

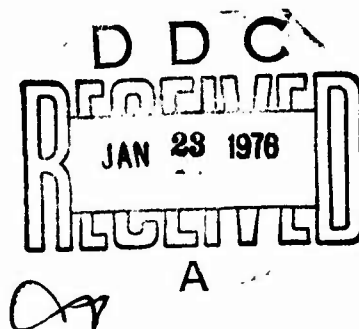
ADA019674

REPORT NO. U-75-27

STEADY-STATE COMBUSTION OF NONMETALLIZED COMPOSITE SOLID
PROPELLANT

DR. R. L. GLICK

THIOKOL CORPORATION
HUNTSVILLE DIVISION
HUNTSVILLE, ALABAMA 35807



JULY 1975

INTERIM REPORT FOR PERIOD 1 MAY 1974 - 30 JUNE 1975

Approved for public release;
distribution unlimited.

PREPARED FOR

DEPARTMENT OF THE AIR FORCE
AIR FORCE OFFICE OF SCIENTIFIC RESEARCH (AFSC)
1400 WILSON BOULEVARD
ARLINGTON, VA 22209

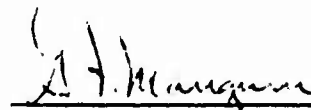
NOTICE

Research sponsored by the Air Force Office of Scientific Research (AFSC), United States Air Force, under Contract F44620-74-C-0080. The United States Government is authorized to reproduce and distribute reprints for governmental purposes notwithstanding any copyright notation hereon.

FOREWORD

This is an interim report covering the work completed under Contract F44620-74-C-0080 for the period 1 May 1974 through 30 June 1975. Publication of this report does not constitute Air Force approval of the findings or conclusions contained herein. It is published only for the exchange of data and stimulation of ideas.

The program is monitored by Capt. L. R. Lawrence, Jr., of the Air Force. Mr. G. F. Mangum is the Project Director and Dr. M. Miller is the Program Manager.



G. F. Mangum
Project Director

ACCESSION for	
NTIS	Yellie 10/10
DDC	5-10-75
UNANNOUNCED	
DISTRIBUTION	
BY	
DATE	
A	

CONTENTS

	<u>Page</u>
ABSTRACT	iv
INTRODUCTION	1
STEADY-STATE COMBUSTION OF NONMETALLIZED COMPOSITE SOLID PROPELLANT	2
Development of Theory	2
Modifications to BDP Model	13
Implementation of Polydisperse BDP Model	14
T-BURNER VENT FLOW STUDY	22
ON REDUCTION OF SOLID ROCKET DATA WHEN THE PRESSURE-TIME IS NON-NEUTRAL	25
PUBLICATIONS DERIVED FROM PROGRAM	30
NOMENCLATURE	31
REFERENCES	34
APPENDIX A - COMPUTER PROGRAM	
APPENDIX B - HYDRAULIC ANALOGY	

FIGURES

<u>No.</u>	<u>Title</u>	<u>Page</u>
1	Schematic of Propellant Surface	4
2	Schematic of Particle Packing	7
3	δ / D versus ζ_0	15
4	Burning Rate as a Function of Oxidizer Mass Fraction	16
5	Burning Rate as a Function of Oxidizer Mass Fraction	17
6	Oxidizer Size Distribution Function	19
7	Burning Rate as a Function of Oxidizer Size	20
8	Monodisperse Pseudo-Propellant Mass Fraction as a Function of Oxidizer Particle Size	21
9	Burning Rate as a Function of Pressure for the Polydisperse Propellant	23

ABSTRACT

Monodisperse BDP combustion model was extended to nonmetallized propellants with mixed, polydisperse oxidizers by embedding monodisperse model in statistical framework including mixture ratio effects. Basically, polydisperse propellant is "disassembled and rearranged" to form sequence of monodisperse pseudo-propellants whose rates are computed via monodisperse model. Re-assembly provides real propellant's burning rate. Approach provides information pertaining to distribution of regression rates and surface structure among different size ox. particles. Preliminary results suggest that significant factor in rate increases wrought by introduction of small oxidizer modes is mixture ratio alterations in larger modes.

Hydraulic T-burner analog was constructed and employed to visualize vent flow phenomena. Studies showed that flow enters vent with axial momentum and that that momentum is partially transformed to vent into Karman vortex sheet. Fact that flow enters vent with axial momentum invalidates boundary condition of Culick analysis for flow turning gain; "correct" boundary condition leads to null vent gain. Experimental facts consistent with proof that in formal one-dimensional flow vent gain violates second law of thermodynamics.

Logical and consistent way to reduce solid rocket data when pressure-time history is not neutral was derived. Since current techniques are not self-consistent in this situation, these results open door to reclamation of performance data heretofore rejected.

INTRODUCTION

Since 1972 when Culick⁽¹⁾ first found that formal analysis of the linearized, one-dimensional equations of change led to acoustic/mean flow interactions (A/MFI), the rather surprising flow turning gain associated with a T-burner's vent has been regarded skeptically. The situation was not improved by the appearance of another "theory" predicting different A/MFI⁽²⁾ and indecisive results obtained from T-burner tests aimed at evaluating A/MFI. The situation in 1973* is described in some detail by Shoner⁽³⁾.

It is not surprising that Culick's one-dimensional results conflict with results stemming from the theory developed by McClure, Hart, and Cantrell⁽⁵⁾ in an area where mixing and viscous effects are important. Culick's theory implicitly includes mixing while MHC's theory explicitly (through the inviscid media assumption) disallows mixing. Clearly, what is required is qualitative knowledge of the flow phenomena so that "intelligent" modeling of A/MFI can be accomplished. A cost effective approach to obtaining qualitative information about multi-dimensional nonsteady flows is to employ the hydraulic analogy. Accordingly, a proposal was prepared and submitted to AFOSR with the expressed purpose of examining the vent region flow in a T-burner with the hydraulic analogy.

Since 1970 steady-state composite propellant combustion modeling has been dominated by the Beckstead, Derr, Price (BDP) model⁽⁶⁾. Although the basic model applied solely to additive-free propellant with spherical, monodisperse oxidizer, Cohen, Derr, and Price⁽⁷⁾ extended the model to propellants with aluminum and bimodal oxidizer. Sammons⁽⁸⁾ subsequently extended the model to propellants with polydisperse oxidizer.

Since composite solid propellant is a random packing of solid particles filled with binder and the deflagration wave traverses the solid, the burning surface must also possess random structure. Because of the discrete particulate nature and random structure of the burning surface, a classical steady state where state variables are invariant in time cannot exist; at any fixed time spatial variations of state variables are random to some length scale; at any fixed position relative to the burning surface the state variables are random in time to some time scale. Consequently, steady-state combustion can only mean that statistical means are stationary in time.

In the monodisperse BDP model the random, nonsteady phenomena at the burning surface is "averaged" into a mean state in a particle's life. Treating this state as quasi-steady and applying mass and energy conservation, kinetics principles, etc., an implicit "relation" for burning rate is obtained. No derivation has been given for the averaging procedure. Cohen, Derr, and Price⁽⁷⁾ extended the model to bi-modal distributions by assuming all particle sizes burn at the

*The situation in 1974 was not greatly changed; see discussion in Reference 4.

same rate. This seems highly improbable. On the other hand, Sammons⁽⁸⁾ extended the model to polydispersions by apparently assuming that the polydispersion could be averaged into a single particle. No derivation was given for this averaging procedure.

In 1973 Glick⁽⁹⁾⁽¹⁰⁾ advanced a statistical combustion modeling formalism that applied to polydisperse situations and eliminated the aforementioned approximations. Consequently, a proposal was prepared and submitted to AFOSR with the expressed purpose of embedding the basic BDP combustion model in this statistical formalism.

These separate proposals were ultimately combined into a single program with the following objectives:

- Construct a hydraulic analogue of a T-burner utilizing a water table.
- Investigate the flow pattern in the vent region of the T-burner analogue to determine whether or not acoustic energy is convected out the vent.
- Compare the experimental results in qualitative fashion with the predictions of present T-burner theories.
- Adapt the Beckstead, Derr, Price combustion model as modified by Sammons to the contractor's statistical combustion model. Investigate the properties of the resulting model as it pertains to propellants with polydispersions of spherical, mixed oxidizers.

This program was monitored, in the best sense of the word, by Capt. L. R. Lawrence, Jr. This report describes in detail the work that was accomplished under this program.

STEADY-STATE COMBUSTION OF NONMETALLIZED COMPOSITE SOLID PROPELLANT

Development of Theory

The most obvious feature of composite solid propellants is their heterogeneous structure. Since high specific impulse is desirable for propulsion systems, total solids content is generally as large as possible. Since composite propellant is essentially a packing of solid particles filled with binder, high total solids content demands a dense packing. To achieve a dense packing, the particles must be polydisperse with a broad range of particle sizes so that the smaller particles can fill the voids in the packing of the larger particles. Therefore, virtually all practical propellants are polydisperse. In the past ammonium perchlorate (AP) was the preferred oxidizer specie. Consequently, propellants with mixed oxidizers were rare. However, recent emphasis on reduced visual

signature has aroused interest in oxidizers other than AP and propellants with non-AP oxidizer, mixtures of non-AP oxidizers, and AP and non-AP mixtures are being explored. Therefore, realistic combustion modeling must consider, in the least, propellants with mixed, polydisperse oxidizers.

Composite propellants are created by mixing their several ingredients together. Therefore, a randomly packed, particulate structure is expected above some length scale. Since the deflagrating surface transverses the solid, the arrangement/structure of oxidizer particles on the burning surface must also be random above some length scale. Because of this randomness and the discontinuous chemistry wrought by heterogeneity, composite propellant combustion is never steady-state in the sense that state variables are invariant in time; at any time state variables are spatially random above some length scale; at any fixed position relative to the mean burning surface state variables vary randomly in time above some time scale. Consequently, analysis of "steady-state" combustion must be directed toward the determination of state variable means and distributions.

Consider now a large, quasi-planar deflagrating surface of composite solid propellant (see Figure 1). Application of mass conservation to the control surface yields

$$\frac{dm_{cv}}{dt} = \oint_{S_b} m'' dS - \oint_{S_p} m'' dS \quad (1)$$

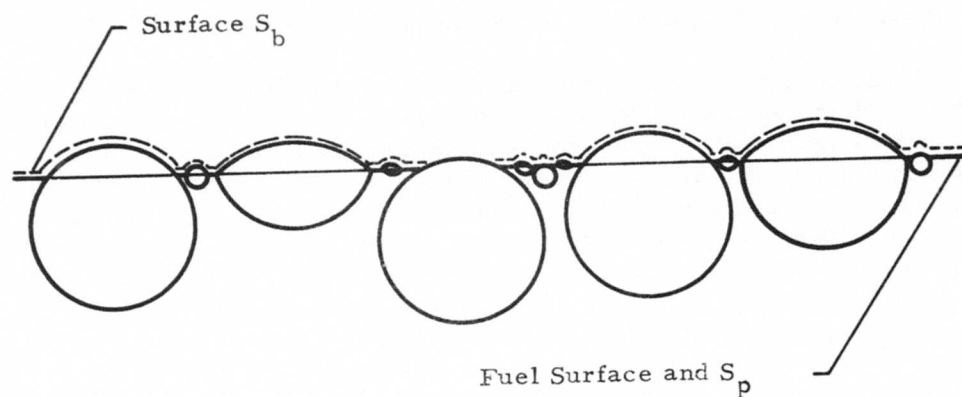
Experience shows that when $dp = dT_i = 0$ $\lim_{S_p \rightarrow \infty} \frac{dm_{cv}}{dt} = 0$. Consequently, for steady-state combustion

$$\oint_{S_p} m'' dS = \oint_{S_b} m'' dS \quad (2)$$

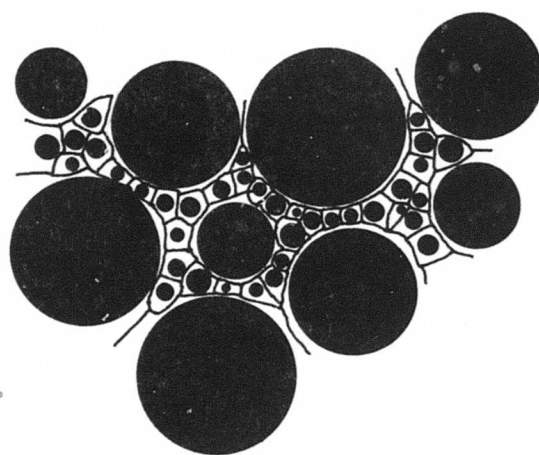
Applying the mean value theorem for integrals to the LHS of Eq. (1) yields

$$\bar{m}_t = \oint_{S_b} m'' dS / S_p = \bar{r} \rho_t \quad (3)$$

The surface S_b may be visualized as a jigsaw puzzle-like arrangement of oxidizer particle/fuel surface pairs. For composite propellant with polydisperse, mixed oxidizers, some of these oxidizer particle/fuel surface pairs will have the same particle diameter and specie. Therefore, rearrange the oxidizer particle/fuel surface pairs so that those with common particle diameters and species are neighbors. This rearrangement creates a sequence of monodisperse propellant subsurfaces. If it is assumed that combustion of all oxidizer particle/fuel surface pairs are independent, the deflagration rate of any monodisperse subsurface can be computed by application of any monodisperse combustion (BDP for example) model. Consequently, proper summation of these subsurface rates should yield the burning rate of composite propellant with mixed, polydisperse oxidizer.



ELEVATION



PLAN

Figure 1. Schematic of Propellant Surface

To accomplish this approach rearrange the burning surface's oxidizer particle/fuel surface pairs into Q monodisperse subsurfaces. Then Eq. (3) becomes

$$\bar{m}_t'' = \sum_{i=1}^Q \left(\sum_{k=1}^s \oint_{\Delta S_{b,d,k}} m_{d,k}'' dS \right) / S_p \quad (4)$$

where $\Delta S_{b,d,k}$ is the portion of S_b occupied by and $m_{d,k}''$ is the mass flux from oxidizer particle/fuel surface pairs possessing oxidizer particles with $D \leq D \leq D + \Delta D$ and specie k . Application of the mean value theorem for integrals to the RHS of Eq. (4) yields

$$\bar{m}_t'' = \sum_{i=1}^Q \left(\sum_{k=1}^s \bar{m}_{d,k}'' \Delta S_{b,d,k} \right) / S_p \quad (5)$$

The term $\bar{m}_{d,k}'' \Delta S_{b,d,k}$ is the mass flow of products from the monodisperse subsurface $\Delta S_{b,d,k}$. Therefore,

$$\bar{m}_{d,k}'' \Delta S_{b,d,k} = \bar{m}_{p,d,k}'' \Delta S_{p,d,k} \quad (6)$$

where $\bar{m}_{p,d,k}''$ is the mean mass flux (based on planar area) from the monodisperse subsurface $\Delta S_{b,d,k}$ and $\Delta S_{p,d,k}$ is the projection of $\Delta S_{b,d,k}$ on S_p .

If $\Delta N_{p,d,k}$ is the number of oxidizer particles on S_p with $D \leq D \leq D + \Delta D$ and specie k per unit area of S_p ,

$$\Delta S_{p,d,k} / S_p = \Delta \bar{S}_{p,d,k} \Delta N_{p,d,k} \quad (7)$$

where $\Delta \bar{S}_{p,d,k}$ is the average planar surface for an oxidizer particle/fuel surface pair possessing oxidizer particles with $D_i \leq D_i \leq D_i + \Delta D$ and specie k .

Define a distribution function $F_{p,d,k}$ such that

$$\Delta N_{p,d,k} = N F_{p,d,k} \Delta D \quad (8)$$

Then combining Eqs. (5) - (8) yields

$$\bar{m}_t = N \sum_{k=1}^s \left(\sum_{i=1}^Q \bar{m}_{p,d,k}'' \Delta \bar{S}_{p,d,k} F_{p,d,k} \Delta D \right) \quad (9)$$

Passing to the limit of the sum on i as $Q \rightarrow \infty$ yields

$$\bar{m}_t'' = N \sum_{k=1}^s \oint_D \bar{m}_{p,d,k}'' \Delta \bar{S}_{p,d,k} F_{p,d,k} dD = \bar{r} \rho_t \quad (10)$$

Equation (10) is a statistical formalism that enables the mean burning rate of propellant with mixed, polydisperse oxidizers to be computed from the mean burning rates ($\bar{m}_{p,d,k} = \bar{r}_{d,k} \rho_{t,d,k}$) of the sequence of monodisperse psuedo-propellants that "compose" it IF THE COMBUSTION OF EACH OXIDIZER PARTICLE/FUEL SURFACE PAIR IS INDEPENDENT. This approach permits consideration of mixed oxidizers and avoids the requirement that a single particle be selected to represent a polydispersion. Since a polydispersion is represented as a polydispersion, information concerning the variation of surface geometry, temperature, regression rate, etc. can also be computed.

The next step is to investigate the statistical characteristics of the burning surface and thereby relate $\Delta \bar{S}_{p,d,k}$, $F_{p,d,k}$, and the properties of the monodisperse psuedo-propellants to propellant formulation variables. Assuming that the statistical characteristics of the random packing are homogeneous and isotropic, the statistical characteristics of surface S_p can be explored within the propellant. Figure 2 illustrates a random polydisperse packing schematically. Clearly, particles with $D \leq D \leq D + dD$ must lie within $z = \pm D/2$ to intersect plane S . Therefore, if $dN_{v,d}$ is the number of particles per unit volume with $D \leq D \leq D + dD$, the number of these particles that intersect S per unit area of S is

$$dN_{p,d} = dN_{v,d} D \quad (11)$$

The volume fraction of spherical particles with diameter D is

$$d\zeta_d = (\pi D^3 / 6) dN_{v,d} \quad (12)$$

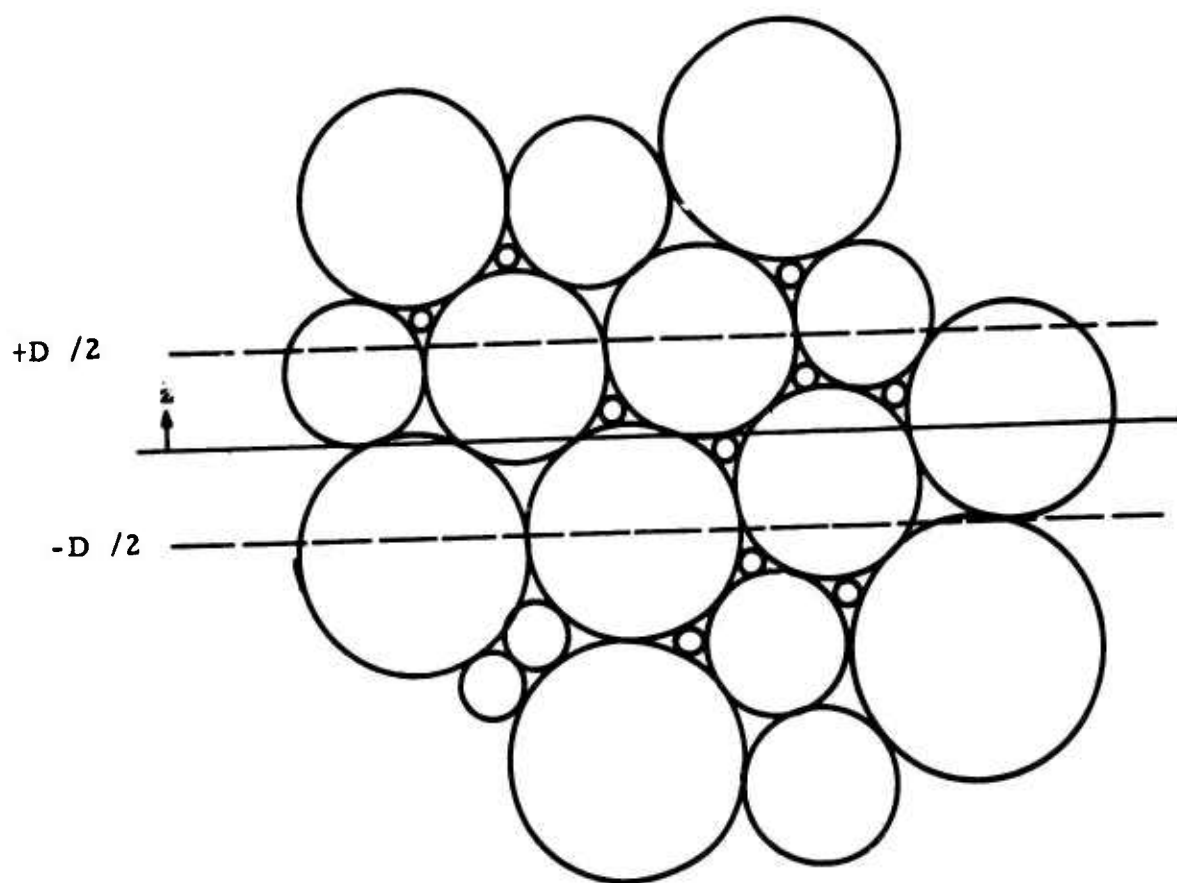


Figure 2 Schematic of Particle Packing

Therefore,

$$dN_{p,d} = (6/\pi D^2) d\zeta_d \quad (13)$$

If the number fraction of particles with $D \leq D \leq D + dD$ and species k in the propellant is $\eta_{d,k}^*$, the number of these particles per unit area of S is

$$dN_{p,d,k} = (6/\pi D^2) \eta_{d,k} d\zeta_d = (6/\pi D^2) d\zeta_{d,k} \quad (14)$$

Now move the plane a distance Δz . The volume of oxidizer particles with $D \leq D \leq D + dD$ in the swept volume is

$$dV_d = d\zeta_d S \Delta z \quad (15)$$

However, the statistical characteristics are homogeneous and isotropic. Therefore, this volume is also swept out by intersections of S with oxidizer particles having $D \leq D \leq D + dD$. Since $dS_{p,d} = (\pi \bar{D}_d^2/4) dN_{p,d}$,

$$dV_d = (\pi \bar{D}_d^2/4) dN_{p,d} \Delta z \quad (16)$$

Combining Eqs. (13), (15), and (16) yields the mean particle intersection diameter

$$\bar{D}_d = \sqrt{2/3} D \quad (17)$$

Therefore, the average oxidizer particle intersection area is

$$\Delta \bar{S}_{o,d,k} = \pi D_{d,k}^2/6 \quad (18)$$

* Note that $\sum \eta_{d,k} = 1$. Since all these particles have same diameter, $\eta_{d,k}$ is $k = 1$ also a volume fraction.

It is important to note that \bar{D}_d , $dN_{v,d}$ and $dN_{p,d}$ are functions of D alone. This means that statistical characteristics of the monodisperse cuts in a polydisperse propellant are the same as those in a monodisperse propellant. In short, each monodisperse cut behaves as if it alone occupied the propellant. Notice the similarity to mixtures of perfect gases.

The mean statistical characteristics of the fuel surface in each monodisperse cut of oxidizer fuel surface pairs cannot be determined exactly because it requires a statistical determination of how the smaller particles pack inside the packing of larger particles. This information is unavailable. Therefore, approximations must be introduced. Examination of the characteristics of regular geometric packings⁽¹¹⁾ suggests that the mean volume of fuel associated with a particle should be roughly proportional to its surface or $\bar{\Delta V}_{f,d} \propto D^2$. However, to allow for some variation assume

$$\bar{\Delta V}_{f,d} = C D^n \quad (19)$$

where n is a parameter to be determined experimentally. Since oxidizer volume is proportional to D^3 , $d(O/F)/dD \geq 0$ when $n \geq 3$. Particle diameter alone is important in a packing. Therefore, $\bar{\Delta V}_{f,d,k} = \bar{\Delta V}_{f,d}$.

The volume fraction of fuel associated with particles having $D \leq D \leq D + dD$ and species k is

$$dV_{f,d} = \bar{\Delta V}_{f,d} dN_{v,d} \quad (20)$$

The volume fraction of fuel in the real propellant is $1 - \zeta_o$; it is also the integral of Eq. (20) over all particle diameters. Employing this fact and Eqs. (12) and (20) yields after integrating over all diameters

$$C = [\pi (1 - \zeta_o)/6] / \int_D^\infty D^{n-3} d\zeta_d \quad (21)$$

With both particle diameter and mean volume of fuel associated with that particle diameter "known" the volume and mass fractions and the density of a pseudo-propellant formed from mono-diameter and specie oxidizer particle/fuel surface pairs can be computed. The volume fraction is $\bar{\Delta V}_{o,d,k} / (\bar{\Delta V}_{o,d,k} + \bar{\Delta V}_{f,d,k})$ so

$$\zeta_{d,k}^* = (1 + 6CD^{n-3}/\pi)^{-1} \quad (22)$$

The mass fraction is $\overline{\Delta m}_{o,d,k} / (\overline{\Delta m}_{o,d,k} + \overline{\Delta m}_{f,d,k})$ so

$$\alpha_{d,k}^* = [1 + 6C\rho_f D^{n-3} / (\pi \rho_{o,k})]^{-1} \quad (23)$$

The pseudo-propellant's density is

$$\rho_{d,k}^* = \rho_{o,k} \zeta_{d,k}^* / \alpha_{d,k}^* \quad (24)$$

Since $\zeta_{d,k}^* = S_{o,d,k}^* / S_{p,d,k}^* = \Delta \bar{S}_{o,d,k} / \Delta \bar{S}_{d,k}$, Eq. (18) becomes

$$\Delta \bar{S}_{d,k} = \pi D^2 / (6 \zeta_{d,k}^*) \quad (25)$$

The mass flux in Eq. (10) corresponds to the mean mass flux stemming from combustion of pseudo-propellant. Therefore,

$$\overline{m}_{p,d,k}'' = \overline{m}_{d,k}'' = \overline{r}_{d,k}^* \rho_{d,k}^* \quad (26)$$

The only tasks remaining are to relate $F_{p,d,k}$ and $d\zeta_{d,k}$ to the independent propellant formulation variables $\alpha_{k,j}$, $F_{k,j}$, M_k , and s . The volume fraction of oxidizer specie k with diameter D is defined as

$$d\zeta_{d,k} = dV_{o,d,k} / V_t \quad (27)$$

Since $dV_{o,d,k} = dm_{o,d,k} / \rho_{o,k}$ and $V_t = m_T / \rho_t$

$$d\zeta_{d,k} = (dm_{o,d,k} / m_t) (\rho_t / \rho_{o,k}) \quad (28)$$

However, $F_{k,j} = dm_{o,d,k,j} / (m_{o,k,j} dD)$ and $dm_{o,d,k} = \sum_{j=1}^{M_k} dm_{o,d,k,j}$
 Therefore,

$$d\zeta_{d,k} = (\rho_t / \rho_{o,k}) \sum_{j=1}^{M_k} \alpha_{k,j} F_{k,j} dD \quad (29)$$

$$\text{Since } dV_{o,d} = \sum_{k=1}^s dV_{o,d,k}$$

$$d\zeta_d = \sum_{k=1}^s (\rho_t / \rho_{o,k}) F_k dD \quad (30)$$

where

$$F_k = \sum_{j=1}^{M_k} F_{k,j} \alpha_{k,j} \quad (31)$$

$$\text{Since } \zeta_o = V_o / V_t, \quad V_o = \sum_{k=1}^s \sum_{j=1}^{M_k} V_{o,k,j}, \text{ and } V = m / \rho,$$

$$\zeta_o = \rho_t \sum_{k=1}^s \sum_{j=1}^{M_k} (\alpha_{k,j} / \rho_{o,k}) \quad (32)$$

$$\text{Since } \rho_t = (V_t / m_t)^{-1}, \quad V_t = \sum_{k=1}^s \sum_{j=1}^{M_k} V_{o,k,j} + V_f, \text{ and } V = m / \rho,$$

$$\rho_t = [\rho_f^{-1} + \sum_{k=1}^s \sum_{j=1}^{M_k} (\rho_{o,k}^{-1} - \rho_f^{-1}) \alpha_{k,j}]^{-1} \quad (33)$$

By definition $NF_{p,k,d} dD = dN_{p,d,k}$. Employing Eq. (14) it is seen that

$$NF_{p,k,d} dD = 6 d \zeta_{d,k} / (\pi D^2) \quad (34)$$

Employing this result and Eqs. (25) and (30), Eq. (10) can be rewritten as

$$\bar{r} \rho_t = \frac{\bar{m}''}{m_t} = \rho_t \sum_{k=1}^s \rho_{o,k}^{-1} \oint_D (\bar{m}_{d,k}''^* / \zeta_{d,k}^*) F_k dD \quad (35)$$

Therefore

$$\bar{r} = \sum_{k=1}^s \rho_{o,k}^{-1} \oint_D (\bar{m}_{d,k}''^* / \zeta_{d,k}^*) F_k dD \quad (36)$$

Eqs. (21 - 24), (31 - 33), and (36) put \bar{r} in terms of real propellant data. Since interest is focused on the BDP model herein,

$$\bar{m}_{d,k}''^* = \bar{m}_{BDP}'' (D, \alpha_{d,k}^*, \rho_{d,k}^*, \zeta_{d,k}^*, \text{etc.}) \quad (37)$$

Modifications to BDP Model

The reason for polydisperse propellants is high total solids. Consequently, with "real" propellants the BDP model must operate in the $\zeta_o \approx 1$ regime. Unfortunately, examination of the model⁽⁶⁾ shows that the b parameter (mean distance from center of oxidizer particle to center of binder separating particles) is given by

$$b = D [1 + \sqrt{3/2} (\delta/D)] / \sqrt{6} \quad (38)$$

where

$$\delta/D = [\pi / (6 \zeta_o)]^{1/3} - (2/3)^{1/3} \quad (39)$$

Clearly, as ζ_o approaches unity, both δ/D and b must approach zero with the proviso that $\delta/D > 0$ and $b > 0$. Examination of Eq. (39) shows that δ/D changes sign at $\zeta_o \approx 0.785$. Consequently, Eqs. (38) and (39) and hence the BDP model cannot be employed for propellants with $\zeta_o \geq 0.785$. This represents no difficulty for monodisperse propellants because packing considerations limit ζ_o to values below this limit.⁽¹¹⁾ However, this is a very real difficulty with monodisperse psuedo-propellants.

The aforementioned difficulty occurs because the fuel surface of an oxidizer particle/fuel surface pair is assumed to be annular with $D_i = \bar{D}$ and $D_o = 2b$. However, in reality the binder surface is not an annulus but an irregular quadrilateral. Consequently, this assumption "loses" the fuel in the corners between the quadrilateral and the "inscribed" annulus. The simplest way to overcome this difficulty is to assume that b is the dimension of an annulus possessing the fuel surface associated with the mean oxidizer particle/fuel surface pair. In other words, b is defined by

$$\pi b^2 - \pi \bar{D}^2 / 4 = \Delta \bar{S}_f \quad (40)$$

The fraction of planar surface occupied by fuel is $1 - \zeta_o$. The number of particles/unit planar surface is given by Eq. (13). Therefore,

$$\Delta \bar{S}_f = (1 - \zeta_o) \pi D^2 / (6 \zeta_o) \quad (41)$$

$$b = D / \sqrt{6 \zeta_o} \quad (42)$$

and

$$\delta/D = (\zeta_o^{-1/2} - 1) / \sqrt{6} \quad (43)$$

Examination of the BDP computer program⁽¹²⁾⁽¹³⁾ shows that the FORTRAN expression employed for δ/D is not equivalent to Eq. (39) but represents

$$\delta/D = [\pi/(6\zeta_0)]^{1/3} - (2/3)^{1/2} \quad (44)$$

This expression is positive for $\zeta_0 < 0.961$.

Figure 3 compares Eqs. (39), (43), and (44). It is seen that Eq. (43) has correct behavior for $\zeta_0 \approx 1$ and agrees well with Eq. (39) for $\zeta_0 \approx 0$.

Numerical tests were made to determine the effect of oxidizer mass fraction on burning rate. Tests were made with both Eqs. (38) (44) (denoted as BDP) and (42) (43) (denoted as Mod. BDP). Figure 4 presents results when $D = 1 \mu$ and $p = 932$ psi. It is clear that the solutions are discontinuous at both high and low mass fractions for both normal and modified BDP models. For oxidizer mass fractions greater than the upper discontinuity point and less than the lower discontinuity point, the models gave negative values for the diffusion flame standoff distances in both cases. Consequently, the difficulty appears to stem from the Burke-Schumann solution. Since the BDP model with the single term approximation to the Burke-Schumann solution was employed herein and Sammons multiple term version showed no evidence of discontinuities at a mass fraction of 0.86,⁽¹³⁾ this defect can probably be remedied by employing the Sammons version of the BDP model. However, we did not have this version. Consequently, another remedy was sought. Because the diffusion flame standoff distances increased rapidly to very large values when the discontinuities were approached from the other direction, a negative diffusion flame standoff distance was replaced by a very large value whenever it occurred. This gives continuity with intermediate mass fraction results. Figure 5 illustrates rate versus mass fraction results with this modification.

Calculations at $D = 100 \mu$ and $p = 932$ psi exhibited behavior similar to the aforementioned. However, as will be observed below, the aforementioned results did not completely eliminate "discontinuous" behavior.

Implementation of Polydisperse BDP Model

The modified monodisperse BDP combustion model was extended to non-metallized propellants with a polydisperse oxidizer by embedding the model in the previously described statistical framework. A complete listing of the computer program and a description of its use with a sample problem is provided in Appendix A.

Since parametric studies were anticipated, a log normal distribution of oxidizer particle size was assumed for each mode.

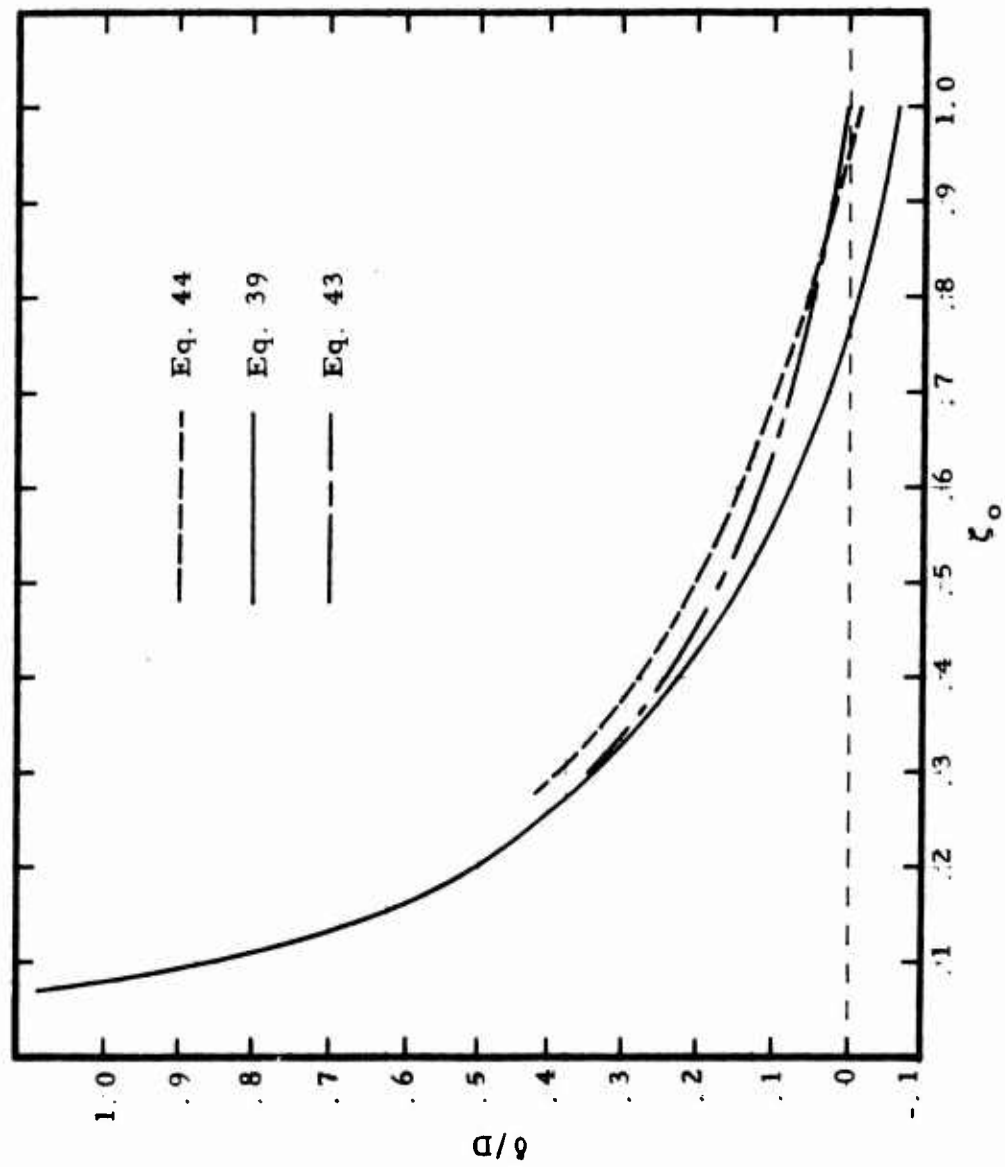


Figure 3. δ/D versus ζ_0 .

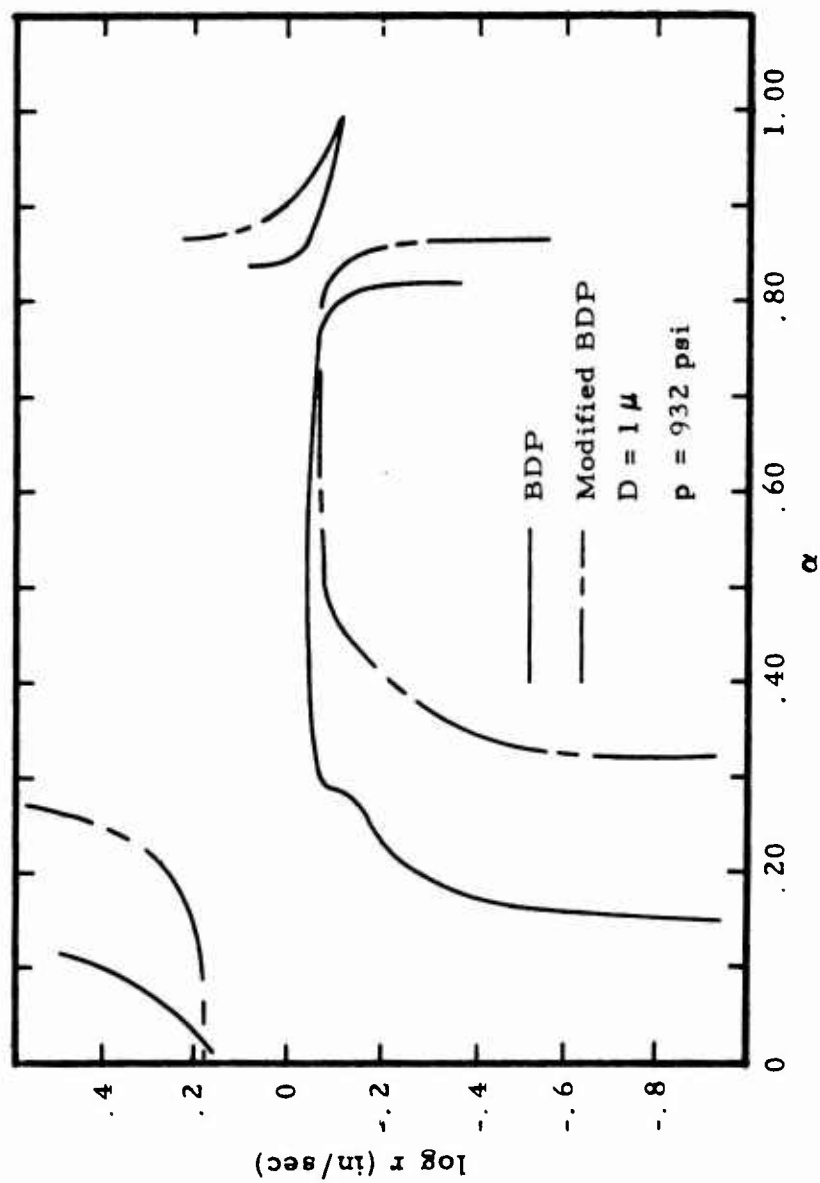


Figure 4. Burning Rate as a Function of Oxidizer Mass Fraction

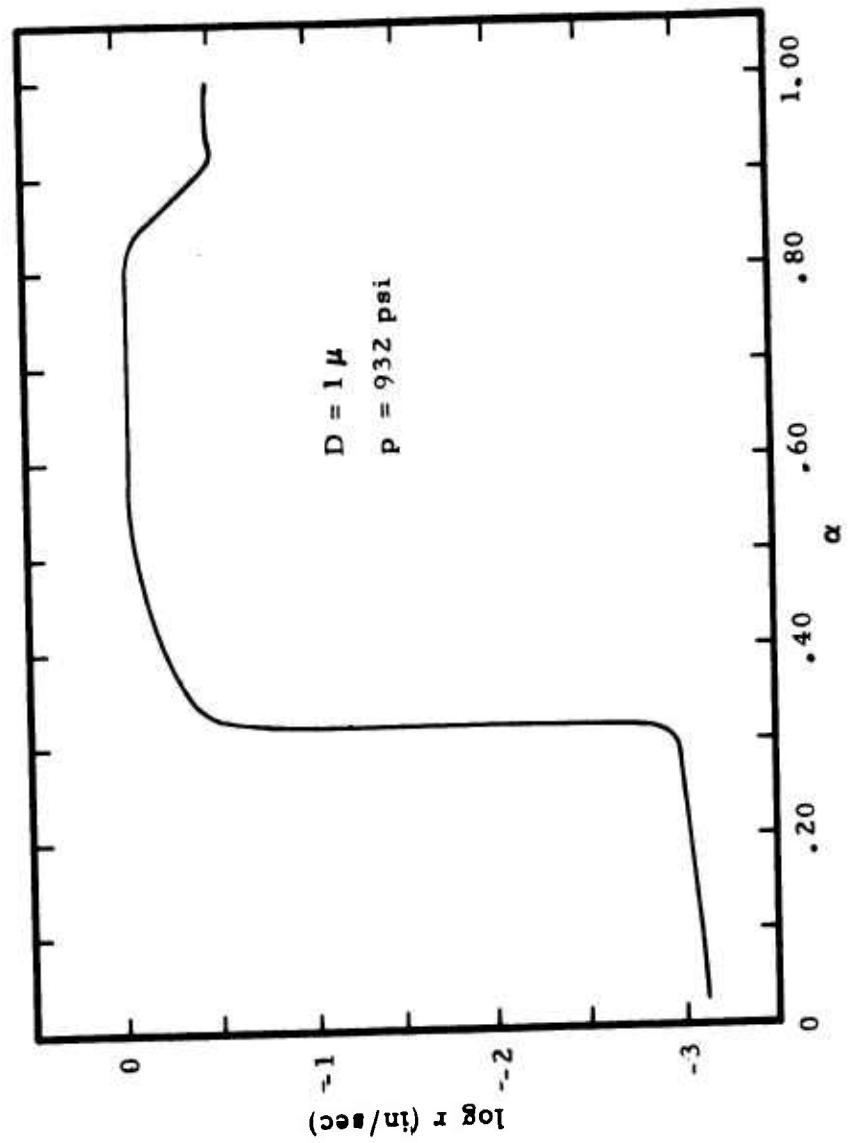


Figure 5. Burning Rate as a Function of Oxidizer Mass Fraction

$$y = \frac{1}{\sigma \sqrt{2\pi}} \exp \left[-\frac{1}{2} \left(\frac{x - m}{\sigma} \right)^2 \right] \quad (45)$$

where

$$x = \ln D$$

$$m = \ln \bar{D}_m$$

$$\sigma = \ln \sigma^*$$

This assumption is reasonably realistic and permits each mode to be characterized with minimum input information, thereby assisting parametric studies of particle size effects. Thus, in addition to the standard BDP input parameters, the number of modes, the weight mean diameter and standard deviation of diameter for each mode and the mass fraction of each mode relative to the total mass of oxidizer are needed to characterize the polydisperse oxidizer size distributions in the computer program.

The initial test of the computer program was made with a polydisperse bimodal AP propellant. Oxidizer size distribution data are shown in Table 1. The distributions are depicted in Fig. 6.

TABLE 1

<u>Mode</u>	<u>Mass Fraction of Total Propellant</u>	<u>\bar{D} [μ]</u>	<u>σ^* [μ]</u>
1	0.45	16	2.0
2	0.45	200	1.4

The computer program solves for the mass flux associated with each monodisperse psuedo-propellant in the propellant and sums these fluxes in accordance with Eq. (36) to determine mean propellant burning rate. Figure 7 presents the monodisperse psuedo-propellant burning rates as a function of particle size for several values of n . * Figure 8 illustrates how oxidizer mass fraction varies in the psuedo-propellant family. Viewing Figures 7 and 8 together shows the following:

*Recall that n is an empirical parameter controlling how oxidizer mass fraction varies in the psuedo-propellant family.

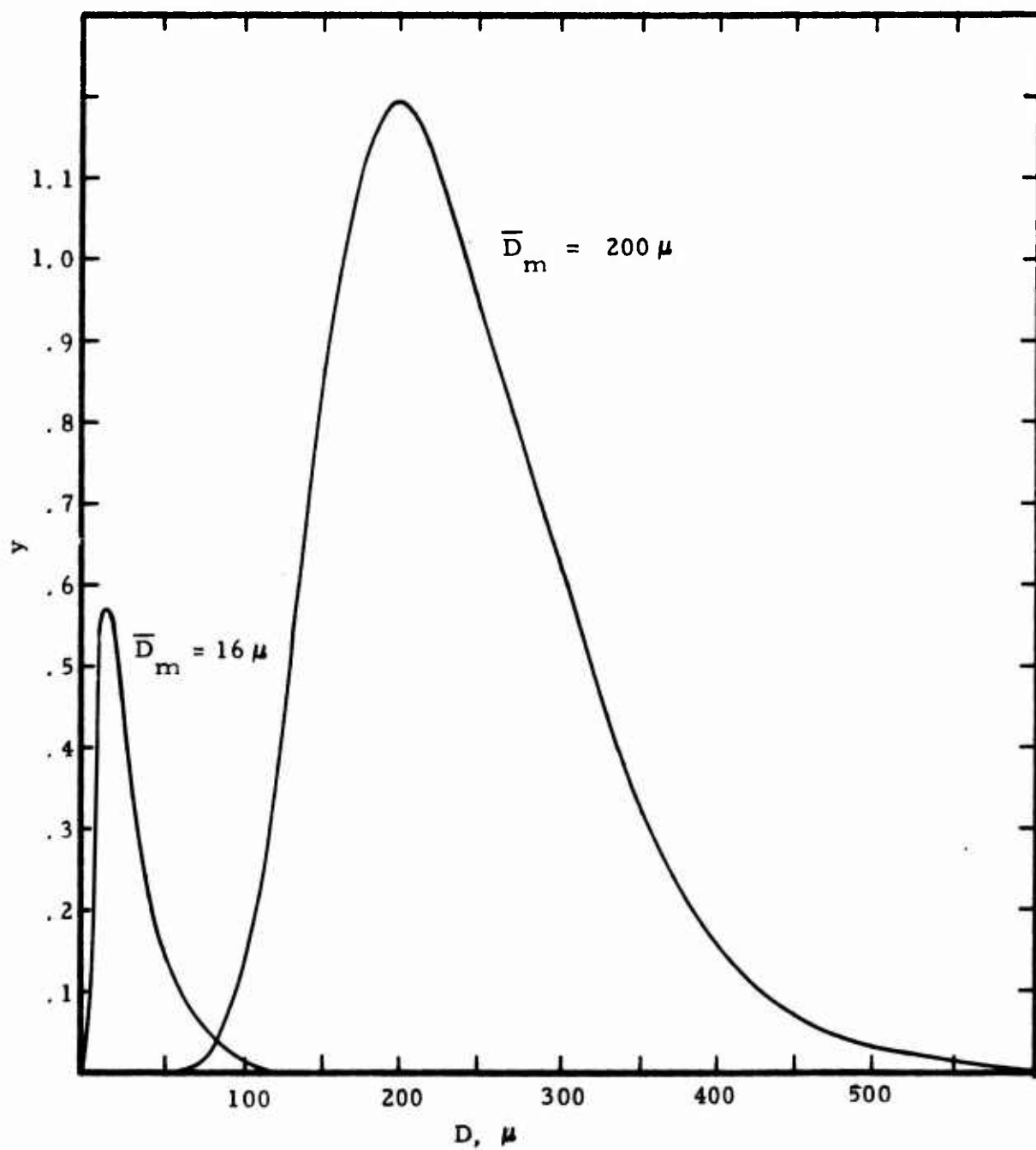


Figure 6. Oxidizer Size Distribution Function

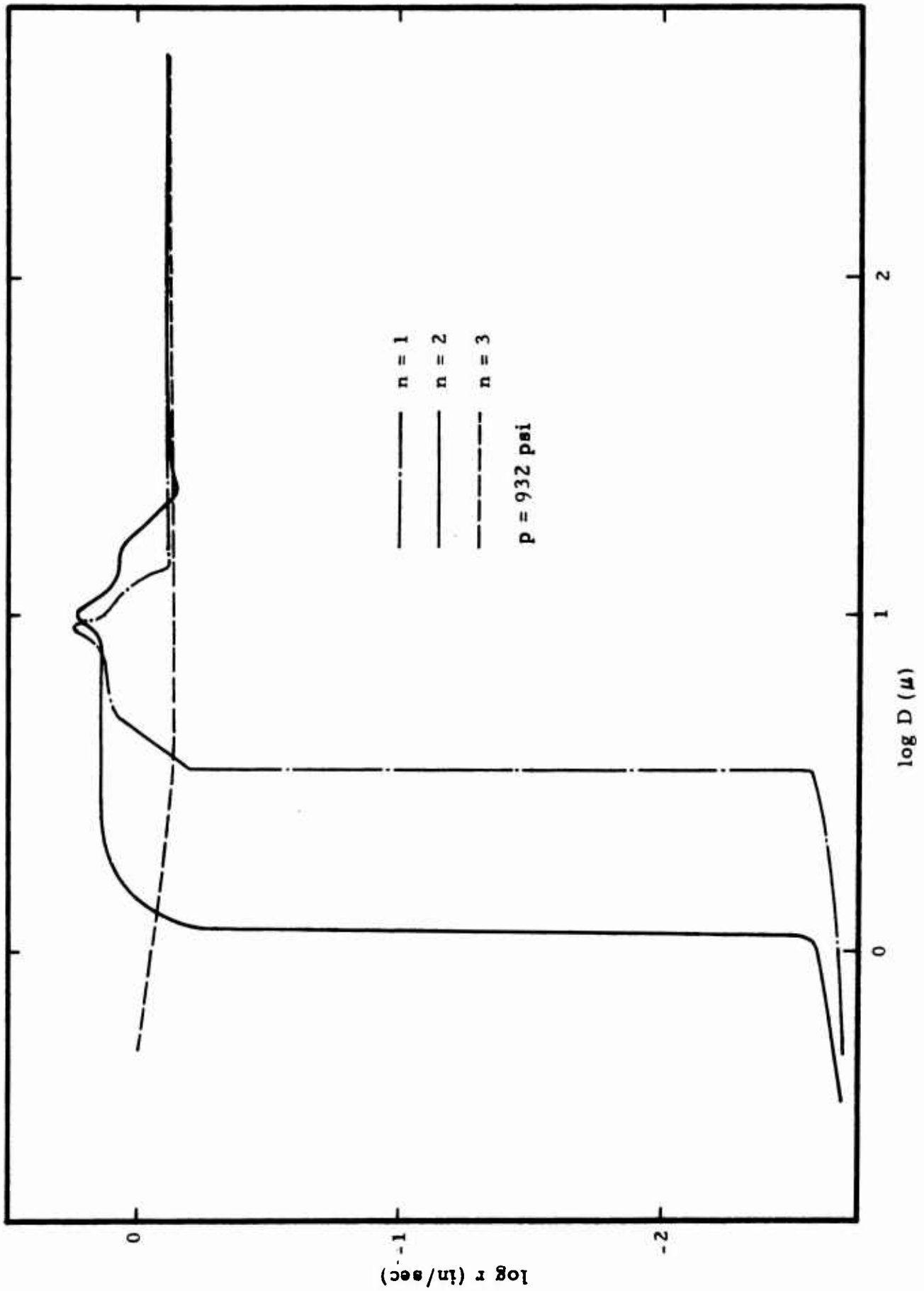


Figure 7. Burning Rate as a Function of Oxidizer Size

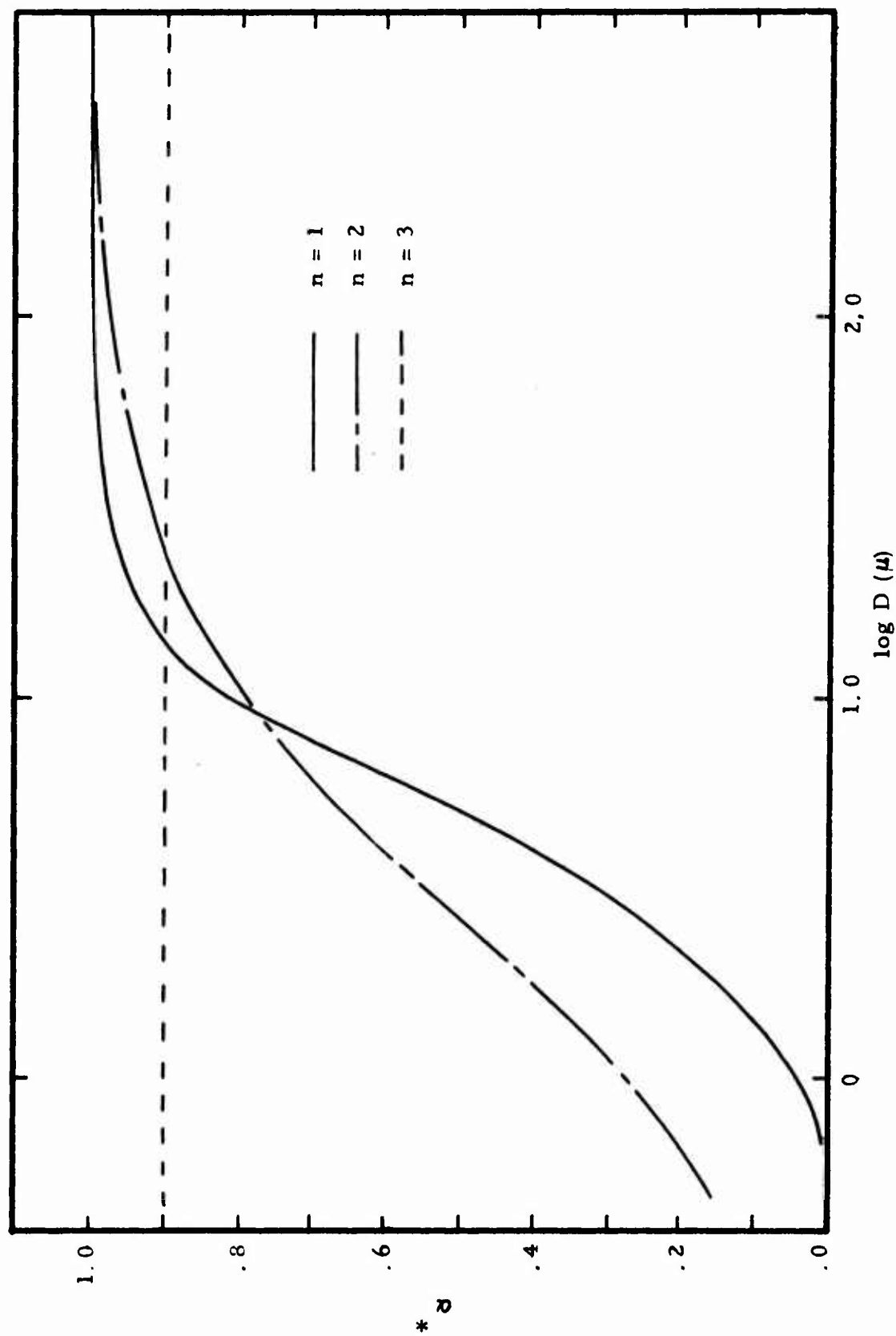


Figure 8. Monodisperse Psuedo-Propellant Mass Fraction as a Function of Oxidizer Particle Size

- o Rate does not vary with particle size by any simple expression reminiscent of the GDF relationship. (14)
- o The way fuel is apportioned among the psuedo-propellants (n) has an enormous effect on the burning rates of the smaller particle sizes.
- o The way fuel is apportioned among the psuedo-propellants (n) has little effect on the burning rates of the larger particle sizes.

The fact that a simple $r \propto D^{-1}$ relationship is not evident suggests that smaller particles do not necessarily augment burning rate by any intrinsically higher rate mechanism. Rather, they appear to partially augment rate by leaning the mixture ratio of the larger particles.

Figure 9 presents the burning rate of the initial case propellant versus pressure. A reasonable exponent is predicted and, somewhat surprisingly, the results are not strongly dependent upon the value of n.

T-BURNER VENT FLOW STUDY

Culick⁽¹⁾⁽¹⁵⁾ has shown, through analysis of the one-dimensional equations of change that a mean flow/acoustics surface interactions term arises naturally in stability analyses. For regions where $d\hat{p}/dz \neq 0$ this term represents a loss of acoustic energy when there is mass addition and a gain of acoustic energy when there is mass subtraction. The latter has led to speculation that the vent of a T-burner yields a gain of acoustic energy for waves in the burner.

However, Culick⁽¹⁵⁾ demonstrates that the adiabatic process leading to a mean flow/acoustic surface interaction loss dissipates acoustic energy into heat. Since acoustic energy is completely available energy, available energy is degraded into heat by this process. Therefore, this process is thermodynamically irreversible. Consequently, the reverse process - the mean flow/acoustics surface interaction gain - is thermodynamically impossible.

This result is almost as surprising as the original mean flow/acoustics surface interaction gain because it contradicts results that arise solely from the equations of change. However, the equations of change do not suffice to define reality because a second law of thermodynamics exists. Therefore, a mean flow/acoustics surface interaction gain process must be a second law violator. Reflection shows that this is the situation because formal reversal of the mean flow/acoustics surface interaction loss implies complete conversion of heat into available energy in an adiabatic process - a phenomena that is disallowed by the second law of thermodynamics.

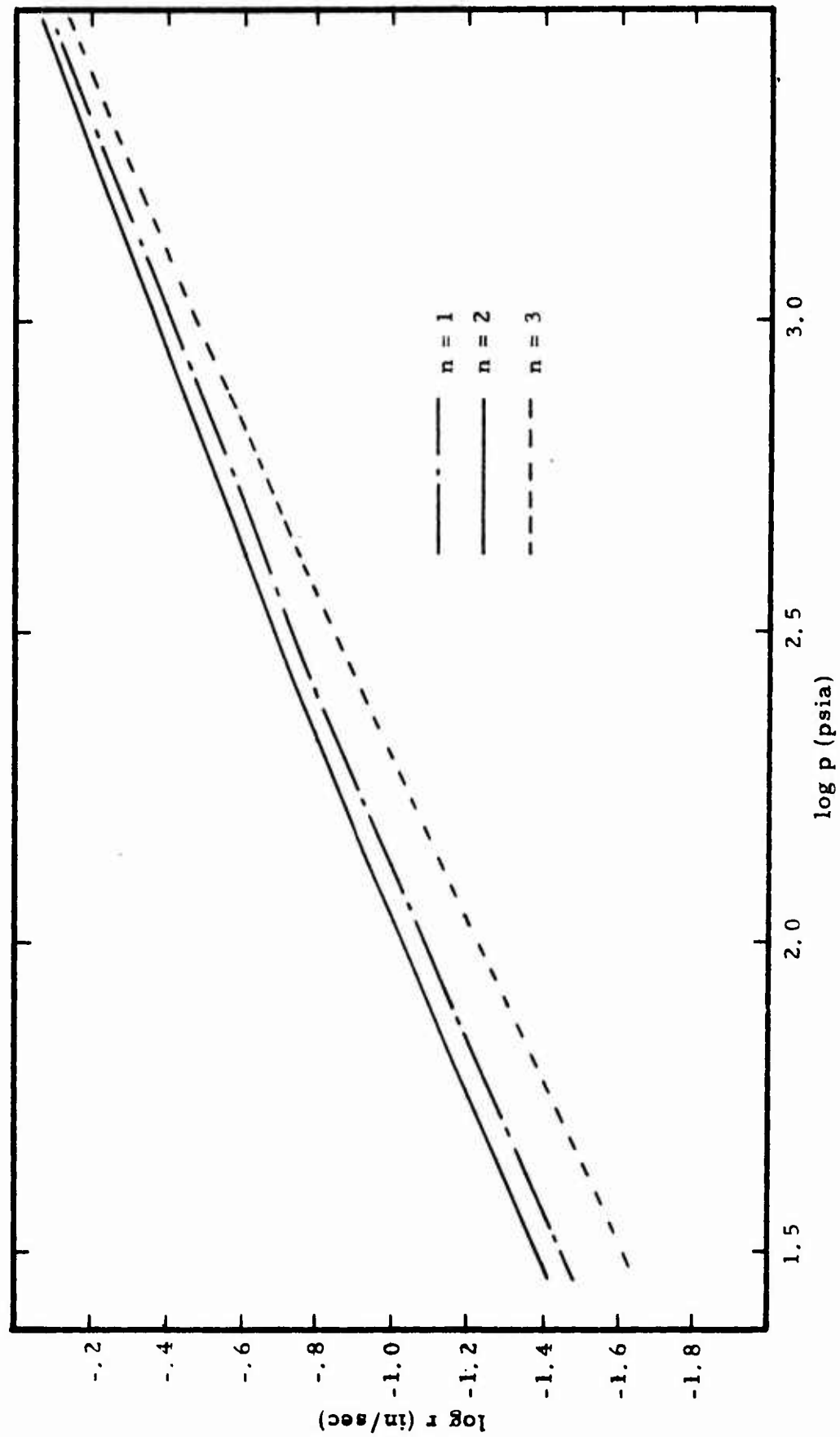


Figure 9. Burning Rate as a Function of Pressure for the Polydisperse Propellant

Why does this result occur and what is the correct result for a mean flow/acoustic surface interaction when there is mass subtraction? The only "arbitrary" assumption in Culick's analysis is that mass enters and leaves with zero velocity. Is this assumption "legitimate"? Since the one-dimensional equations of change must be valid in the quasi-steady limit, is this assumption "legitimate" in steady-flow? Shapiro⁽¹⁶⁾ shows that it is legitimate for mass addition but violates the second law of thermodynamics for mass subtraction. Moreover, Shapiro shows that the second law requires that mass be rejected with free stream conditions in a steady, one-dimensional flow. Clearly, the mean flow/acoustic surface interactions gain arises from this improper boundary condition. For a proper one-dimensional analysis, Culick's equations must be formulated so they are in harmony with these quasi-steady flow constraints because this is the limit as frequency goes to zero. Culick has also solved this problem⁽¹⁵⁾ and finds in this case that the mean flow/acoustic surface interactions term is zero when there is mass subtraction. Therefore, a properly formulated one-dimensional analysis shows that the vent is neither gain nor loss.

It is important to note that this "new" result is in harmony with physical results. First, atmospheric T-burner test results reported by Horton and Coates⁽²⁾ demonstrate conclusively that gases at the vent of a T-burner possess axial velocity. Second, hydraulic analogy tests reported by Glick⁽¹⁷⁾ show that in a T-burner with a vent pipe the gases enter the vent with axial momentum and that that axial momentum is transformed in the vent into a Karman vortex sheet. Third, Culick⁽¹⁸⁾ has shown that a flow field like that revealed by the hydraulic analogy studies leads to a vent condition that is neither gain nor loss.

In summary, theoretical and experimental evidence seems to be converging on a null vent condition.

ON REDUCTION OF SOLID ROCKET DATA WHEN THE PRESSURE-TIME HISTORY IS NON-NEUTRAL

Reducing pressure- and thrust-time, propellant mass and web, and nozzle geometry data to determine mean burning rate, mean characteristic velocity, delivered (mean) specific impulse, mean pressure, and mean nozzle geometry is reasonably straightforward with neutral pressure-time histories and minimal nozzle erosion because pressure and nozzle geometry are unique in this situation. However, when the pressure-time history is non-neutral, pressure (and usually nozzle geometry) is no longer unique and choosing the correct mean pressure becomes a problem. It is important to note that functional relationships exist between dependent (r , C^* , I_{sp}) and independent (p , ϵ , etc.) variables. Indeed, one purpose of performance testing is to determine these relationships experimentally. Consequently, when means of dependent variables are defined, means of the independent variables must be derived from these definitions. In other words, when the independent variables (pressure, etc.) vary during a test firing, their means cannot be arbitrarily defined. In Ref. 19 constraints are placed upon independent variable variations during a test. If variations exceed constraints, that data is unacceptable. Although this approach eliminates non-neutral independent variable problems and yields quality performance data, it is not cost effective.

The objectives of this work are twofold. First, to derive general equations defining consistent independent variable means when motor operation is in the quasi-steady regime and pressure and throat area are the independent variables. Second, to obtain first approximation "solutions" to these equations.

Reference 19 defines mean burning rate, mean characteristic velocity,* and delivered specific impulse as

$$\bar{r} = w/t_b \quad (46)$$

$$\bar{C}^* = g \int_{t_I}^{t_I + t_a} A_t p dt / m_p \quad (47)$$

$$I_{sp, d} = \int_{t_I}^{t_I + t_a} F dt / m_p \quad (48)$$

Eq. (47) is a generalization of the more commonly employed $\bar{C}^ = g \bar{A}_t$

$$\int_{t_I}^{t_I + t_a} p dt / m.$$

The mean independent variables are defined as*

$$\bar{p}_t = \int_{t_I}^{t_I + t_a} p \, dt / t_a \quad (49)$$

$$\bar{A}_t = \left[A_t (t_I + t_a) + A_t (0) \right] / 2 \quad (50)$$

$$\bar{\epsilon} = A_e (t_I + t_a) / \bar{A}_t \quad (51)$$

Since functionals $r(p)$, $C^*(p)$, and $I_{sp}(p, \epsilon)$ are presumed to exist, consistent means for p and ϵ require that

$$\bar{r} = r(\bar{p}_r) \quad (52a)$$

$$\bar{C}^* = C^*(\bar{p}_C) \quad (52b)$$

$$I_{sp, d} = I_{sp}(\bar{p}_I, \bar{\epsilon}_I) \quad (52c)$$

where \bar{p}_r , \bar{p}_C , and \bar{p}_I are mean pressures for burning rate, characteristic velocity, and specific impulse, respectively and $\bar{\epsilon}_I$ is the mean expansion ratio for specific impulses. Since $w = \int_0^t r(p) \, dt$, Eq. (46) can be written as

*For non-neutral pressure-time histories, Reference 19 suggests that the mass averaged pressure

$$\bar{p}_m \approx \frac{\int_{t_I}^{t_I + t_a} p^2 \, dt}{\int_{t_I}^{t_I + t_a} p \, dt}$$

replace the time averaged pressure \bar{p}_t .

$$r(\bar{p}_r) = \int_{t_I}^{t_I + t_b} r(p) dt / t_b \quad (53)$$

For quasi-steady conditions $I = \int_{t_I}^{t_I + t_a} I_{sp} dm^*$, $m = \int_{t_I}^{t_I + t_a} \dot{m} dt$, and $\dot{m} = A_t p g / C^*$.

Therefore, Eqs. (47) and (48) can be rewritten as

$$C^*(\bar{p}_C) = \int_{t_I}^{t_I + t_a} A_t p dt / \int_{t_I}^{t_I + t_a} [A_t p / C^*(p)] dt \quad (54)$$

$$I_{sp}(\bar{p}_I, \bar{\epsilon}_I) = g \int_{t_I}^{t_I + t_a} [I_{sp}(p, \epsilon) A_t p / C^*(p)] dt \quad (55)$$

Equation (55) does not specify \bar{p}_I and $\bar{\epsilon}_I$ uniquely. Therefore, it is necessary to introduce an arbitrary definition. Since specific impulse and characteristic velocity are both thermodynamic parameters, it is logical that both should possess the same mean pressure. Consequently, assume

$$\bar{p} = \bar{p}_I = \bar{p}_C \quad (56)$$

Examination of Eqs. (53 - 55) shows the following: (a) they are implicit equations; (b) the function desired must be known to determine the desired mean; (c) since r , C^* , and I_{sp} are, in general, neither proportional to p nor independent of p , $\bar{p}_r \neq \bar{p} \neq \bar{p}_m \neq \bar{p}_t$ for non-neutral pressure-time histories; and (d) when the pressure-time history is neutral, $\bar{p}_r = \bar{p} = \bar{p}_m = \bar{p}_t$. Item (b) shows that when the pressure-time history is non-neutral motor test data cannot be reduced on a single firing basis. If the dependent variable is assumed to be an M

*This shows that specific impulse is a mass averaged quantity. Consequently, it has been argued that \bar{p}_m should be employed with $I_{sp, d}^{(21)}$, e.g., $\bar{p}_I = \bar{p}_m$. Following this same argument, $\bar{p}_r = \bar{p}_t$.

parameter function of the independent variables, at least M tests are required and data for the M firings must be reduced simultaneously. Items (c) and (d) show that although the CPIA recommendations are exact for neutral pressure-time histories, they are not precisely valid for non-neutral pressure-time histories.

First approximation "solutions" to Eqs. (53 - 56) are obtained by assuming $r = ap^n$, $\bar{C}^*/\bar{C} = 1 + \alpha(p - \bar{p})$, $I_{sp}/I_{sp,d} = 1 + \beta(p - \bar{p}) + \delta(\epsilon - \bar{\epsilon})$.

Then, Eqs. (53 - 56) become*

$$\bar{p}_r = \left(\int_{t_I}^{t_I + t_b} p^n dt / t_b \right)^{1/n} \quad (57)$$

$$\bar{p} = \frac{\int_{t_I}^{t_I + t_a} A_t p^2 dt}{\int_{t_I}^{t_I + t_a} A_t p dt} \quad (58)$$

$$\bar{\epsilon} = \beta(\bar{p}_m - \bar{p})/\delta + A_e \left[\bar{p}_t (1 + \alpha \bar{p}) + \alpha \int_{t_I}^{t_I + t_a} p^2 dt \right] / \int_{t_I}^{t_I + t_a} A_t p dt \quad (59)$$

If A_t is constant, $\bar{p} = \bar{p}_m$ and $\bar{\epsilon} = A_e/A_t$. Therefore, the CPIA recommendations for non-neutral pressure-time histories are valid as first approximations.

The magnitude of the errors involved with employing \bar{p}_t for \bar{p}_r [Eq. (57)] and \bar{p} [Eq. (58)] can be readily estimated. Expanding the integrands of Eqs. (57) and (58) in a Taylor's series about $p = \bar{p}_t$ gives

$$p^n = \left[1 + n(\Delta p/\bar{p}_t) + n(n-1)(\Delta p/\bar{p}_t)^2/2! + n(n-1)(n-2)(\Delta p/\bar{p}_t)^3/ \right. \quad (60)$$

$$\left. 3! + \dots \right] \bar{p}_t^n$$

*Equation (57) has been obtained previously by Brock. (20)

When $n < 1$, this series has alternating sign. Consequently, when convergent,

$$p^n \approx [1 + n (\Delta p / \bar{p}_t) + n(n-1) (\Delta p / \bar{p}_t)^2 / 2!] \bar{p}_t^n \quad (61)$$

with error less than $[n(n-1)(n-2) (\Delta p / \bar{p}_t)^3 / 3!]$. (21) Substitution of Eq. (61) into Eq. (57), integrating, and applying the mean value theorem for integrals gives

$$\bar{p}_r \approx \bar{p}_t \left[1 + n(n-1) \left[(\Delta p / \bar{p}_t)^2 \right] / 2 \right]^{1/n} \quad (62)$$

Substitution of Eq. (61) with $n=2$ into Eq. (58), assuming A_t is constant, integrating, and applying the mean value theorem for integrals gives

$$\bar{p} = \bar{p}_t \left\{ 1 + \left[(\Delta p / \bar{p}_t)^2 \right] \right\} \quad (63)$$

Examination of Eqs. (62) and (63) shows that when $\Delta p / \bar{p}_t$ is small, \bar{p}_r and \bar{p} agree with \bar{p}_t to first order accuracy. However, when $\Delta p / \bar{p}_t$ is large, significant deviations can occur. Calculations presented by Brock⁽²⁰⁾ support this.

In summary, this work has shown that consistent reduction of motor test data when the pressure-time history is non-neutral falls outside conventional procedure. As long as deviations from neutrality are small, errors relative to established procedure are small. However, when deviations become large, significant errors can result. This work has assumed that motor operations falls in the quasi-steady regime and that pressure and throat area are the only independent variables. However, burning rate depends on flow over the burning surface and the thermodynamic parameters depend at least upon stay time and nozzle geometry. Therefore, what has been presented here is just a ripple on the surface of the basic problem of extracting all possible truth from available data.

FUTURE PLANS

Future efforts will be expended in four directions:

- modification of the BDP combustion model
- generation and implementation of propellant burning rate computer codes
- consideration of transient burning phases within the steady-state statistical framework
- application of the hydraulic analogy to determine mean flow effects on mode shape.

In the first, extension of the model to include spheriodal particles and surface tension effects will be explored. In the second, computer codes for predicting burning rates in additive free propellants will be developed. In the third, basic problems in statistical combustion modeling will be explored. Specifically, transient effects and statistical formulations with nonplanar burning surfaces will be pursued. In the latter, hydraulic analogy test sequences with real motor geometry and distributed mass addition will be employed to assess mode shape deviations wrought by mean flow effects. This will be accomplished by determining the resonant frequency and then measuring amplitude and phase along the motor length (light absorption technique). Comparison of results at no flow with acoustic approximation results "defines" analogy errors; comparison of analogy results at various port Mach numbers "indicates" mean flow errors.

PUBLICATIONS DERIVED FROM PROGRAM

1. On Reduction of Solid Rocket Data When the Pressure-Time History is Non-Neutral, accepted for publication, Journal Spacecraft and Rockets, 1975.
2. Hydraulic Analogy Study: T-Burner Vent Gain/Loss, CPIA Publication No. 261, Vol. 1, 1974, pp. 491-498.
3. Comment on "The Stability of One-Dimensional Motions in a Rocket Motor", accepted for publication, Combustion Science and Technology, 1975.

NOMENCLATURE

Latin Symbols

A_e	nozzle exit area
A_t	nozzle throat area
b	$\overline{D} + \Delta$
C	constant defined by Eq. (19)
C^*	characteristic velocity
D	diameter
F	distribution function
g	gravitational acceleration
h	water depth
I	delivered impulse
I_{sp}	specific impulse
$I_{sp, d}$	delivered specific impulse
m	mass
\dot{m}	mass flow rate
m''	mass flux
M_k	number of modes associated with k^{th} oxidizer species
n	exponent defined by Eq. (19)
p	pressure
Q	number of subdivisions
r	burning rate
s	number of oxidizer species
S	surface area

t	time
t_a	action time
t_b	burn time
t_I	time when p first becomes $0.05 \bar{p}_t$
u	velocity component in x direction
v	velocity component in y direction
V	volume
w	propellant web or velocity component in z direction
x, y, z	coordinates in inertial reference frame
y	$dm_{o,j,k} / (m_{o,j,k} dD)$
z	distance normal to S

Greek Symbols

α	mass oxidizer/mass propellant
ζ	volume oxidizer/volume propellant
δ	width of fuel annulus surrounding mean oxidizer particle
Δ	denotes a small quantity
$\eta_{d,k}$	fraction of oxidizer particles on burning surface with $D \leq D \leq D + dD$ and species k
ϵ	nozzle expansion ratio
σ^*	standard deviation of oxidizer particle size distribution
ρ	density

Special Symbols

$(\bar{\quad})$	denotes a mean
$(\quad)^*$	pertains to a monodisperse, psuedo-propellant
$(\hat{\quad})$	denotes a fluctuating term such that $(\hat{\quad}) = 0$
$(\quad)^+$	denotes a non-dimensional quantity

Subscripts

b	denotes burning surface
d	denotes oxidizer particles with $D \leq D \leq D + dD$
f	denotes fuel
g	denotes gas
j	denotes oxidizer mode j
k	denotes oxidizer species k
m	denotes weight mean in oxidizer particle size distribution
o	denotes oxidizer or stagnation condition
t	denotes time mean or propellant
p	denotes planar surface
v	denotes per unit volume
w	denotes water

REFERENCES

1. Culick, F. E. C., Derr, R. L., and Price, C. F., "Linear Analysis of One-Dimensional Oscillations in a Variable Area T-Burner", CPIA Pub. 231, Vol. I, pp. 165-196, Dec. 1972.
2. Horton, M. D. and Coates, R. L., "Some Developments in T-Burner Analysis", CPIA Pub. 243, Vol. II, pp. 83-98, Dec. 1973.
3. Schoner, R. J., Review of the Workshop on Combustion/Flow Interaction, CPIA Pub. 243, Vol. II, pp. 107-114, Dec. 1973.
4. Culick, F. E. C., Editor, T-Burner Testing of Metallized Solid Propellants, AFRPL-TR-74-28, pp. 240-258, Oct. 1974.
5. McClure, F. T., Hart, R. W., and Cantrell, R. H., "Interaction between Sound and Flow: Stability of T-Burners", AIAA Journal, 1, 3, pp. 586-590, March 1963.
6. Beckstead, M. W., Derr, R. L., and Price, C. F., "A Model of Solid Propellant Combustion Based on Multiple Flames", AIAA Journal, Vol. 8, No. 12, pp. 2200-2207, Dec. 1970.
7. Cohen, N. S., Derr, R. L., and Price, C. F., "Extended Model of Solid Propellant Combustion Based on Multiple Flames", CPIA Publication 231, Vol. II, pp. 25-42, 1972.
8. Sammons, G. D., "Solid Propellant Combustion Modeling", CPIA Pub. 243, Vol. I, pp. 149-156, Dec. 1973.
9. Glick, R. L., "Statistical Analysis of Non-Metallized Composite Solid Propellant Combustion", CPAI Pub. 243, Vol. I, pp. 157-184, Dec. 1973.
10. Glick, R. L., "On Statistical Analysis of Composite Solid Propellant Combustion", AIAA Journal, 12, 3, pp. 384-385, March 1974.
11. Dallavalle, J. M., Micromeritics, (Pitman Publishing Co., New York, 1948), pp. 123-143.
12. Beckstead, M. W., Derr, R. L., and Price, C. F., "Combustion Tailoring Criteria for Solid Propellants", AFRPL-TR-69-190, Lockheed Propulsion Co., 1969 (Confidential).
13. Sammons, G. D., "Scientific Report: Multiple Flame Combustion Model Fortran IV Computer Program", Rocketdyne Division, Rockwell International, Report R-4827, March 1974.

14. Summerfield, M., et al, "Burning Mechanism of Ammonium Perchlorate Propellants", Solid Propellant Rocket Research, Progress in Astronautics and Rocketry, Vol. I, (Academic Press, New York) pp. 141-182, 1960.
15. Culick, F. E. C., "The Stability of One Dimensional Motions in a Rocket Motor", Combustion Science and Technology, Vol. 7, No. 4, p. 165, 1973.
16. Shapiro, A. H., The Dynamics and Thermodynamics of Compressible Fluid Flow, (Ronald Press Co., New York) Vol. I, p. 234.
17. Glick, R. L., Hydraulic Analogy Study T-Burner Vent Gain/Loss, CPIA Publication No. 261, Vol. I, pp. 491-498, 1974.
18. Levine, J. N. and Culick, F. E. C., "Nonlinear Analysis of Solid Rocket Combustion Instability", AFRPL-TR-74-45, Vol. I, pp. A3-A9, Oct. 1974.
19. Recommended Procedure for the Measurement of Specific Impulse of Solid Propellants, CPAI Publication No. 174, Aug. 1968.
20. Brock, F. H., "Average Burn Rate, Average Pressure Relationships in Solid Rockets", Journal Spacecraft and Rockets, Vol. 3, No. 2, pp. 1802-1803, Dec. 1966.
21. Taylor, A. E., Advanced Calculus, (Ginn and Company, Boston, 1955), p. 563.
22. Hoyt, J. W., "The Hydraulic Analogy for Compressible Gas Flow", Applied Mechanics Reviews, Vol. 15, No. 6, pp. 419-425 (1962).
23. Loh, W. H. T., "Hydraulic Analogy for Two-Dimensional and One-Dimensional Flows", Journal of the Aero/Space Sciences, Vol. 26, No. 6, pp. 389-391 (1959).
24. Liepmann, H. W. and Roshko, A., Elements of Gas Dynamics, (John Wiley, 1957).

APPENDIX A
COMPUTER PROGRAM

COMPUTER PROGRAM DATA INPUT FORMAT

CARD 1: Control Card

NUMBER REQUIRED: One card per run

FUNCTION: Specify run options

FORMAT: (2I6)

Columns 1-6: NJOB, if NJOB = 1 read

propellant parameters, if NOB = 2 read namelist data

Columns 7-12: IPLOT, IPLOT = 2, (Plotting routine
presently deleted)

CARD 2: Title Card

NUMBER REQUIRED: One card per run

FUNCTION: Identify run out at

FORMAT: (20A4)

Columns 2-80: May be used to identify run

CARD 3: Data Card

NUMBER REQUIRED: One card per run

FUNCTION: Specify propellant parameters

FORMAT: (6E12.6)

Columns 1-12: TZERO, initial propellant temperature, deg K

Columns 13-24: ALFA, Oxidizer mass fraction

Columns 25-36: TF, adiabatic flame temperature, deg K

Columns 37-48: GMW, molecular weight of final flame

Columns 49-60: XNUI, stoichiometric ratio of the final flame

Columns 61-80: not used

CARD 4: Data Card

NUMBER REQUIRED: One card per run

FUNCTION: Specify propellant parameters

FORMAT: (6E12.6)

Columns 1-12: QFUEL, heat of pyrolysis of the fuel binder, cal/g

Columns 13-24: RHOF, density of fuel binder, g/cm^3

Columns 25-36: AF, arrhenius frequency factor of fuel binder,
 $\text{g/cm}^2\text{-sec}$

Columns 37-48: EF, activation energy of the fuel binder, cal/mole

Columns 49-60: XNUP, primary flame stoichiometric ratio

Columns 61-72: PMW, primary flame molecular weight

Columns 73-80: not used

CARD 5: Data Card

NUMBER REQUIRED: One card per run

FUNCTION: Specify propellant parameters

FORMAT: (6E12.6)

Columns 1-12: QL, latent heat of vaporization of the oxidizer, cal/g

Columns 13-24: RHOX, density of the oxidizer, g/cm^3

Columns 25-36: AOX, arrhenius frequency factor of the oxidizer
 $\text{g/cm}^2\text{-sec}$

Columns 37-48: EOX, activation energy of the oxidizer cal/mole

Columns 49-60: TAP, temperature of the AP flame, deg K

Columns 61-72: AP, AP=1 if oxidizer rate constants specified,

AP = -1 or 0 if oxidizer rate constant to be calculated by
program. If -1, mass flux of oxidizer taken as $1.9 \text{ g/cm}^2\text{-sec}$
in rate constant calculation. If 0, mass flux of oxidizer taken
as $1.66 \text{ g/cm}^2\text{-sec}$ in rate constant calculation.

Columns 73-80: not used

CARD 6: Data Card

NUMBER REQUIRED: One card per run

FUNCTION: Specify propellant parameters

FORMAT: (6E12.6)

Columns 1-12: CIGN, oxidizer ignition delay parameter, sec(atm)^m
 cm^{-n+1} where $m=\text{POWIGN}$ and $n=\text{POWD}$

Columns 13-24: POWIGN, pressure exponent in oxidizer particle
ignition particle ignition delay term

Columns 25-36: POWD, diameter exponent in oxidizer particle ignition
delay term

Columns 37-48: PSTART, pressure to start incremental calcu-
lations, atm

Columns 49-60: PSTOP, pressure to stop incremental calculations, atm

Columns 60-72: CONF, CONF=0 if parabolic flame assumed, CONF=1
if conical flame assumed

Columns 73-80: not used

CARD 7: Data Card

NUMBER REQUIRED: One card per run

FUNCTION: Specify propellant parameters

FORMAT: (6E12.6)

Columns 1-12: KPF, rate constant of primary flame, $\text{g}/\text{cm}^3\text{-sec-atm}$)

Columns 13-24: KAP1, rate constant of AP flame at low pressure,
 $\text{g}/(\text{cm}^3\text{-sec-atm})$

Columns 25-36: KAP2, rate constant of AP flame at high pressure,
 $\text{g}/\text{cm}^3\text{-sec-atm})$

Columns 37-48: XN1, reaction order of primary flame

Columns 49-60: XN2, reaction order of AP flame at low pressure

Columns 61-72: XN3, reaction order of AP flame at high pressure

Columns 72-80: not used

CARD 8: Data Card

NUMBER REQUIRED: One card per run

FUNCTION: Specify propellant parameters

FORMAT: (6E12.6)

Columns 1-12: CSUBP, average heat capacity of solids and gases,
 $\text{cal}/\text{g-}^\circ\text{K}$

Columns 13-24: XLAMB, average thermal conductivity of the combustion gases, $\text{cal}/\text{cm-sec-}^\circ\text{K}$

Columns 25-36: GAMMA, diffusion parameter, cm^2/sec

Columns 37-48: AFH, flame height factor

Columns 49-60: EPS, exponent for diffusion pressure dependence

Columns 61-72: Y, proportionality constant for short diffusion flame

Columns 72-80: not used

CARD 9: Data Card

NUMBER REQUIRED: One per run

FUNCTION: Specify propellant parameters

FORMAT: (6E12.6)

Columns 1-12: BETA, mass fraction of metal

Columns 13-24: RHOM, density of metal, g/cm^3

Columns 25-36: QM, heat release of metal combustion, cal/g

Columns 37-80: not used

CARD 10: Data Card

NUMBER REQUIRED: One per case

FUNCTION: Specify integration parameters

FORMAT: (3I5, 3F10.5)

Columns 1-5: NMODES, number of oxidizer size distribution modes

Columns 6-10: NCOUNT, number of intervals in the numerical integration of total propellant mass flux

Columns 10-15: NXCOUN, number of intervals in the numerical integration for the proportionality constant C in the equation for the volume of fuel associated with a particle in a polydisperse packing

Columns 16-25: XN, diameter exponent in the equation for the volume of fuel associated with a particle in a polydisperse packing.

Columns 26-35: DDO, oxidizer particle size increment in the numerical integration of total propellant mass flux.

Columns 36-45: XDDO, oxidizer particle size increment in the numerical integration for the proportionality constant C

CARDS 10 to 11 + NMODES: Data Card

NUMBER REQUIRED: One per oxidizer mode size, per case

FUNCTION: Specify oxidizer size distribution parameters

FORMAT: (3F10.5)

Columns 1-10: SIGMA, standard deviation of oxidizer size distribution for a particular mode

Columns 11-20: DBAR, mean oxidizer crystal size for a particular mode, microns

Columns 21-30: YI, mass fraction of oxidizer in a particular mode relative to the total mass of oxidizer.

Columns 31-80: not used

CARD 11 + NMODES: Control Card

NUMBER REQUIRED: One card per case

FUNCTION: Start next case or terminate run

FORMAT: (I4)

Columns (1-4): NSTOP, if NSTOP > 1 terminate program, if NSTOP ≤ 1 begin next case

CARD 12 + NMODES: Data Card

NUMBER REQUIRED: One card per additional case

FUNCTION: Specify propellant parameters

FORMAT: NAMELIST/NAM1/

REMARKS: Used only when more than one case is run.

CARD 13 + NMODES: Data Card

NUMBER REQUIRED: One card per additional case

FUNCTION: See Card 10

FORMAT: See Card 10

CARD 13 + NMODES_{case one} to (12 + NMODES_{case one} + NMODES_{case two}):
Data Card

NUMBER REQUIRED: One per mode in case two

FUNCTION: See Cards 11 to 10 + NMODES_{case one}

FORMAT: See Cards 11 to 10 + NMODES_{case one}

CARD 13 + NMODES_{case one} + NMODES_{case two}: Control Card

NUMBER REQUIRED: One per additional case

FUNCTION: See Card 11 + NMODES_{case one}

FORMAT: See Card 11 + NMODES_{case one}

COMPUTER PROGRAM LISTING

AND

SAMPLE CALCULATION

```

0001      IMPLICIT REAL*8 (A-H,O-Z)
0002      REAL*8 KAP1,KAP2,KPF,MOX,MT
0003      COMMON AL,
1      A2,
2      BESS,
3      CIGN,
4      EOX,
5      HDP,
6      KPF,
7      POND,
8      QFUEL,
9      QPF,
10     Q,
11     RHOX,
12     RHOSP,
13     TF,
14     TAV,
15     XLAMR,
16     XN1,
17     XN2,
18     XN3,
19     XN4,
20     XN5,
21     XN6,
22     XN7,
23     XN8,
24     XN9,
25     XN10,
26     XN11,
27     XN12,
28     XN13,
29     XN14,
30     XN15,
31     XN16,
32     XN17,
33     XN18,
34     XN19,
35     XN20,
36     XN21,
37     XN22,
38     XN23,
39     XN24,
40     XN25,
41     XN26,
42     XN27,
43     XN28,
44     XN29,
45     XN30,
46     XN31,
47     XN32,
48     XN33,
49     XN34,
50     XN35,
51     XN36,
52     XN37,
53     XN38,
54     XN39,
55     XN40,
56     XN41,
57     XN42,
58     XN43,
59     XN44,
60     XN45,
61     XN46,
62     XN47,
63     XN48,
64     XN49,
65     XN50,
66     XN51,
67     XN52,
68     XN53,
69     XN54,
70     XN55,
71     XN56,
72     XN57,
73     XN58,
74     XN59,
75     XN60,
76     XN61,
77     XN62,
78     XN63,
79     XN64,
80     XN65,
81     XN66,
82     XN67,
83     XN68,
84     XN69,
85     XN70,
86     XN71,
87     XN72,
88     XN73,
89     XN74,
90     XN75,
91     XN76,
92     XN77,
93     XN78,
94     XN79,
95     XN80,
96     XN81,
97     XN82,
98     XN83,
99     XN84,
100    XN85,
101    XN86,
102    XN87,
103    XN88,
104    XN89,
105    XN90,
106    XN91,
107    XN92,
108    XN93,
109    XN94,
110    XN95,
111    XN96,
112    XN97,
113    XN98,
114    XN99,
115    XN100,
116    XN101,
117    XN102,
118    XN103,
119    XN104,
120    XN105,
121    XN106,
122    XN107,
123    XN108,
124    XN109,
125    XN110,
126    XN111,
127    XN112,
128    XN113,
129    XN114,
130    XN115,
131    XN116,
132    XN117,
133    XN118,
134    XN119,
135    XN120,
136    XN121,
137    XN122,
138    XN123,
139    XN124,
140    XN125,
141    XN126,
142    XN127,
143    XN128,
144    XN129,
145    XN130,
146    XN131,
147    XN132,
148    XN133,
149    XN134,
150    XN135,
151    XN136,
152    XN137,
153    XN138,
154    XN139,
155    XN140,
156    XN141,
157    XN142,
158    XN143,
159    XN144,
160    XN145,
161    XN146,
162    XN147,
163    XN148,
164    XN149,
165    XN150,
166    XN151,
167    XN152,
168    XN153,
169    XN154,
170    XN155,
171    XN156,
172    XN157,
173    XN158,
174    XN159,
175    XN160,
176    XN161,
177    XN162,
178    XN163,
179    XN164,
180    XN165,
181    XN166,
182    XN167,
183    XN168,
184    XN169,
185    XN170,
186    XN171,
187    XN172,
188    XN173,
189    XN174,
190    XN175,
191    XN176,
192    XN177,
193    XN178,
194    XN179,
195    XN180,
196    XN181,
197    XN182,
198    XN183,
199    XN184,
200    XN185,
201    XN186,
202    XN187,
203    XN188,
204    XN189,
205    XN190,
206    XN191,
207    XN192,
208    XN193,
209    XN194,
210    XN195,
211    XN196,
212    XN197,
213    XN198,
214    XN199,
215    XN200,
216    XN201,
217    XN202,
218    XN203,
219    XN204,
220    XN205,
221    XN206,
222    XN207,
223    XN208,
224    XN209,
225    XN210,
226    XN211,
227    XN212,
228    XN213,
229    XN214,
230    XN215,
231    XN216,
232    XN217,
233    XN218,
234    XN219,
235    XN220,
236    XN221,
237    XN222,
238    XN223,
239    XN224,
240    XN225,
241    XN226,
242    XN227,
243    XN228,
244    XN229,
245    XN230,
246    XN231,
247    XN232,
248    XN233,
249    XN234,
250    XN235,
251    XN236,
252    XN237,
253    XN238,
254    XN239,
255    XN240,
256    XN241,
257    XN242,
258    XN243,
259    XN244,
260    XN245,
261    XN246,
262    XN247,
263    XN248,
264    XN249,
265    XN250,
266    XN251,
267    XN252,
268    XN253,
269    XN254,
270    XN255,
271    XN256,
272    XN257,
273    XN258,
274    XN259,
275    XN260,
276    XN261,
277    XN262,
278    XN263,
279    XN264,
280    XN265,
281    XN266,
282    XN267,
283    XN268,
284    XN269,
285    XN270,
286    XN271,
287    XN272,
288    XN273,
289    XN274,
290    XN275,
291    XN276,
292    XN277,
293    XN278,
294    XN279,
295    XN280,
296    XN281,
297    XN282,
298    XN283,
299    XN284,
300    XN285,
301    XN286,
302    XN287,
303    XN288,
304    XN289,
305    XN290,
306    XN291,
307    XN292,
308    XN293,
309    XN294,
310    XN295,
311    XN296,
312    XN297,
313    XN298,
314    XN299,
315    XN300,
316    XN301,
317    XN302,
318    XN303,
319    XN304,
320    XN305,
321    XN306,
322    XN307,
323    XN308,
324    XN309,
325    XN310,
326    XN311,
327    XN312,
328    XN313,
329    XN314,
330    XN315,
331    XN316,
332    XN317,
333    XN318,
334    XN319,
335    XN320,
336    XN321,
337    XN322,
338    XN323,
339    XN324,
340    XN325,
341    XN326,
342    XN327,
343    XN328,
344    XN329,
345    XN330,
346    XN331,
347    XN332,
348    XN333,
349    XN334,
350    XN335,
351    XN336,
352    XN337,
353    XN338,
354    XN339,
355    XN340,
356    XN341,
357    XN342,
358    XN343,
359    XN344,
360    XN345,
361    XN346,
362    XN347,
363    XN348,
364    XN349,
365    XN350,
366    XN351,
367    XN352,
368    XN353,
369    XN354,
370    XN355,
371    XN356,
372    XN357,
373    XN358,
374    XN359,
375    XN360,
376    XN361,
377    XN362,
378    XN363,
379    XN364,
380    XN365,
381    XN366,
382    XN367,
383    XN368,
384    XN369,
385    XN370,
386    XN371,
387    XN372,
388    XN373,
389    XN374,
390    XN375,
391    XN376,
392    XN377,
393    XN378,
394    XN379,
395    XN380,
396    XN381,
397    XN382,
398    XN383,
399    XN384,
400    XN385,
401    XN386,
402    XN387,
403    XN388,
404    XN389,
405    XN390,
406    XN391,
407    XN392,
408    XN393,
409    XN394,
410    XN395,
411    XN396,
412    XN397,
413    XN398,
414    XN399,
415    XN400,
416    XN401,
417    XN402,
418    XN403,
419    XN404,
420    XN405,
421    XN406,
422    XN407,
423    XN408,
424    XN409,
425    XN410,
426    XN411,
427    XN412,
428    XN413,
429    XN414,
430    XN415,
431    XN416,
432    XN417,
433    XN418,
434    XN419,
435    XN420,
436    XN421,
437    XN422,
438    XN423,
439    XN424,
440    XN425,
441    XN426,
442    XN427,
443    XN428,
444    XN429,
445    XN430,
446    XN431,
447    XN432,
448    XN433,
449    XN434,
450    XN435,
451    XN436,
452    XN437,
453    XN438,
454    XN439,
455    XN440,
456    XN441,
457    XN442,
458    XN443,
459    XN444,
460    XN445,
461    XN446,
462    XN447,
463    XN448,
464    XN449,
465    XN450,
466    XN451,
467    XN452,
468    XN453,
469    XN454,
470    XN455,
471    XN456,
472    XN457,
473    XN458,
474    XN459,
475    XN460,
476    XN461,
477    XN462,
478    XN463,
479    XN464,
480    XN465,
481    XN466,
482    XN467,
483    XN468,
484    XN469,
485    XN470,
486    XN471,
487    XN472,
488    XN473,
489    XN474,
490    XN475,
491    XN476,
492    XN477,
493    XN478,
494    XN479,
495    XN480,
496    XN481,
497    XN482,
498    XN483,
499    XN484,
500    XN485,
501    XN486,
502    XN487,
503    XN488,
504    XN489,
505    XN490,
506    XN491,
507    XN492,
508    XN493,
509    XN494,
510    XN495,
511    XN496,
512    XN497,
513    XN498,
514    XN499,
515    XN500,
516    XN501,
517    XN502,
518    XN503,
519    XN504,
520    XN505,
521    XN506,
522    XN507,
523    XN508,
524    XN509,
525    XN510,
526    XN511,
527    XN512,
528    XN513,
529    XN514,
530    XN515,
531    XN516,
532    XN517,
533    XN518,
534    XN519,
535    XN520,
536    XN521,
537    XN522,
538    XN523,
539    XN524,
540    XN525,
541    XN526,
542    XN527,
543    XN528,
544    XN529,
545    XN530,
546    XN531,
547    XN532,
548    XN533,
549    XN534,
550    XN535,
551    XN536,
552    XN537,
553    XN538,
554    XN539,
555    XN540,
556    XN541,
557    XN542,
558    XN543,
559    XN544,
560    XN545,
561    XN546,
562    XN547,
563    XN548,
564    XN549,
565    XN550,
566    XN551,
567    XN552,
568    XN553,
569    XN554,
570    XN555,
571    XN556,
572    XN557,
573    XN558,
574    XN559,
575    XN560,
576    XN561,
577    XN562,
578    XN563,
579    XN564,
580    XN565,
581    XN566,
582    XN567,
583    XN568,
584    XN569,
585    XN570,
586    XN571,
587    XN572,
588    XN573,
589    XN574,
590    XN575,
591    XN576,
592    XN577,
593    XN578,
594    XN579,
595    XN580,
596    XN581,
597    XN582,
598    XN583,
599    XN584,
600    XN585,
601    XN586,
602    XN587,
603    XN588,
604    XN589,
605    XN590,
606    XN591,
607    XN592,
608    XN593,
609    XN594,
610    XN595,
611    XN596,
612    XN597,
613    XN598,
614    XN599,
615    XN600,
616    XN601,
617    XN602,
618    XN603,
619    XN604,
620    XN605,
621    XN606,
622    XN607,
623    XN608,
624    XN609,
625    XN610,
626    XN611,
627    XN612,
628    XN613,
629    XN614,
630    XN615,
631    XN616,
632    XN617,
633    XN618,
634    XN619,
635    XN620,
636    XN621,
637    XN622,
638    XN623,
639    XN624,
640    XN625,
641    XN626,
642    XN627,
643    XN628,
644    XN629,
645    XN630,
646    XN631,
647    XN632,
648    XN633,
649    XN634,
650    XN635,
651    XN636,
652    XN637,
653    XN638,
654    XN639,
655    XN640,
656    XN641,
657    XN642,
658    XN643,
659    XN644,
660    XN645,
661    XN646,
662    XN647,
663    XN648,
664    XN649,
665    XN650,
666    XN651,
667    XN652,
668    XN653,
669    XN654,
670    XN655,
671    XN656,
672    XN657,
673    XN658,
674    XN659,
675    XN660,
676    XN661,
677    XN662,
678    XN663,
679    XN664,
680    XN665,
681    XN666,
682    XN667,
683    XN668,
684    XN669,
685    XN670,
686    XN671,
687    XN672,
688    XN673,
689    XN674,
690    XN675,
691    XN676,
692    XN677,
693    XN678,
694    XN679,
695    XN680,
696    XN681,
697    XN682,
698    XN683,
699    XN684,
700    XN685,
701    XN686,
702    XN687,
703    XN688,
704    XN689,
705    XN690,
706    XN691,
707    XN692,
708    XN693,
709    XN694,
710    XN695,
711    XN696,
712    XN697,
713    XN698,
714    XN699,
715    XN700,
716    XN701,
717    XN702,
718    XN703,
719    XN704,
720    XN705,
721    XN706,
722    XN707,
723    XN708,
724    XN709,
725    XN710,
726    XN711,
727    XN712,
728    XN713,
729    XN714,
730    XN715,
731    XN716,
732    XN717,
733    XN718,
734    XN719,
735    XN720,
736    XN721,
737    XN722,
738    XN723,
739    XN724,
740    XN725,
741    XN726,
742    XN727,
743    XN728,
744    XN729,
745    XN730,
746    XN731,
747    XN732,
748    XN733,
749    XN734,
750    XN735,
751    XN736,
752    XN737,
753    XN738,
754    XN739,
755    XN740,
756    XN741,
757    XN742,
758    XN743,
759    XN744,
760    XN745,
761    XN746,
762    XN747,
763    XN748,
764    XN749,
765    XN750,
766    XN751,
767    XN752,
768    XN753,
769    XN754,
770    XN755,
771    XN756,
772    XN757,
773    XN758,
774    XN759,
775    XN760,
776    XN761,
777    XN762,
778    XN763,
779    XN764,
780    XN765,
781    XN766,
782    XN767,
783    XN768,
784    XN769,
785    XN770,
786    XN771,
787    XN772,
788    XN773,
789    XN774,
790    XN775,
791    XN776,
792    XN777,
793    XN778,
794    XN779,
795    XN780,
796    XN781,
797    XN782,
798    XN783,
799    XN784,
800    XN785,
801    XN786,
802    XN787,
803    XN788,
804    XN789,
805    XN790,
806    XN791,
807    XN792,
808    XN793,
809    XN794,
810    XN795,
811    XN796,
812    XN797,
813    XN798,
814    XN799,
815    XN800,
816    XN801,
817    XN802,
818    XN803,
819    XN804,
820    XN805,
821    XN806,
822    XN807,
823    XN808,
824    XN809,
825    XN810,
826    XN811,
827    XN812,
828    XN813,
829    XN814,
830    XN815,
831    XN816,
832    XN817,
833    XN818,
834    XN819,
835    XN820,
836    XN821,
837    XN822,
838    XN823,
839    XN824,
840    XN825,
841    XN826,
842    XN827,
843    XN828,
844    XN829,
845    XN830,
846    XN831,
847    XN832,
848    XN833,
849    XN834,
850    XN835,
851    XN836,
852    XN837,
853    XN838,
854    XN839,
855    XN840,
856    XN841,
857    XN842,
858    XN843,
859    XN844,
860    XN845,
861    XN846,
862    XN847,
863    XN848,
864    XN849,
865    XN850,
866    XN851,
867    XN852,
868    XN853,
869    XN854,
870    XN855,
871    XN856,
872    XN857,
873    XN858,
874    XN859,
875    XN860,
876    XN861,
877    XN862,
878    XN863,
879    XN864,
880    XN865,
881    XN866,
882    XN867,
883    XN868,
884    XN869,
885    XN870,
886    XN871,
887    XN872,
888    XN873,
889    XN874,
890    XN875,
891    XN876,
892    XN877,
893    XN878,
894    XN879,
895    XN880,
896    XN881,
897    XN882,
898    XN883,
899    XN884,
900    XN885,
901    XN886,
902    XN887,
903    XN888,
904    XN889,
905    XN890,
906    XN891,
907    XN892,
908    XN893,
909    XN894,
910    XN895,
911    XN896,
912    XN897,
913    XN898,
914    XN899,
915    XN900,
916    XN901,
917    XN902,
918    XN903,
919    XN904,
920    XN905,
921    XN906,
922    XN907,
923    XN908,
924    XN909,
925    XN910,
926    XN911,
927    XN912,
928    XN913,
929    XN914,
930    XN915,
931    XN916,
932    XN917,
933    XN918,
934    XN919,
935    XN920,
936    XN921,
937    XN922,
938    XN923,
939    XN924,
940    XN925,
941    XN926,
942    XN927,
943    XN928,
944    XN929,
945    XN930,
946    XN931,
947    XN932,
948    XN933,
949    XN934,
950    XN935,
951    XN936,
952    XN937,
953    XN938,
954    XN939,
955    XN940,
956    XN941,
957    XN942,
958    XN943,
959    XN944,
960    XN945,
961    XN946,
962    XN947,
963    XN948,
964    XN949,
965    XN950,
966    XN951,
967    XN952,
968    XN953,
969    XN954,
970    XN955,
971    XN956,
972    XN957,
973    XN958,
974    XN959,
975    XN960,
976    XN961,
977    XN962,
978    XN963,
979    XN964,
980    XN965,
981    XN966,
982    XN967,
983    XN968,
984    XN969,
985    XN970,
986    XN971,
987    XN972,
988    XN973,
989    XN974,
990    XN975,
991    XN976,
992    XN977,
993    XN978,
994    XN979,
995    XN980,
996    XN981,
997    XN982,
998    XN983,
999    XN984,
1000   XN985,
1001   XN986,
1002   XN987,
1003   XN988,
1004   XN989,
1005   XN990,
1006   XN991,
1007   XN992,
1008   XN993,
1009   XN994,
1010   XN995,
1011   XN996,
1012   XN997,
1013   XN998,
1014   XN999,
1015   XN1000,
1016   XN1001,
1017   XN1002,
1018   XN1003,
1019   XN1004,
1020   XN1005,
1021   XN1006,
1022   XN1007,
1023   XN1008,
1024   XN1009,
1025   XN1010,
1026   XN1011,
1027   XN1012,
1028   XN1013,
1029   XN1014,
1030   XN1015,
1031   XN1016,
1032   XN1017,
1033   XN1018,
1034   XN1019,
1035   XN1020,
1036   XN1021,
1037   XN1022,
1038   XN1023,
1039   XN1024,
1040   XN1025,
1041   XN1026,
1042   XN1027,
1043   XN1028,
1044   XN1029,
1045   XN1030,
1046   XN1031,
1047   XN1032,
1048   XN1033,
1049   XN1034,
1050   XN1035,
1051   XN1036,
1052   XN1037,
1053   XN1038,
1054   XN1039,
1055   XN1040,
1056   XN1041,
1057   XN1042,
1058   XN1043,
1059   XN1044,
1060   XN1045,
1061   XN1046,
1062   XN1047,
1063   XN1048,
1064   XN1049,
1065   XN1050,
1066   XN1051,
1067   XN1052,
1068   XN1053,
1069   XN1054,
1070   XN1055,
1071   XN1056,
1072   XN1057,
1073   XN1058,
1074   XN1059,
1075   XN1060,
1076   XN1061,
1077   XN1062,
1078   XN1063,
1079   XN1064,
1080   XN1065,
1081   XN1066,
1082   XN1067,
1083   XN1068,
1084   XN1069,
1085   XN1070,
1086   XN1071,
1087   XN1072,
1088   XN1073,
1089   XN1074,
1090   XN1075,
1091   XN1076,
1092   XN1077,
1093   XN1078,
1094   XN1079,
1095   XN1080,
1096   XN1081,
1097   XN1082,
1098   XN1083,
1099   XN1084,
1100   XN1085,
1101   XN1086,
1
```

```

FORTRAN IV C LEVEL 21          MAIN          DATE = 75197          09/58/38          *****
C          SUBROUTINE CONCAL (J)          CONCAL          *****
0001      IMPLICIT REAL*8 (A-H,O-Z)          469 0040
0002      THIS SUBROUTINE INCREMENTS THE PRESSURE          469 0041
0003      DIMENSION FAC(10)          469 0042
0004      REAL*8 KAP1, KAP2, KPF, MOX, MT          ANSI(50), 469 0004
0005      COMMON A1, AZ, AF, AFH, BSQR, DZERO, HDM, KAP2, P, 469 0045
1          1 BESS, BESS(50), BETAF, DELDI, 469 0046
2          2 CIGN, CON1, CSUBP, GAM, 469 0047
3          3 EFX, ETA, GAMMA, KAP1, 469 0050
4          4 HOP, KPF, MOX, MT, QFF, RF, 469 0051
5          5 POWIGN, QL, PSTART, R, RAP, 469 0012
6          6 COMMON QFUEL, RHOF, RHOD, RON, SDX, 469 0053
1          1 RHOSP, TF, TIT(20), TZERO, 469 0014
2          2 TAV, XN1, XN2, XN3, XNU1
3          3 COMMON XNUP, XALFA, PMW, ETAP, EPS
COMMON/DOUBLE/TS,C3P,C4P,XS1PF,XSTPD,XSTARD,XSTAP
COMMON/XINT/ IJIM, IPLOT, K, MEM1, NP1
1      IF (J) 2, 2, 15          469 0057
2      FAC(1)=1.0
0011      FAC(2)=1.77
0012      FAC(3)=3.17
0013      FAC(4)=5.62
0014      FAC(5)=10.0
0015      JJ = 0
0016      I = 1
0017      IF (JJ - 1) 16, 20, 20
0018      16 XMULT = PSTART
0019      JJ = 1
0020      I = 1
0021      IF (1-6) 50,21,21
0022      21 XMULT = XMULT*10.
0023      I = 2
0024      P = XMULT*FAC(I)
0025      I = I + 1
0026      RETURN
0027      END
0028
          469 0068
          469 0069
          469 0070
          469 0071
          469 0072
          469 0073
          469 0075
          469 0076
          469 0077
          469 0078
          469 0079
          469 0080

```

```

0001 C *****
0002 SURROUTINE STEMP
0003 IMPLICIT REAL*8 (A-H,O-Z)
0004 EXTERNAL DYN
0005 REAL*8 KAP1, KAP2, KPF, MOX, MT
COMMON A1,
1 A2, AFH, ALFAST,
2 BESS, BESI(50), BETAF, BSQR,
3 CIGN, CON1, DELDT, DZERO,
4 EOX, ETA, GAMMA, HON,
5 HDP, HOP, KAP1, KAP2,
6 KPF, P,
COMMON QFUEL, PCMIGN, PSTOP, QAP,
1 QF, R,
2 RHOSP, RHOP, RHOX, RAP,
3 TF, TIT(20), TIT1(20), TZERO,
4 XLAMB, XN1, XN2, XN3, XNUST,
5 XNU, XNUST
COMMON XJUP, KALFA, PMW, ETAP, EPS
COMMON/DOUBLE/TS-C3P-CAP,XSTPF,XSTPD,XSTARD,XSTAP
COMMON/XINT/ IJIM, IPLOI, K, MEH1, NPI
COMMON/ETAY/ Y
DIMENSION ARG1ST(20), AN(5)
ALFA = ALFAST
XNU = XNUST
XNU2 = (1.000 - ALFAST)*XNU1/ALFAST
XNUQ = (1.000 - ALFAST)*XNUP/ALFAST
RHOP = RHOSP
BSQR = (DZERO**2/6.000)*(1.000/XNU) *1.00-08
CELOI = (1.000/(DSQRT(XNU)) - 1.000)*(1.000/(DSQRT(6.000)))
CON1 = DSQRT(XNU)
ARG = 3.9300*CON1
CALL BESSEL (0.0, ARG, AN)
BESS = AN(3)
DUM1 = 3.21500*CON1*(1.000 + XNU2)*BESS/(XNU2 - (1.000 + XNU2)*CON
11**2)
0024 IF (DUM1) 40, 40, 41
0025 41 ETA = DLOG (DUM1)
0026 GO TO 42
0027 40 ETA = DLOG (-1.29300*DUM1/3.21500)
0028 42 DUM1 = -1.29300*CON1*(1.000 + XNUQ)*BESS/(XNUQ - (1.000 + XNUQ)*CO
11**2)
0029 IF (DUM1) 20, 20, 21
0030 20 ETAP = DLOG (3.21500*DUM1/(-1.29300))
0031 GO TO 22
0032 21 ETAP = DLOG (DUM1)
0033 22 QFF = CSUBP*((TF - 298.000) - ALFA*(TAP - 298.000) + (1.000 - ALFA
1)/(CSUBP*QFUEL)/ALFA
QPF = CSUBP*((TF - 298.000) + ALFA*(QL/CSUBP + (1.000 - ALFA) *
1 QFUEL/CSUBP)
QAP = CSUBP*(TAP - 298.000) + QL
ETA = Y/ETA
ETAP = Y/ETAP
CON2 = GAMMA*TAV**0.7500/62.0600*GMW
C3 = 2.000*CON2*ETA*AFH
C4 = (7.6600*CON2)**2/BSQR
32 MNC = XN2
RATC = KAP1
MT = RHOP*R
XNT = 0.0000
469 0081 *****
469 0082
469 0085 ANS(150), 469 0004
469 0086 DZERO, 469 0085
469 0087 HON, 469 0086
469 0088 KAP2, 469 0087
469 0089 P, 469 0090
469 0090 QF, 469 0091
469 0091 R, 469 0092
469 0092 RAP, 469 0093
469 0093 TAP, 469 0094
469 0094 XNU1 469 0014
469 0097
469 0185
469 0186
469 0101
469 0102
469 0103
469 0104

```

```

C
0001 *****
0002 SUPROUTINE INPUT (M1)
0003 IMPLICIT REAL*8 (A-H,O-Z)
0004 REAL*8 KAP1, KAP2, KPF, MOX, MT
0005 COMMON AL,
1 A2, AF, AFH, ALFAST,
2 BESS(50), BETAF, BSQR,
3 CIGN, CON1, CSUSP, DELOI,
4 EOX, ETA, GAMMA, KAP1,
5 HDP, KPF, MOX, MT,
6 POMIGN, PSTART, QFF,
COMMON QFUEL, QL, QPF, R,
1 RHCF, RHGX, RCHSP, RCHX, RCN, SOX,
2 TAV, TF, TIT(20), TZERO,
3 XLAMB, XN1, XN2, XN3, XNU1
COMMON XNUP, XALFA, PMH, ETAP, EPS
COMMON /PBC/ CONF
COMMON /RMN/ BETA, RHOM, QM
COMMON/DNURLE/TS,C3P,C4P,XSTPF,XSTPD,XSTARD,XSTAP
COMMON/XINT/ IJIN, IPLOT, K, MEM1, NP1
COMMON/ETAY/ Y
DIMENSION AN(4)
NAMELIST /NAME1/ IPLOT, NJOB, ITIT, TZERO, ALFA, TF, GMW, XNU1,
1 DZERO, QFUEL, RHOF, AF, EF, XNUP, PMH, QL, RHGX, AOX, EOX, TAP,
1 AP, CIGN, POMIGN, POWD, PSTART, PSTOP, CONF, KPF, KAP1, KAP2, QM
1 XN1, XN2, XN3, CSURP, XLAMB, GAMMA, AFH, EPS, Y, BETA, RHOM, QM
DATA NJOB/1/
GO TO (1, 2), NJOB
1 READ (5,800) NJOB, IPLOT
READ (5,801) (TIT(I), I=1,8)
READ (5,802) TZERO, XALFA, TF, GMW, XNU1, XDZERO
READ (5,802) QFUEL, RHCF, AF, EF, XNUP, PMH
READ (5,802) QL, RHGX, AOX, EOX, TAP, AP
READ (5,802) CIGN, POMIGN, POWD, PSTART, PSTOP, CONF
READ (5,802) KPF, KAP1, KAP2, XN1, XN2, XN3
READ (5,802) CSURP, XLAMB, GAMMA, AFH, EPS, Y
READ (5,802) BETA, RHOM, QM
NJOB = 2
GO TO 10
2 READ (5,NAME1)
IF (NJOB - 2) 3, 3, 11
3 CONTINUE
4 CONTINUE
10 CONTINUE
11 CONTINUE
ITIT = 0
IF (AP) 22, 21, 20
CALCULATE OXIDIZER RATE CONSTANT, AS NONE WAS GIVEN
22 MOX70 = 1.900
GO TO 23
21 MOX70 = 1.6800
23 TS70 = -COX/(1.98700* DLGG(MOX70/ADK))
ZS70 = DLOG ((TAP + QL/CSURP - 298.000)/(OL/CSURP - 298.000 +
1 TS70))
KAP1 = CSURP/XLAMB*MOX70**2/(70.000**XN2*ZS70)
KAP2 = KAP1
V = (TAP + TF)/2.000
20 RETURN
201 FORMAT (30H AP CENTERED PRIMARY FLAME
202 FORMAT (30H AP CENTERED FINAL FLAME
800 FORMAT (2I2)
801 FORMAT (A10)
802 FORMAT (6E12.6)
END
0006
0007
0008
0009
0010
0011
0012
0013
0014
0015
0016
0017
0018
0019
0020
0021
0022
0023
0024
0025
0026
0027
0028
0029
0030
0031
0032
0033
0034
0035
0036
0037
0038
0039
0040
0041
0042
0043
0044
0045
0046
0047
0048
0049
0050
*****
469 0133
469 0004
469 0136
469 0137
469 0138
469 0141
469 0142
469 0012
469 0144
469 0014
469 0148
469 0149
469 0151
469 0152
469 0153
469 0154
469 0155
469 0156
469 0157
469 0158
469 0159
469 0161
469 0162
469 0163
469 0164
469 0165
469 0166
469 0167
469 0168
469 0169
469 0170
469 0179
469 0204
469 0205
469 0207
469 0208
469 0212
469 0213
469 0216
469 0217
469 0218
469 0219
469 0220
469 0221
469 0222

```

09/58/38

DATE = 15197

STMP

FORTRAN IV G LEVEL 21

```

0045      C 51      BEGINNING OF COMPETING FLAME CALCULATION
0046      17 = 0
0047      18 = 0
0048      ARGST(1) = TS
0049      ARGST(3) = C3
0050      ARGST(4) = C4
0051      ARGST(5) = RATC
0052      ARGST(6) = XNC
0053      CONVERGENCE CALCULATION ON TS FOLLOWS
0054      XTS = TS - 808(DON, ARGST)
0055      IF (DABS (1.000 - XTS/TS) - .00100) 60, 60, 61
0056      61 IF (TS - XTS) 86, 85, 85
0057      85 17 = 1
0058      IF (XTS.LT.500.000) XTS = 500.000
0059      XLOW = XTS
0060      GO TO 87
0061      86 18 = 1
0062      IF (XTS-GE.1400.) XUP = 1400.000
0063      IF (XTS.LT.1400.) XUP = XTS
0064      IF (17 + 18 - 2) 88, 89, 89
0065      88 ARGST(1) = XTS
0066      GO TO 80
0067      89 ANS = 0.000
0068      TS HAS BOUNCED -- GO TO BRUTE FORCE
0069      N = 15
0070      XTS = 2(DON, ARGST, XUP, XLOW, ANS, N)
0071      CONTINUE
0072      R = MT/RHOP
0073      RETURN
0074      END

```

```

0001      C ***** FINRAT
0002      SUBROUTINE FINRAT (XMT,D,FZERO,DOO,XXMU,NCOUNT)
0003      IMPLICIT REAL*8 (A-H,O-Z)
0004      COMMON/XRAT/ RHOP,8R
0005      DIMENSION XMT(100), FZERO(100), XXMU(100), D(100)
0006      A = 0.000
0007      LL = 1
0008      2 XL1 = XMT(LL)*XXMU(LL)*FZERO(LL)/D(LL)
0009      XL2 = XMT(LL+1)*XXMU(LL+1)*FZERO(LL+1)/D(LL+1)
0010      IF (D(LL+1).LT.5.000) GO TO 10
0011      IF (D(LL+1).LT.30.000) GO TO 11
0012      IF (D(LL+1).LT.60.000) GO TO 12
0013      IF (D(LL+1).LT.120.000) GO TO 13
0014      IF (D(LL+1).LT.240.000) GO TO 14
0015      GO TO 15
0016      10 DOO = .500
0017      GO TO 3
0018      11 DOO = 1.000
0019      GO TO 3
0020      12 DOO = 5.000
0021      GO TO 3
0022      13 DOO = 10.000
0023      GO TO 3
0024      14 DOO = 20.000
0025      GO TO 3
0026      15 DOO = 40.000
0027      3 APART = (XL1 + XL2)*DOO/2.000
0028      LL = LL + 1
0029      A = A + APART
0030      IF (LL - NCOUNT) 2, 4, 4
0031      4 RR = A/RHOP
0032      RETURN
0033      END

```

```

0001 *****
0002 DOUBLE PRECISION FUNCTION DON (ARGLST)
0003 IMPLICIT REAL*8 (A-H,O-Z)
0004 CALCULATE TS FOR COMPETING FLAMES
      REAL*8 KAP1, KAP2, KPF, MOX, MT
      COMMON A1, A2, AF, AFH, ALFAST,
1      BESS, BESS1(50), BETAF, BSQR,
2      CIGN, CON1, CSUBP, DELDI,
3      EDX, ETA, GAMMA, GNV,
4      HDP, KPF, MOX, MT,
5      KPF, PCWIGN, PSTART, QAP,
6      COMMON OFUEL, QL, RAP,
1      RHOF, RHOSP, RHOX, RON,
2      TAV, TF, TIT(20), TIT1(20), TZERO,
3      XLAMP, XN1, XN2, XN3, XNUST,
      COMMON XNUP, XALFA, PMW, ETAP, EPS
      COMMON /PBC/ CONF
      COMMON /RWV/ BETA, RHOM, QM
      COMMON/DOUBLE/TS,C3P,C4P,XSTPF,XSTPD,XSTARD,XSTAP
      COMMON/XINT/IJIM, IPLOT, K, MEM1, NP1
      DIMENSION ARGLST(20)
      IF (ARGLST(1).GT.0.230D40) GO TO 99
      TS = ARGLST(1)
      C3 = ARGLST(3)
      C4 = ARGLST(4)
      RATC = ARGLST(5)
      XNC = ARGLST(6)
      WDCP = RHOSP
      ALFA = ALFAST
      XNU = XNUST
80      C2P = GAMMA*TS**0.75D0/82.06D0*PMW
      C3P = 2.00D0*C2P*ETAP*AFH
      C4P = (7.66D0*C2P)**2/RSQR
      MOX = AOX*DEXP(-EOX/(1.987D0*TS))
      CALL SOXCAL (TS, SOX)
      MT = MOX*SOX/ALFA
      XSTPF = MT/(KPF*P**XN1)
      DUM2=1.0D0 + C4P/(MOX**2)
      IF (DUM2 - 1.01D0) 121, 121, 122
121      DUM3 = 0.50D0*C4P/(MOX**2)
      GO TO 124
122      DUM3 = DSQRT (DUM2) - 1.0D0
124      XSTPD = C3P/(MOX*DUM3)
      IF(XSTPD-LT.0.00D) XSTPD = 1.0D0
      XSTAP = MOX/(RATC*P**XNC)
      IF (XSTAP - XSTPF - XSTPD/AFH) 51, 51, 52
52      BETAF = 1.0D0
      GO TO 55
51      BETAF = AFH*(XSTAP - XSTPF)/XSTPD
      IF (CONF) 54, 54, 53
53      BETAF = 2.00D0*BETAF - BETAF**2
      COMMON (CONICAL) FLAME
54      IJIM = 2
56      IF (BETAF) 56, 55, 55
55      BETAF = 0.0D0
      CONTINUE
      DUM2 = 1.0D0 + C4/(MOX**2)

```


09/58/38

DATE = 75197

FORTAN IV G LEVEL 21

DON

```

0047 IF (DUM2 - 1.0100) 10, 10, 11
0048 11 DUM3 = DSQRT (DUM2) - 1.000
0049 GO TO 91
0050 10 DUM3 = 0.500+C4/(MOX**2)
0051 91 XSTARD = C3/(MOX*DUM3)
0052 IF (XSTARD-LT.0.000) XSTARN = 1.000
0053 DUM2 = 1.000 + C4P/(MOX**2)
0054 IF (DUM2 - 1.0100) 12, 12, 13
0055 13 DUM3 = DSQRT(DUM2) - 1.000
0056 GO TO 92
0057 12 DUM3 = 0.500+C4P/(MOX**2)
0058 92 XSTPD = C3P/(MOX*DUM3)
0059 IF (XSTPD-LT.0.000) XSTPD = 1.000
0060 93 XSTAP = MOX/(RATC*P**XNC)
0061 94 XSTPF = MT/(KPF*P**XN1)
0062 95 ZAP = CSURP*MOX*XSTAP/XLAMB
0063 96 ZAT = ZAP + CSURP*MCX*XSTARD/XLAMB
0064 IF (BETAF - 1.000) 97, 90, 90
0065 90 ZPF = CSURP*MT/XLAMB*(XSTPF + XSTPD)
0066 GO TO 98
0067 97 ZPF = CSURP*MT/XLAMB*(XSTAP*AFH + XSTPF)
0068 98 IF (ZPF-LT.-164.000) ZPF = -164.000
0069 IF (ZAP-LT.-164.000) ZAP = -164.000
0070 IF (ZAT-LT.-164.000) ZAT = -164.000
0071 IF (ZPF-GT.164.000) ZPF = 164.000
0072 IF (ZAP-GT.164.000) ZAP = 164.000
0073 IF (ZAT-GT.164.000) ZAT = 164.000
0074 XTS = ZERO - ALFA*QL/CSURP - (1.000 - ALFA - BETAF)*QFUEL/CSURP
1 - BETAF*OM/CSURP + (1.000 - BETAF)*(ALFA*QAP/CSURP*DEXP(-ZAP) +
2 QFF/CSURP*DEXP(-ZAT)*ALFA) + BETAF*QPF/CSURP*DEXP(-ZPF)
C
0075 XTS = AMAX1 (XTS, 500.)
0076 IF ( XTS.LF.500.000) XTS = 500.000
0077 DON = ARGLS1(1) - XTS
0078 GO TO 100
0079 99 DON = ARGLS1(1)
0080 100 RETURN
END

```



```

FORTRAN IV G LEVEL 21          OUTPUT          DATE = 75197          09/58/38          469 0002

0049      101      FORMAT (1H1.8A10/)
0050      102      FORMAT (8X,4HPRES,5X,4HPRES,7X,2HBR,9X,2HBR)
0051      103      FORMAT (5X,FT-2,2X,F7.1,2I2X,F9.4)
0052      104      FORMAT (8X,4HATMS,5X,4HPSIA,5X,6HCM/SEC,5X,6HIN/SEC/)
0053      106      FORMAT (19H PROPELLANT DATA IS)
0054      107      FORMAT (6X,20HWT, PERCENT OXID. = ,F6.1)
0055      108      FORMAT (6X,16HPROP. DENSITY = ,F5.2)
0056      109      FORMAT (6X,8HQFUEL = ,F6.1,5X,12HTF(DEC K) = ,F6.0,5X,9HMOL WT = ,F6.2)
0057      110      FORMAT (6X,13HPRI MOL WT = ,F6.2)
0058      111      FORMAT (6X,13HDIFF PARAM = ,F11.4,3X,9HST RAT = ,F6.2,3X,13HPRI ST
0059      112      FORMAT (38H OXIDIZER IGNITION AND BURNING DATA IS)
0060      113      FORMAT (6X,7HICIGN = ,F6.1,6X,9HPONIGN = ,F6.3,6X,7HPDWD = ,F6.1,
0061      114      FORMAT (6X,5HEF = ,F8.0,6X,7HE OX = ,F8.0,6X,5HAF = ,E10.3,6X,
0062      115      FORMAT (6X,11HORDER, PF = ,F6.3,3X,12HRT CON, PF = ,E10.3,3X,
0063      116      FORMAT (6X,11HORDER, LP = ,F6.3,3X,12HRT CON, LP = ,E10.3/
0064      117      FORMAT (6X,17HMOXID. FLM TEMP = ,F7.1,9X,14HGAS CONDUCT = ,F8.5,
0065      118      FORMAT (6X,17HAV FLM HT FACT = ,F7.4/)
0066      119      FORMAT (27H PROPELLANT INITIAL TEMP IS, F6.1, 15H DEG CENTIGRADE//)
0067      120      FORMAT (75X,12HCASE NUMBER ,F3.0)
0068      121      FORMAT (47H EXPONENT FOR DIFFUSION PRESSURE DEPENDENCE IS ,F6.3/)
0069      122      FORMAT (130H CONICAL FLAME ASSUMED
0070      123      FORMAT (1H1.30H PARABOLIC FLAME ASSUMED
0071      124      END

C
*****      SOXCAL
SUBROUTINE SOXCAL (TS1, SOX1)
IMPLICIT REAL*8 (A-H,O-Z)
PEAL=9 KAP1, KAP2, KPF, MOX, MT
COMMON A1,
1      A2,
2      BESS,
3      CIGN,
4      EOX,
5      KPF,
6      POWD,
COMMON QFUEL,
1      RHOF,
2      TAV,
3      XLAM,
COMMON XNUP, XALFA, PMW, ETAP, EPS
COMMON DOUBLE/TS,C3P,C4P,XSTPF,XSTPD,XSTARD,XSTAP
COMMON/XINT/ IJIM, IPLOT, K, MEM1, NP1
ALFA = ALFAST
RHOF = RHOSP
XNU = XNUST
RF = AF*EXPI-EF/(1.98700*TS1)/RHOF
RAP = MDX/RHDX
RON = RAP*CIGN*(DZERG*.00100)**POWD/(P**POWIGN)
HDP = A1*(1.000 - RAP/RF) + RON
HON = A2*(1.000 - RAP/RF) + RON
IF (HDP-GE-0.788500) HDP = 0.788500
IF (HON-LE-0.211500) HDP = -0.211500
IF (HON-GE-0.211500) HON = 0.211500
IF (HON-LE-0.788500) HON = 0.788500
SOX1 = 3.000*XNU*(HDP**2 + HON**2)
1      XNU*(HDP**2 + HON**2)
RETURN
END

0001      0001      *****
0002      0002      SUBROUTINE SOXCAL (TS1, SOX1)
0003      0003      IMPLICIT REAL*8 (A-H,O-Z)
0004      0004      PEAL=9 KAP1, KAP2, KPF, MOX, MT
0005
0006
0007
0008
0009
0010
0011
0012
0013
0014
0015
0016
0017
0018
0019
0020
0021
0022
0023

```


FORTRAN IV G LEVEL	21	CONVR2	DATE = 75197	09/50/38	PAGE 0002
0034	1	XINC=XINC*0.500		469 0522	
0035		TOP=BOT+XINC		469 0523	
0036		IVAL=IVAL-1		469 0524	
0037		IF (IVAL) 12,12,11		469 0525	
0038	12	CONVR2=TOP		469 0526	
0039		GO TO 99		469 0527	
0040	11	ARGLST(1)=TOP		469 0528	
0041		ATOP=XNAME(ARGLST)		469 0529	
0042		GO TO 50		469 0530	
	C			469 0531	
	C	IN THE NEXT INTERVAL , MOVE AND HALVE		469 0532	
	C			469 0533	
0043	2	XINC=XINC*0.500		469 0534	
0044		BOT=TOP		469 0535	
0045		TOP=BOT+XINC		469 0536	
0046		ABOT=ATOP		469 0537	
0047		IVAL=IVAL-1		469 0538	
0048		IF (IVAL) 22,22,21		469 0539	
0049	22	CONVR2=TOP		469 0540	
0050		GO TO 99		469 0541	
0051	21	ARGLST(1)=TOP		469 0542	
0052		ATOP=XNAME(ARGLST)		469 0543	
0053		GO TO 50		469 0544	
	C			469 0546	
	C	ONE OF THE END POINTS IS EXACT		469 0547	
	C			469 0548	
0054	40	IF (ATOP-ANS) 42,41,42		469 0549	
0055	41	CONVR2=TOP		469 0550	
0056		GO TO 99		469 0551	
0057	42	CONVR2=BOT		469 0552	
0058	99	CONTINUE		469 0553	
0059		ARGLST(1) = CONVR2		469 0554	
0060		ADUM = XNAME (ARGLST)		469 0555	
0061		RETURN		469 0556	
0062		END		469 0557	

[illegible]

```

0001 C *****
0002 SUBROUTINE INPUT1(JJ,M,D,FZERO,XNU,NCCOUNT,ODOO)
0003 IMPLICIT REAL*8 (A-H,O-Z)
0004 REAL*8 KAP1,KAP2,KPF,MOX,MT
      COMMON AL, A2, AF, AFH, ALFAST, ANSI(50),
      1 ADX, BESS, CON1, CSUBP, DELDI, DZERO,
      2 FF, HOP, KAP1, KAP2, KPF, MOX, MT,
      3 KPF, POMIGN, PSTART, PSTOP, QAP, QFF,
      4 COMMON QFUEL, QL, QPF, P, RAP, QF,
      5 RHOF, RHOSP, RHOF, RHOF, RHOF, RHOF,
      6 TAV, TF, TIT(20), TIT(20), TZERO,
      7 XLAMP, XN1, XN2, XN3, XNU1
      COMMON XNUP, XALFA, PMW, ETAP, EPS
      COMMON/XPUT/NXCCUN
      COMMON/XRAT/ RHOP,RR
      DIMENSION YI(10), FZERO(100), D(100), XFZERO(1000), XO(1000), DBAR
      1 IFM = 1, 1, 1, 15
      2 READ(5,100) NMODES, NCCOUNT,NXCCUN,XN,ODO,XDDO
      3 DI = 1.000
      4 FSUM = 0.000
      5 JJ = 1
      6 DO 10 II=1,NMODES
      7 READ(5,101) SIGMAI(II), DBAR(II), YI(II)
      8 CONTINUE
      9 DO 12 III=1,NXCCUN
      10 DO 11 JJJ=1,NMODES
      11 CALL DISTF(DI, JJJ, ITT, YVECR, DBART, SIGMAI)
      12 XFSUM = YI(JJJ)/YVECR
      13 FSUM = FSUM + XFSUM
      14 XFZERO(III) = FSUM
      15 XO(III) = DI
      16 DI = DI + XDDO
      17 FSUM = 0.000
      18 CONTINUE
      19 CONTINUE
      20 XNU = 1.000/(1.000 + RHOF*(1.000-XALFA)/(RHOF*XALFA))
      21 RHOF = RHOF*(1.000-XALFA)/(RHOF*XALFA)
      22 CALL CCAL (XFZERO,XO,XN,XNU,C,XDDO)
      23 CONTINUE
      24 RE-COUNT D AND FZERO
      25 DI = 0.500
      26 DO 22 IZZ=1,NCCOUNT
      27 FSUM = 0.000
      28 DO 21 JZZ=1,NMODES
      29 CALL DISTF(DI,JZZ,IZZ,YVECR,DBART,SIGMAI)
      30 XFSUM = YI(JZZ)/YVECR
      31 FSUM = FSUM + XFSUM
      32 CONTINUE
      33 FZERO(IZZ) = FSUM
      34 C(IZZ) = DI
      35 IF(ODI-LT-5.000) GO TO 31
      36 IF(ODI-LT-30.000) GO TO 32
      37 IF(ODI-LT-60.000) GO TO 33
      38
0005
0006
0007
0008
0009
0010
0011
0012
0013
0014
0015
0016
0017
0018
0019
0020
0021
0022
0023
0024
0025
0026
0027
0028
0029
0030
0031
0032
0033
0034
0035
0036
0037
0038
0039
0040
0041
0042
0043
0044
0045
0046

```

```

FORTRAN IV G LEVEL 21 INPUTI DATE = 5197
0047 IF(D1.LT.,120.000) GO TO 34
0048 IF(D1.LT.,240.000) GO TC 35
0049 GO TO 36
0050 CI = D1 + .500
0051 GO TO 22
0052 DI = D1 + 1.000
0053 GO TO 22
0054 CI = D1 + 5.000
0055 GO TO 22
0056 CI = D1 + 10.000
0057 GO TO 22
0058 DI = D1 + 20.000
0059 GO TO 22
0060 DI = D1 + 40.000
0061 CONTINUE
0062 15
0063 DZERO = 0(JJ)
0064 XNUST = 1.000/(1.000+(6.000*C*DZERO** (XN-3.000)/(3.141592D0)
0065 ALFAST = 1.000/(1.000+(6.000*C*RHOF*DZERO** (XN-3.000)/(3.141592D0)
0066 1 *RHOF))
0067 RHOSP = RHOF*XNUST/ALFAST
0068 RETURN
0069 100 FORMAT(3F10.5)
0070 101 FORMAT(3F10.5)
END

C ***** CCAL
SUBROUTINE CCAL(XFZERO,XD,XN,XMU,C,XDDO)
IMPLICIT REAL*8 (A-H,O-Z)
COMMON/XPUT/NXCOUN
DIMENSION XFZERO(1000), XD(1000)
A = 0.000
B1 = 3.141592D0*(1.000-XMU)/(6.000*XNU)
JJ = 1
2 XL1 = XFZERO(JJ)*XD(JJ)**(XN-4.000)
XL2 = XFZERO(JJ+1)*XD(JJ+1)**(XN-4.000)
APART = (XL1 + XL2)*XDDO/2.000
JJ = JJ + 1
A = A + APART
IF (JJ - NXCOUN) 2, 4, 4
4 C = B1/A
RETURN
END

***** DISTF
SUBROUTINE DISTF(DI,JJJ,I1I,YVECR,DBARI,SIGMAI)
IMPLICIT REAL*8 (A-H,O-Z)
DIMENSION DBARI(10), SIGMAI(10)
X = NLG(I1I)
XM = DLOG(DBART(JJJ))
SIG = DLOG(SIGMAI(JJJ))
YVECR = SIG*2.506628275000*DEXP(.500*((X-XM)/SIG)**2)
RETURN
END

***** XSTOR
SUBROUTINE XSTOR (JJ,XMT,XNUST,XMU,M,T,XNMU)
IMPLICIT REAL*8 (A-H,O-Z)
REAL*8 MT
DIMENSION XMT(100), XNMU(100)
XMT(JJ) = MT
XNMU(JJ) = XNU/XNUST
JJ = JJ + 1
RETURN
END

*****
SURROUTINE XSTOR (JJ,XMT,XNUST,XMU,M,T,XNMU)
IMPLICIT REAL*8 (A-H,O-Z)
REAL*8 MT
DIMENSION XMT(100), XNMU(100)
XMT(JJ) = MT
XNMU(JJ) = XNU/XNUST
JJ = JJ + 1
RETURN
END

*****
SURROUTINE XSTOR (JJ,XMT,XNUST,XMU,M,T,XNMU)
IMPLICIT REAL*8 (A-H,O-Z)
REAL*8 MT
DIMENSION XMT(100), XNMU(100)
XMT(JJ) = MT
XNMU(JJ) = XNU/XNUST
JJ = JJ + 1
RETURN
END

```


P = 2 atm									
JJ	R, C _m /w	FZEROP	DZERO, μ	XSTPF, μ	XSTAP, μ	XSTPD, μ	XSTAPD, μ	ALFAST, α [*]	KMUST, μ [*]
1	0.0022	0.0000	0.5	0.33	2.14	10000.00	10000.00	0.1600	0.0870
2	0.0025	0.0001	1.0	0.41	2.76	10000.00	10000.00	0.2759	0.1601
3	0.2187	0.0008	1.5	36.86	280.44	5.04	6.31	0.3637	0.2223
4	0.2180	0.0032	2.0	38.37	296.27	3.05	3.57	0.4325	0.2759
5	0.2144	0.0080	2.5	39.11	305.36	2.57	2.99	0.4878	0.3227
6	0.2108	0.0156	3.0	39.65	312.34	2.37	2.77	0.5334	0.3637
7	0.2076	0.0260	3.5	40.08	318.06	2.27	2.69	0.5714	0.4001
8	0.2048	0.0389	4.0	40.46	322.98	2.21	2.66	0.6038	0.4325
9	0.2023	0.0539	4.5	40.78	327.25	2.16	2.65	0.6316	0.4616
10	0.2001	0.0704	5.0	41.06	331.18	2.12	2.66	0.6558	0.4879
11	0.1965	0.1057	6.0	41.56	337.86	2.05	2.68	0.6957	0.5334
12	0.1937	0.1413	7.0	41.98	343.44	1.94	2.70	0.7273	0.5715
13	0.1915	0.1745	8.0	42.35	348.31	1.80	2.69	0.7530	0.6039
14	0.1898	0.2039	9.0	42.71	352.78	1.60	2.65	0.7742	0.6317
15	0.1887	0.2287	10.0	43.10	357.20	1.27	2.58	0.7921	0.6558
16	0.1869	0.2487	11.0	43.22	359.35	1.42	2.47	0.8074	0.6770
17	0.1829	0.2640	12.0	42.76	356.47	2.81	2.31	0.8205	0.6957
18	0.1785	0.2751	13.0	42.15	352.25	4.51	2.09	0.8320	0.7124
19	0.1729	0.2825	14.0	41.17	344.87	7.07	1.77	0.8421	0.7274
20	0.1643	0.2865	15.0	39.45	331.10	11.50	1.02	0.8511	0.7438
21	0.1486	0.2878	16.0	35.91	302.13	21.07	2.65	0.8591	0.7530
22	0.1006	0.2867	17.0	24.48	206.61	56.90	4.09	0.8663	0.7641
23	0.0679	0.2837	18.0	16.61	140.52	10000.00	5.88	0.8727	0.7743
24	0.0673	0.2791	19.0	16.55	140.24	10000.00	8.35	0.8786	0.7836
25	0.0666	0.2732	20.0	16.46	139.67	10000.00	12.06	0.8840	0.7921
26	0.0657	0.2665	21.0	16.31	138.55	10000.00	18.29	0.8889	0.8001
27	0.0642	0.2590	22.0	16.01	136.18	10000.00	30.98	0.8934	0.8074
28	0.0608	0.2509	23.0	15.22	129.60	10000.00	70.68	0.8976	0.8142
29	0.0512	0.2425	24.0	12.86	109.65	10000.00	10000.00	0.9014	0.8206
30	0.0513	0.2339	25.0	12.91	110.18	10000.00	10000.00	0.9050	0.8265
31	0.0513	0.2252	26.0	12.96	110.67	10000.00	10000.00	0.9083	0.8321
32	0.0513	0.2164	27.0	13.04	111.12	10000.00	10000.00	0.9114	0.8373
33	0.0514	0.2077	28.0	13.08	111.54	10000.00	10000.00	0.9143	0.8422
34	0.0514	0.1992	29.0	13.11	111.93	10000.00	10000.00	0.9170	0.8468
35	0.0514	0.1907	30.0	13.25	113.85	10000.00	10000.00	0.9195	0.8511
36	0.0514	0.1521	35.0	13.36	115.02	10000.00	10000.00	0.9302	0.8696
37	0.0514	0.1201	40.0	13.45	115.95	10000.00	10000.00	0.9384	0.8840
38	0.0514	0.0946	45.0	13.51	116.69	10000.00	10000.00	0.9449	0.8956
39	0.0514	0.0746	50.0	13.56	117.31	10000.00	10000.00	0.9501	0.9050
40	0.0514	0.0593	55.0	13.61	117.83	10000.00	10000.00	0.9545	0.9129
41	0.0514	0.0477	60.0	13.67	118.64	10000.00	10000.00	0.9581	0.9196
42	0.0514	0.0344	70.0	13.73	119.26	10000.00	10000.00	0.9639	0.9303
43	0.0514	0.0340	80.0	13.77	119.75	10000.00	10000.00	0.9682	0.9384
44	0.0513	0.0484	90.0	13.80	120.14	10000.00	10000.00	0.9717	0.9449
45	0.0513	0.0798	100.0	13.82	120.46	10000.00	10000.00	0.9744	0.9501
46	0.0513	0.1283	110.0	13.88	121.15	10000.00	10000.00	0.9767	0.9545
47	0.0513	0.1915	120.0	13.91	121.46	10000.00	10000.00	0.9786	0.9581
48	0.0513	0.3402	140.0	13.94	121.91	10000.00	10000.00	0.9816	0.9639
49	0.0512	0.4770	160.0	13.97	122.43	10000.00	10000.00	0.9839	0.9682
50	0.0512	0.5651	180.0	13.99	122.71	10000.00	10000.00	0.9856	0.9717
51	0.0512	0.5932	200.0	13.94	121.91	10000.00	10000.00	0.9870	0.9744
52	0.0511	0.5697	220.0	13.94	121.91	10000.00	10000.00	0.9882	0.9767
53	0.0512	0.5120	240.0	13.97	122.21	10000.00	10000.00	0.9892	0.9786
54	0.0512	0.3596	280.0	13.98	122.43	10000.00	10000.00	0.9907	0.9816
55	0.0511	0.2235	320.0	13.93	122.43	10000.00	10000.00	0.9919	0.9839
56	0.0512	0.1289	360.0	14.01	122.71	10000.00	10000.00	0.9928	0.9856
57	0.0511	0.0710	400.0	14.00	122.71	10000.00	10000.00	0.9935	0.9871
58	0.0511	0.0381	440.0	14.00	122.71	10000.00	10000.00	0.9941	0.9882
59	0.0511	0.0201	480.0	14.03	122.97	10000.00	10000.00	0.9946	0.9892
60	0.0511	0.0105	520.0	14.03	122.97	10000.00	10000.00	0.9950	0.9900

p = 3.54 atm

JJ	$\rho, \text{ gm/cc}$	FZEROP	DZERC, μ	XSTPF, μ	XSTAP, μ	XSTDP, μ	XSTARD, μ	ALFAST, α^*	XNUST, γ^*
1	C-0022	0.0000	0.5	0.14	0.77	10000.00	10000.00	0.1600	0.0870
2	C-0025	0.0001	1.0	0.17	0.99	10000.00	10000.00	0.2759	0.1601
3	C-0166	0.0008	1.5	22.66	148.37	5.04	6.31	0.3637	0.2223
4	C-0198	0.0032	2.0	23.90	158.54	3.05	3.57	0.4325	0.2759
5	C-0155	0.0080	2.5	24.44	163.63	2.57	2.99	0.4876	0.3227
6	C-0136	0.0156	3.0	24.80	167.27	2.37	2.77	0.5334	0.3637
7	C-0060	0.0260	3.5	25.09	170.22	2.27	2.69	0.5714	0.4001
8	C-0389	0.0389	4.0	25.33	172.67	2.21	2.66	0.6038	0.4325
9	C-2983	0.0539	4.5	25.53	174.79	2.16	2.65	0.6316	0.4616
10	C-2951	0.0704	5.0	25.71	176.67	2.12	2.66	0.6558	0.4879
11	C-2899	0.1057	6.0	26.03	179.97	2.05	2.68	0.6957	0.5334
12	C-2858	0.1413	7.0	26.30	182.85	1.94	2.70	0.7273	0.5715
13	C-2828	0.1745	8.0	26.56	185.42	1.80	2.69	0.7530	0.6039
14	C-2806	0.2039	9.0	26.81	187.86	1.60	2.65	0.7742	0.6317
15	C-2795	0.2287	10.0	27.10	190.45	1.27	2.58	0.7921	0.6558
16	C-2765	0.2487	11.0	27.15	191.31	1.42	2.47	0.8074	0.6770
17	C-2682	0.2640	12.0	26.63	188.07	2.81	2.31	0.8205	0.6957
18	C-2591	0.2751	13.0	25.98	183.88	4.51	2.09	0.8320	0.7124
19	C-2472	0.2825	14.0	25.00	177.28	7.07	1.77	0.8421	0.7274
20	C-2592	0.2865	15.0	23.36	165.94	11.50	1.02	0.8511	0.7408
21	C-1970	0.2878	16.0	20.22	143.97	21.07	2.65	0.8591	0.7530
22	C-1324	0.2867	17.0	13.68	97.58	56.90	4.09	0.8663	0.7641
23	C-1087	0.2837	18.0	11.30	80.73	10000.00	5.88	0.8727	0.7743
24	C-1075	0.2791	19.0	11.23	80.33	10000.00	8.35	0.8786	0.7836
25	C-1060	0.2732	20.0	11.12	79.67	10000.00	12.06	0.8840	0.7921
26	C-1039	0.2665	21.0	10.95	78.53	10000.00	18.29	0.8889	0.8001
27	C-1004	0.2590	22.0	10.63	76.33	10000.00	30.98	0.8934	0.8074
28	C-0930	0.2509	23.0	9.88	71.02	10000.00	70.68	0.8976	0.8142
29	C-0807	0.2425	24.0	8.60	61.91	10000.00	10000.00	0.9014	0.8206
30	C-0808	0.2339	25.0	8.64	62.22	10000.00	10000.00	0.9050	0.8265
31	C-0808	0.2252	26.0	8.67	62.50	10000.00	10000.00	0.9083	0.8321
32	C-0809	0.2164	27.0	8.70	62.77	10000.00	10000.00	0.9114	0.8373
33	C-0809	0.2077	28.0	8.73	63.01	10000.00	10000.00	0.9143	0.8422
34	C-0810	0.1992	29.0	8.76	63.25	10000.00	10000.00	0.9170	0.8468
35	C-0810	0.1907	30.0	8.78	63.46	10000.00	10000.00	0.9195	0.8511
36	C-0812	0.1521	35.0	8.88	64.37	10000.00	10000.00	0.9302	0.8696
37	C-0812	0.1201	40.0	8.96	65.06	10000.00	10000.00	0.9384	0.8840
38	C-0813	0.0946	45.0	9.02	65.60	10000.00	10000.00	0.9449	0.8956
39	C-0813	0.0746	50.0	9.07	66.04	10000.00	10000.00	0.9501	0.9050
40	C-0813	0.0593	55.0	9.11	66.40	10000.00	10000.00	0.9545	0.9129
41	C-0813	0.0477	60.0	9.14	66.70	10000.00	10000.00	0.9581	0.9196
42	C-0813	0.0344	70.0	9.19	67.17	10000.00	10000.00	0.9639	0.9303
43	C-0813	0.0340	80.0	9.22	67.53	10000.00	10000.00	0.9682	0.9384
44	C-0812	0.0464	90.0	9.25	67.82	10000.00	10000.00	0.9717	0.9449
45	C-0812	0.0798	100.0	9.27	68.04	10000.00	10000.00	0.9744	0.9501
46	C-0812	0.1283	110.0	9.29	68.23	10000.00	10000.00	0.9767	0.9545
47	C-0812	0.1915	120.0	9.31	68.38	10000.00	10000.00	0.9786	0.9581
48	C-0812	0.3402	140.0	9.33	68.63	10000.00	10000.00	0.9816	0.9639
49	C-0811	0.4770	160.0	9.35	68.81	10000.00	10000.00	0.9839	0.9682
50	C-0811	0.5651	180.0	9.36	68.96	10000.00	10000.00	0.9856	0.9717
51	C-0811	0.5932	200.0	9.38	69.07	10000.00	10000.00	0.9870	0.9744
52	C-0810	0.5697	220.0	9.37	69.07	10000.00	10000.00	0.9882	0.9767
53	C-0811	0.5120	240.0	9.39	69.25	10000.00	10000.00	0.9892	0.9786
54	C-0910	0.3596	280.0	9.40	69.37	10000.00	10000.00	0.9907	0.9816
55	C-0909	0.2235	320.0	9.40	69.37	10000.00	10000.00	0.9919	0.9839
56	C-0810	0.1289	360.0	9.42	69.54	10000.00	10000.00	0.9928	0.9856
57	C-0809	0.0710	400.0	9.42	69.54	10000.00	10000.00	0.9935	0.9871
58	C-0810	0.0381	440.0	9.43	69.64	10000.00	10000.00	0.9941	0.9882
59	C-0910	0.0201	480.0	9.43	69.64	10000.00	10000.00	0.9946	0.9892
60	C-0809	0.0105	520.0	9.43	69.64	10000.00	10000.00	0.9950	0.9900

P=6.34 atm									
JJ	R, G ₁ /m	FZEROP	DZERO, μ	XSTPF, μ	XSTPD, μ	XSTARD, μ	ALFAST, α°	XMUST, γ°	
1	0.0022	0.0000	0.5	0.06	0.27	10000.00	0.1600	0.0870	
2	0.0025	0.0001	1.0	0.07	0.35	10000.00	0.2759	0.1601	
3	0.4320	0.0008	1.5	13.50	76.09	10000.00	0.3637	0.2223	
4	0.4665	0.0032	2.0	14.54	82.95	5.04	0.4325	0.2759	
5	0.4626	0.0080	2.5	14.95	85.87	3.05	0.4878	0.3227	
6	0.4563	0.0156	3.0	15.20	87.79	2.37	0.5334	0.3637	
7	0.4500	0.0260	3.5	15.39	89.27	2.27	0.5714	0.4001	
8	0.4442	0.0389	4.0	15.55	90.49	2.21	0.6038	0.4325	
9	0.4391	0.0539	4.5	15.68	91.53	2.16	0.6316	0.4616	
10	0.4345	0.0704	5.0	15.80	92.44	2.12	0.6558	0.4879	
11	0.4271	0.1057	6.0	16.00	94.03	2.05	0.6957	0.5334	
12	0.4215	0.1413	7.0	16.18	95.43	1.94	0.7273	0.5715	
13	0.4176	0.1745	8.0	16.36	96.81	1.80	0.7530	0.6039	
14	0.4152	0.2039	9.0	16.55	98.20	1.60	0.7742	0.6317	
15	0.4148	0.2287	10.0	16.78	99.79	1.27	0.7921	0.6558	
16	0.4097	0.2487	11.0	16.79	100.02	1.42	0.8074	0.6770	
17	0.3920	0.2640	12.0	16.24	96.94	2.81	0.8205	0.6957	
18	0.3727	0.2751	13.0	15.59	93.21	4.51	0.8320	0.7124	
19	0.3472	0.2825	14.0	14.65	87.73	7.07	0.8421	0.7274	
20	0.3098	0.2865	15.0	13.17	78.99	11.50	0.8511	0.7408	
21	0.2345	0.2878	16.0	10.04	60.30	21.07	0.8591	0.7530	
22	0.1931	0.2867	17.0	8.32	50.04	56.90	0.8663	0.7641	
23	0.1747	0.2837	18.0	7.57	45.58	10000.00	0.8727	0.7743	
24	0.1719	0.2791	19.0	7.49	45.14	10000.00	0.8786	0.7836	
25	0.1684	0.2732	20.0	7.37	44.47	10000.00	0.8840	0.7921	
26	0.1635	0.2665	21.0	7.19	43.41	10000.00	0.8889	0.8001	
27	0.1557	0.2590	22.0	6.87	41.54	10000.00	0.8934	0.8074	
28	0.1409	0.2509	23.0	6.25	37.79	10000.00	0.8976	0.8142	
29	0.1278	0.2425	24.0	5.69	34.42	10000.00	0.9014	0.8206	
30	0.1280	0.2339	25.0	5.71	34.60	10000.00	0.9050	0.8265	
31	0.1281	0.2252	26.0	5.73	34.77	10000.00	0.9083	0.8321	
32	0.1283	0.2164	27.0	5.76	34.92	10000.00	0.9114	0.8373	
33	0.1284	0.2077	28.0	5.78	35.07	10000.00	0.9143	0.8422	
34	0.1285	0.1992	29.0	5.80	35.21	10000.00	0.9170	0.8468	
35	0.1286	0.1907	30.0	5.81	35.33	10000.00	0.9195	0.8511	
36	0.1289	0.1521	35.0	5.89	35.86	10000.00	0.9302	0.8696	
37	0.1291	0.1201	40.0	5.94	36.27	10000.00	0.9384	0.8840	
38	0.1293	0.0946	45.0	5.99	36.58	10000.00	0.9449	0.8956	
39	0.1294	0.0746	50.0	6.02	36.84	10000.00	0.9501	0.9050	
40	0.1294	0.0593	55.0	6.05	37.05	10000.00	0.9545	0.9129	
41	0.1295	0.0477	60.0	6.07	37.22	10000.00	0.9581	0.9196	
42	0.1295	0.0344	70.0	6.11	37.50	10000.00	0.9639	0.9303	
43	0.1295	0.0340	80.0	6.13	37.71	10000.00	0.9682	0.9384	
44	0.1295	0.0484	90.0	6.15	37.87	10000.00	0.9717	0.9449	
45	0.1295	0.0798	100.0	6.17	38.00	10000.00	0.9744	0.9501	
46	0.1295	0.1283	110.0	6.18	38.11	10000.00	0.9767	0.9545	
47	0.1295	0.1915	120.0	6.19	38.20	10000.00	0.9786	0.9581	
48	0.1294	0.3402	140.0	6.21	38.34	10000.00	0.9816	0.9639	
49	0.1294	0.4770	160.0	6.22	38.45	10000.00	0.9849	0.9682	
50	0.1294	0.5651	180.0	6.23	38.53	10000.00	0.9856	0.9717	
51	0.1294	0.5932	200.0	6.24	38.60	10000.00	0.9870	0.9744	
52	0.1292	0.5697	220.0	6.24	38.60	10000.00	0.9882	0.9767	
53	0.1293	0.5120	240.0	6.25	38.70	10000.00	0.9892	0.9786	
54	0.1293	0.3596	280.0	6.26	38.77	10000.00	0.9907	0.9816	
55	0.1291	0.2235	320.0	6.26	38.77	10000.00	0.9916	0.9839	
56	0.1293	0.1289	360.0	6.27	38.87	10000.00	0.9928	0.9856	
57	0.1292	0.0710	400.0	6.27	38.87	10000.00	0.9935	0.9871	
58	0.1293	0.0381	440.0	6.28	38.93	10000.00	0.9941	0.9882	
59	0.1292	0.0201	480.0	6.28	38.93	10000.00	0.9946	0.9892	
60	0.1291	0.0105	520.0	6.28	38.93	10000.00	0.9950	0.9900	

p=11.24 σ_{rms}

JJ	R _j C ₀ /msec	FZEROP	DZERO, μ	XSTPF, μ	XSTAP, μ	XSTDP, μ	XSTARD, μ	ALFAST, σ^*	XNJUST, μ^*
1	0.0022	0.0000	0.5	0.02	0.10	10000.00	10000.00	0.1600	0.0870
2	0.0025	0.0001	1.0	0.03	0.12	10000.00	10000.00	0.2759	0.1601
3	0.6219	0.0008	1.5	7.87	38.39	5.04	6.31	0.3637	0.2223
4	0.6625	0.0032	2.0	8.75	43.19	3.05	3.57	0.4325	0.2759
5	0.6621	0.0080	2.5	9.06	44.97	2.57	2.99	0.4878	0.3227
6	0.6554	0.0156	3.0	9.25	46.04	2.37	2.77	0.5334	0.3637
7	0.6474	0.0260	3.5	9.38	46.81	2.27	2.69	0.5714	0.4001
8	0.6398	0.0389	4.0	9.49	47.42	2.21	2.66	0.6038	0.4325
9	0.6328	0.0539	4.5	9.57	47.93	2.16	2.65	0.6316	0.4616
10	0.6267	0.0704	5.0	9.65	48.38	2.12	2.66	0.6558	0.4879
11	0.6167	0.1057	6.0	9.79	49.17	2.05	2.68	0.6957	0.5334
12	0.6096	0.1413	7.0	9.92	49.90	1.94	2.70	0.7273	0.5715
13	0.6052	0.1745	8.0	10.05	50.63	1.80	2.69	0.7530	0.6039
14	0.6037	0.2039	9.0	10.19	51.45	1.60	2.65	0.7742	0.6317
15	0.6061	0.2287	10.0	10.39	52.51	1.27	2.58	0.7921	0.6558
16	0.5978	0.2487	11.0	10.38	52.51	1.42	2.47	0.8074	0.6770
17	0.5597	0.2640	12.0	9.82	49.76	2.81	2.31	0.8205	0.6957
18	0.5192	0.2751	13.0	9.20	46.65	4.51	2.09	0.8320	0.7124
19	0.4672	0.2825	14.0	8.35	42.38	7.07	1.77	0.8421	0.7274
20	0.3697	0.2865	15.0	6.66	33.81	11.50	1.02	0.8511	0.7408
21	0.3230	0.2878	16.0	5.86	29.77	21.07	2.65	0.8591	0.7530
22	0.2932	0.2867	17.0	5.35	27.22	56.90	4.09	0.8643	0.7641
23	0.2756	0.2837	18.0	5.06	25.75	10000.00	5.88	0.8727	0.7743
24	0.2692	0.2791	19.0	4.57	25.31	10000.00	8.35	0.8786	0.7836
25	0.2612	0.2732	20.0	4.84	24.70	10000.00	12.06	0.8840	0.7921
26	0.2503	0.2665	21.0	4.66	23.79	10000.00	18.29	0.8889	0.8001
27	0.2343	0.2590	22.0	4.38	22.38	10000.00	30.98	0.8934	0.8074
28	0.2101	0.2509	23.0	3.95	20.15	10000.00	70.68	0.8976	0.8142
29	0.1998	0.2425	24.0	3.76	19.24	10000.00	10000.00	0.9014	0.8206
30	0.2001	0.2339	25.0	3.78	19.35	10000.00	10000.00	0.9050	0.8265
31	0.2004	0.2252	26.0	3.80	19.45	10000.00	10000.00	0.9083	0.8321
32	0.2007	0.2164	27.0	3.82	19.54	10000.00	10000.00	0.9114	0.8373
33	0.2009	0.2077	28.0	3.83	19.63	10000.00	10000.00	0.9143	0.8422
34	0.2011	0.1992	29.0	3.84	19.71	10000.00	10000.00	0.9170	0.8468
35	0.2013	0.1907	30.0	3.86	19.78	10000.00	10000.00	0.9195	0.8511
36	0.2021	0.1521	35.0	3.91	20.10	10000.00	10000.00	0.9302	0.8696
37	0.2027	0.1201	40.0	3.95	20.34	10000.00	10000.00	0.9384	0.8840
38	0.2030	0.0946	45.0	3.98	20.53	10000.00	10000.00	0.9469	0.8956
39	0.2033	0.0746	50.0	4.01	20.68	10000.00	10000.00	0.9501	0.9050
40	0.2035	0.0593	55.0	4.03	20.80	10000.00	10000.00	0.9545	0.9129
41	0.2037	0.0477	60.0	4.05	20.91	10000.00	10000.00	0.9581	0.9196
42	0.2039	0.0344	70.0	4.07	21.07	10000.00	10000.00	0.9639	0.9303
43	0.2040	0.0340	80.0	4.09	21.19	10000.00	10000.00	0.9682	0.9384
44	0.2041	0.0484	90.0	4.11	21.29	10000.00	10000.00	0.9717	0.9449
45	0.2041	0.0798	100.0	4.12	21.37	10000.00	10000.00	0.9744	0.9501
46	0.2041	0.1283	110.0	4.13	21.43	10000.00	10000.00	0.9767	0.9545
47	0.2041	0.1915	120.0	4.14	21.48	10000.00	10000.00	0.9786	0.9581
48	0.2041	0.3402	140.0	4.15	21.57	10000.00	10000.00	0.9816	0.9639
49	0.2041	0.4770	160.0	4.16	21.63	10000.00	10000.00	0.9839	0.9682
50	0.2040	0.5651	180.0	4.16	21.68	10000.00	10000.00	0.9856	0.9717
51	0.2040	0.5932	200.0	4.17	21.72	10000.00	10000.00	0.9870	0.9744
52	0.2037	0.5697	220.0	4.17	21.72	10000.00	10000.00	0.9882	0.9767
53	0.2040	0.5120	240.0	4.18	21.76	10000.00	10000.00	0.9892	0.9785
54	0.2040	0.3596	280.0	4.18	21.82	10000.00	10000.00	0.9907	0.9816
55	0.2037	0.2235	320.0	4.18	21.82	10000.00	10000.00	0.9919	0.9839
56	0.2040	0.1289	360.0	4.19	21.88	10000.00	10000.00	0.9928	0.9856
57	0.2038	0.0710	400.0	4.19	21.88	10000.00	10000.00	0.9935	0.9871
58	0.2039	0.0381	440.0	4.20	21.91	10000.00	10000.00	0.9941	0.9882
59	0.2038	0.0201	480.0	4.20	21.91	10000.00	10000.00	0.9946	0.9892
60	0.2037	0.0105	520.0	4.20	21.91	10000.00	10000.00	0.9950	0.9900

JJ	R ₃ Confine	FZEROP	DZERO, μ	XSTPE, μ	XSTAP, μ	XSTPD, μ	XSTARD, μ	ALFAST, α^*	XNUST, ξ^*
1	C.0022	0.0000	0.5	0.01	0.03	10000.00	10000.00	0.1600	0.0870
2	0.0025	0.0001	1.0	0.01	0.04	10000.00	10000.00	0.2759	0.1601
3	0.7242	0.0008	1.5	3.86	16.13	5.04	6.31	0.3637	0.2223
4	C.9148	0.0032	2.0	5.09	21.81	3.05	3.57	0.4325	0.2759
5	0.9258	0.0080	2.5	5.34	22.95	2.57	2.99	0.4878	0.3227
6	0.5211	0.0156	3.0	5.48	23.57	2.37	2.77	0.5334	0.3637
7	C.9176	0.0260	3.5	5.57	23.98	2.27	2.69	0.5714	0.4001
8	0.5014	0.0389	4.0	5.64	24.29	2.21	2.66	0.6038	0.4325
9	C.8946	0.0539	4.5	5.70	24.54	2.16	2.65	0.6316	0.4616
10	C.8868	0.0704	5.0	5.75	24.76	2.12	2.66	0.6558	0.4879
11	0.8745	0.1057	6.0	5.85	25.17	2.05	2.68	0.6957	0.5334
12	C.8668	0.1413	7.0	5.94	25.56	1.94	2.70	0.7273	0.5715
13	0.8636	0.1745	8.0	6.04	25.99	1.80	2.69	0.7530	0.6039
14	0.8657	0.2039	9.0	6.16	26.50	1.60	2.65	0.7742	0.6317
15	C.8762	0.2287	10.0	6.33	27.22	1.27	2.58	0.7921	0.6558
16	0.8604	0.2487	11.0	6.29	27.07	1.42	2.47	0.8074	0.6770
17	0.7807	0.2640	12.0	5.77	24.83	2.81	2.31	0.8205	0.6957
18	C.6980	0.2751	13.0	5.21	22.41	4.51	2.09	0.8320	0.7124
19	0.5606	0.2825	14.0	4.22	16.14	7.07	1.77	0.8421	0.7274
20	0.5177	0.2865	15.0	3.93	16.89	11.50	1.02	0.8511	0.7408
21	0.4796	0.2878	16.0	3.67	15.76	21.07	2.65	0.8591	0.7530
22	0.4509	0.2867	17.0	3.47	14.92	56.90	4.09	0.8663	0.7641
23	0.4289	0.2837	18.0	3.32	14.28	10000.00	5.88	0.8727	0.7743
24	0.4147	0.2791	19.0	3.23	13.89	10000.00	8.35	0.8786	0.7836
25	0.3973	0.2732	20.0	3.10	13.37	10000.00	12.06	0.8840	0.7921
26	C.3751	0.2665	21.0	2.94	12.69	10000.00	18.29	0.8889	0.8001
27	0.3462	0.2590	22.0	2.73	11.76	10000.00	30.98	0.8934	0.8074
28	0.3154	0.2509	23.0	2.50	10.76	10000.00	70.68	0.8976	0.8142
29	0.3108	0.2425	24.0	2.47	10.64	10000.00	10000.00	0.9014	0.8206
30	0.3115	0.2339	25.0	2.48	10.71	10000.00	10000.00	0.9050	0.8265
31	0.3121	0.2252	26.0	2.49	10.77	10000.00	10000.00	0.9083	0.8321
32	0.3127	0.2164	27.0	2.51	10.83	10000.00	10000.00	0.9114	0.8373
33	0.3132	0.2077	28.0	2.52	10.88	10000.00	10000.00	0.9143	0.8422
34	0.3137	0.1992	29.0	2.53	10.93	10000.00	10000.00	0.9170	0.8468
35	C.3142	0.1907	30.0	2.54	10.97	10000.00	10000.00	0.9195	0.8511
36	0.3159	0.1521	35.0	2.58	11.16	10000.00	10000.00	0.9302	0.8696
37	0.3171	0.1201	40.0	2.61	11.30	10000.00	10000.00	0.9384	0.8840
38	0.3180	0.0946	45.0	2.63	11.41	10000.00	10000.00	0.9449	0.8956
39	0.3186	0.0746	50.0	2.65	11.50	10000.00	10000.00	0.9501	0.9050
40	0.3191	0.0593	55.0	2.66	11.58	10000.00	10000.00	0.9545	0.9129
41	0.3195	0.0477	60.0	2.67	11.64	10000.00	10000.00	0.9581	0.9196
42	0.3201	0.0344	70.0	2.69	11.74	10000.00	10000.00	0.9639	0.9303
43	C.3205	0.0340	80.0	2.71	11.81	10000.00	10000.00	0.9682	0.9384
44	0.3208	0.0484	90.0	2.72	11.87	10000.00	10000.00	0.9717	0.9449
45	C.3211	0.0798	100.0	2.73	11.91	10000.00	10000.00	0.9744	0.9501
46	C.3211	0.1283	110.0	2.74	11.95	10000.00	10000.00	0.9767	0.9545
47	0.3212	0.1915	120.0	2.74	11.98	10000.00	10000.00	0.9786	0.9581
48	C.3212	0.3402	140.0	2.75	12.03	10000.00	10000.00	0.9816	0.9639
49	0.3213	0.4770	160.0	2.76	12.07	10000.00	10000.00	0.9839	0.9682
50	0.3213	0.5651	180.0	2.76	12.10	10000.00	10000.00	0.9856	0.9717
51	0.3213	0.5932	200.0	2.77	12.12	10000.00	10000.00	0.9870	0.9744
52	0.3208	0.5697	220.0	2.77	12.12	10000.00	10000.00	0.9882	0.9767
53	0.3213	0.5120	240.0	2.77	12.16	10000.00	10000.00	0.9892	0.9786
54	0.3213	0.3596	280.0	2.78	12.18	10000.00	10000.00	0.9907	0.9816
55	0.3208	0.2235	320.0	2.78	12.18	10000.00	10000.00	0.9919	0.9839
56	0.3213	0.1289	360.0	2.78	12.22	10000.00	10000.00	0.9928	0.9856
57	C.3210	0.0710	400.0	2.78	12.22	10000.00	10000.00	0.9935	0.9871
58	0.3213	0.0381	440.0	2.79	12.24	10000.00	10000.00	0.9941	0.9882
59	C.3211	0.0201	480.0	2.79	12.24	10000.00	10000.00	0.9946	0.9892
60	0.3209	0.0105	520.0	2.79	12.24	10000.00	10000.00	0.9950	0.9900

P = 35.40 ΔT_{ref}									
JJ	R_{surface}	FIEROP	DZERO, μ	XSTPF, μ	XSTAP, μ	STPD, μ	XSTARD, μ	ALFAST, μ^*	XNUST, μ^*
1	0.0022	0.0000	0.5	0.00	0.01	10000.00	10000.00	0.1600	0.0870
2	C.0025	0.0001	1.0	0.01	0.02	10000.00	10000.00	0.2759	0.1601
3	C.8763	0.0008	1.5	0.01	7.14	5.04	6.31	0.3637	0.2223
4	1.0318	0.0032	2.0	2.49	9.14	3.05	3.57	0.4325	0.2759
5	1.1145	0.0080	2.5	2.73	10.11	2.57	2.77	0.4878	0.3227
6	1.2464	0.0156	3.0	3.15	11.76	2.37	2.69	0.5334	0.3637
7	1.2400	0.0260	3.5	3.22	11.99	2.27	2.66	0.5714	0.4001
8	1.2307	0.0389	4.0	3.26	12.16	2.21	2.65	0.6038	0.4325
9	1.2212	0.0539	4.5	3.31	12.29	2.16	2.65	0.6316	0.4616
10	1.2126	0.0704	5.0	3.34	12.40	2.12	2.66	0.6558	0.4879
11	1.1998	0.1057	6.0	3.41	12.61	2.05	2.68	0.6957	0.5334
12	1.1940	0.1413	7.0	3.47	12.84	1.94	2.70	0.7273	0.5715
13	1.1961	0.1745	8.0	3.55	13.10	1.80	2.69	0.7530	0.6039
14	1.2081	0.2039	9.0	3.65	13.45	1.60	2.65	0.7742	0.6317
15	1.2377	0.2287	10.0	3.80	13.97	1.27	2.58	0.7921	0.6558
16	1.2089	0.2487	11.0	3.75	13.80	1.42	2.47	0.8074	0.6770
17	0.9459	0.2640	12.0	2.97	10.87	2.81	2.31	0.8205	0.6957
18	0.8392	0.2751	13.0	2.66	9.73	4.51	2.09	0.8320	0.7124
19	C.7910	0.2825	14.0	2.53	9.24	7.07	1.77	0.8421	0.7274
20	0.7721	0.2865	15.0	2.49	9.09	11.50	1.02	0.8511	0.7408
21	0.7233	0.2878	16.0	2.35	8.57	21.07	2.65	0.8591	0.7530
22	C.6846	0.2867	17.0	2.24	8.16	56.90	4.09	0.8663	0.7641
23	0.6499	0.2837	18.0	2.14	7.79	10000.00	5.88	0.8727	0.7743
24	0.6200	0.2791	19.0	2.05	7.47	10000.00	8.35	0.8786	0.7836
25	C.5856	0.2732	20.0	1.94	7.09	10000.00	12.06	0.8840	0.7921
26	0.5458	0.2665	21.0	1.82	6.64	10000.00	18.29	0.8889	0.8001
27	0.5034	0.2590	22.0	1.68	6.15	10000.00	30.98	0.8934	0.8074
28	0.4766	0.2509	23.0	1.60	5.84	10000.00	70.68	0.8976	0.8142
29	0.4770	0.2425	24.0	1.61	5.87	10000.00	10000.00	0.9014	0.8206
30	0.4785	0.2339	25.0	1.62	5.91	10000.00	10000.00	0.9050	0.8265
31	0.4798	0.2252	26.0	1.63	5.95	10000.00	10000.00	0.9083	0.8321
32	0.4810	0.2164	27.0	1.64	5.98	10000.00	10000.00	0.9114	0.8373
33	C.4821	0.2077	28.0	1.64	6.01	10000.00	10000.00	0.9143	0.8422
34	0.4831	0.1992	29.0	1.65	6.04	10000.00	10000.00	0.9170	0.8468
35	0.4841	0.1907	30.0	1.66	6.07	10000.00	10000.00	0.9195	0.8511
36	0.4878	0.1521	35.0	1.69	6.18	10000.00	10000.00	0.9302	0.8696
37	0.4904	0.1201	40.0	1.71	6.27	10000.00	10000.00	0.9384	0.8840
38	C.4923	0.0946	45.0	1.73	6.34	10000.00	10000.00	0.9449	0.8956
39	0.4938	0.0746	50.0	1.74	6.39	10000.00	10000.00	0.9501	0.9050
40	0.4949	0.0593	55.0	1.75	6.44	10000.00	10000.00	0.9545	0.9129
41	C.4958	0.0477	60.0	1.76	6.47	10000.00	10000.00	0.9581	0.9196
42	0.4972	0.0344	70.0	1.78	6.53	10000.00	10000.00	0.9639	0.9303
43	C.4982	0.0340	80.0	1.79	6.58	10000.00	10000.00	0.9682	0.9384
44	C.4989	0.0484	90.0	1.80	6.61	10000.00	10000.00	0.9717	0.9449
45	0.4995	0.0798	100.0	1.80	6.64	10000.00	10000.00	0.9744	0.9501
46	0.4999	0.1283	110.0	1.81	6.66	10000.00	10000.00	0.9767	0.9545
47	C.5003	0.1915	120.0	1.81	6.68	10000.00	10000.00	0.9786	0.9581
48	0.5005	0.3402	140.0	1.82	6.71	10000.00	10000.00	0.9816	0.9639
49	C.5007	0.4770	160.0	1.82	6.73	10000.00	10000.00	0.9839	0.9682
50	0.5008	0.5651	180.0	1.83	6.75	10000.00	10000.00	0.9856	0.9717
51	0.5009	0.5932	200.0	1.83	6.76	10000.00	10000.00	0.9870	0.9744
52	C.5001	0.5697	220.0	1.83	6.76	10000.00	10000.00	0.9882	0.9767
53	0.5010	0.5120	240.0	1.84	6.78	10000.00	10000.00	0.9892	0.9786
54	0.5011	0.3596	280.0	1.84	6.80	10000.00	10000.00	0.9907	0.9816
55	C.5004	0.2235	320.0	1.84	6.80	10000.00	10000.00	0.9919	0.9839
56	0.5013	0.1289	360.0	1.84	6.82	10000.00	10000.00	0.9928	0.9856
57	C.5008	0.0710	400.0	1.84	6.82	10000.00	10000.00	0.9935	0.9871
58	C.5013	0.0381	440.0	1.85	6.83	10000.00	10000.00	0.9941	0.9882
59	0.5010	0.0201	480.0	1.85	6.83	10000.00	10000.00	0.9946	0.9892
60	C.5037	0.0105	520.0	1.85	6.83	10000.00	10000.00	0.9950	0.9900

p = 63.40 α

JJ	R, C ₀ /sec	FZEROP	DZERO, μ	XSTP, μ	XSTAP, μ	XSTDP, μ	XSTARD, μ	ALFAST, α^*	XNUST, γ^*
1	C.0022	0.0000	0.5	0.00	0.00	10000.00	10000.00	0.1600	0.0870
2	0.0025	0.0001	1.0	0.00	0.01	10000.00	10000.00	0.2759	0.1601
3	1.0707	0.0008	1.5	1.01	3.13	5.04	6.31	0.3637	0.2223
4	1.3090	0.0032	2.0	1.29	4.10	3.05	3.57	0.4325	0.2759
5	1.3722	0.0080	2.5	1.40	4.68	2.57	2.99	0.4878	0.3227
6	1.3923	0.0156	3.0	1.47	4.68	2.37	2.77	0.5334	0.3637
7	1.3967	0.0260	3.5	1.51	4.81	2.27	2.69	0.5714	0.4001
8	1.3946	0.0389	4.0	1.54	4.91	2.21	2.66	0.6036	0.4325
9	1.3903	0.0539	4.5	1.57	4.98	2.16	2.65	0.6316	0.4616
10	1.3859	0.0704	5.0	1.59	5.05	2.12	2.66	0.6558	0.4879
11	1.3804	0.1057	6.0	1.64	5.16	2.05	2.68	0.6957	0.5334
12	1.3835	0.1413	7.0	1.68	5.29	1.94	2.70	0.7273	0.5715
13	1.4002	0.1745	8.0	1.74	5.45	1.80	2.69	0.7530	0.6039
14	1.4422	0.2039	9.0	1.82	5.71	1.60	2.65	0.7742	0.6317
15	1.7087	0.2287	10.0	2.19	6.88	1.27	2.58	0.7921	0.6558
16	1.4827	0.2487	11.0	1.92	6.01	1.42	2.47	0.8074	0.6770
17	1.2550	0.2640	12.0	1.64	5.12	2.81	2.31	0.8205	0.6957
18	1.1944	0.2751	13.0	1.58	4.91	4.51	2.09	0.8320	0.7124
19	1.1709	0.2825	14.0	1.56	4.85	7.07	1.77	0.8421	0.7274
20	1.1819	0.2865	15.0	1.59	4.93	11.50	1.02	0.8511	0.7408
21	1.0916	0.2878	16.0	1.48	4.58	21.07	2.65	0.8591	0.7530
22	1.0248	0.2867	17.0	1.40	4.32	56.90	4.09	0.8663	0.7641
23	C.9624	0.2837	18.0	1.32	4.08	10000.00	5.88	0.8727	0.7743
24	0.9044	0.2791	19.0	1.25	3.85	10000.00	8.35	0.8786	0.7836
25	0.8439	0.2732	20.0	1.17	3.61	10000.00	12.06	0.8840	0.7921
26	0.7841	0.2665	21.0	1.09	3.36	10000.00	18.29	0.8889	0.8001
27	0.7374	0.2590	22.0	1.03	3.18	10000.00	30.98	0.8934	0.8074
28	0.7258	0.2509	23.0	1.02	3.14	10000.00	70.68	0.8976	0.8142
29	0.7291	0.2425	24.0	1.03	3.16	10000.00	10000.00	0.9014	0.8206
30	0.7322	0.2339	25.0	1.03	3.19	10000.00	10000.00	0.9050	0.8265
31	C.7349	0.2252	26.0	1.04	3.21	10000.00	10000.00	0.9083	0.8321
32	0.7375	0.2164	27.0	1.05	3.23	10000.00	10000.00	0.9114	0.8373
33	0.7398	0.2077	28.0	1.05	3.25	10000.00	10000.00	0.9143	0.8422
34	0.7419	0.1992	29.0	1.06	3.27	10000.00	10000.00	0.9170	0.8468
35	0.7439	0.1907	30.0	1.06	3.28	10000.00	10000.00	0.9195	0.8511
36	C.7517	0.1521	35.0	1.09	3.35	10000.00	10000.00	0.9302	0.8696
37	0.7572	0.1201	40.0	1.10	3.40	10000.00	10000.00	0.9384	0.8840
38	0.7614	0.0946	45.0	1.11	3.44	10000.00	10000.00	0.9449	0.8956
39	0.7645	0.0746	50.0	1.13	3.48	10000.00	10000.00	0.9501	0.9050
40	0.7671	0.0593	55.0	1.13	3.50	10000.00	10000.00	0.9545	0.9129
41	0.7691	0.0477	60.0	1.14	3.52	10000.00	10000.00	0.9581	0.9196
42	C.7723	0.0344	70.0	1.15	3.56	10000.00	10000.00	0.9639	0.9303
43	0.7745	0.0340	80.0	1.16	3.59	10000.00	10000.00	0.9682	0.9384
44	0.7762	0.0484	90.0	1.17	3.61	10000.00	10000.00	0.9717	0.9449
45	0.7775	0.0798	100.0	1.17	3.62	10000.00	10000.00	0.9744	0.9501
46	0.7785	0.1293	110.0	1.18	3.64	10000.00	10000.00	0.9767	0.9545
47	C.7794	0.1915	120.0	1.18	3.65	10000.00	10000.00	0.9786	0.9581
48	0.7806	0.3402	140.0	1.18	3.67	10000.00	10000.00	0.9816	0.9639
49	0.7813	0.4770	160.0	1.19	3.68	10000.00	10000.00	0.9839	0.9682
50	C.7817	0.5651	180.0	1.19	3.69	10000.00	10000.00	0.9856	0.9717
51	0.7820	0.5932	200.0	1.19	3.70	10000.00	10000.00	0.9870	0.9744
52	C.7808	0.5697	220.0	1.19	3.70	10000.00	10000.00	0.9882	0.9767
53	C.7824	0.5120	240.0	1.20	3.71	10000.00	10000.00	0.9892	0.9786
54	0.7827	0.3596	280.0	1.20	3.72	10000.00	10000.00	0.9907	0.9816
55	C.7815	0.2235	320.0	1.20	3.72	10000.00	10000.00	0.9919	0.9839
56	C.7831	0.1289	360.0	1.20	3.73	10000.00	10000.00	0.9928	0.9856
57	0.7824	0.0710	400.0	1.20	3.73	10000.00	10000.00	0.9935	0.9871
58	C.7833	0.0381	440.0	1.20	3.74	10000.00	10000.00	0.9941	0.9882
59	C.7828	0.0201	480.0	1.20	3.74	10000.00	10000.00	0.9946	0.9892
60	0.7824	0.0105	520.0	1.20	3.74	10000.00	10000.00	0.9950	0.9900

$P = 112.40 \text{ atm.}$

JJ	R, cm/sec	FZEROP	OZERO, μ	XSTPF, μ	XSTAP, μ	XSTDP, μ	XSTARD, μ	ALFAST, μ	XNUST, μ
1	C.0022	0.0000	0.5	0.00	10000.00	10000.00	0.1600	0.0870	0.1601
2	C.0025	0.0001	1.0	0.00	10000.00	10000.00	0.2759	0.1601	0.2759
3	1.2389	0.0008	1.5	0.50	6.3	3.04	0.3637	0.2759	0.3637
4	1.6207	0.0032	2.0	0.68	1.87	3.05	0.4325	0.3637	0.4325
5	1.7298	0.0080	2.5	0.75	2.08	2.99	0.4878	0.3637	0.4878
6	1.7707	0.0156	3.0	0.79	2.19	2.97	0.5334	0.3637	0.5334
7	1.7864	0.0260	3.5	0.82	2.26	2.97	0.5714	0.3637	0.5714
8	1.7914	0.0389	4.0	0.84	2.31	2.97	0.6038	0.3637	0.6038
9	1.7917	0.0539	4.5	0.86	2.35	2.97	0.6316	0.3637	0.6316
10	1.7903	0.0704	5.0	0.87	2.39	2.97	0.6558	0.3637	0.6558
11	1.7881	0.1057	6.0	0.90	2.44	2.97	0.6957	0.3637	0.6957
12	1.7911	0.1413	7.0	0.92	2.50	2.97	0.7273	0.3637	0.7273
13	1.8036	0.1745	8.0	0.95	2.56	2.97	0.7530	0.3637	0.7530
14	1.8331	0.2039	9.0	0.98	2.64	2.97	0.7742	0.3637	0.7742
15	1.9104	0.2287	10.0	1.04	2.78	2.97	0.7921	0.3637	0.7921
16	1.8713	0.2487	11.0	1.03	2.75	2.97	0.8074	0.3637	0.8074
17	1.7378	0.2640	12.0	0.96	2.57	2.97	0.8205	0.3637	0.8205
18	1.7099	0.2751	13.0	0.96	2.55	2.97	0.8320	0.3637	0.8320
19	1.7154	0.2825	14.0	0.97	2.57	2.97	0.8421	0.3637	0.8421
20	1.7840	0.2865	15.0	1.02	2.70	2.97	0.8511	0.3637	0.8511
21	1.5957	0.2878	16.0	0.92	2.42	2.97	0.8591	0.3637	0.8591
22	1.4728	0.2867	17.0	0.85	2.24	2.97	0.8663	0.3637	0.8663
23	1.3637	0.2837	18.0	0.79	2.08	2.97	0.8727	0.3637	0.8727
24	1.2664	0.2791	19.0	0.74	1.94	2.97	0.8786	0.3637	0.8786
25	1.1776	0.2732	20.0	0.69	1.81	2.97	0.8840	0.3637	0.8840
26	1.1084	0.2665	21.0	0.65	1.71	2.97	0.8889	0.3637	0.8889
27	1.0782	0.2590	22.0	0.64	1.67	2.97	0.8934	0.3637	0.8934
28	1.0814	0.2509	23.0	0.64	1.68	2.97	0.9014	0.3637	0.9014
29	1.0880	0.2425	24.0	0.65	1.70	2.97	0.9050	0.3637	0.9050
30	1.0940	0.2339	25.0	0.65	1.71	2.97	0.9083	0.3637	0.9083
31	1.0995	0.2252	26.0	0.66	1.72	2.97	0.9114	0.3637	0.9114
32	1.1045	0.2164	27.0	0.66	1.74	2.97	0.9143	0.3637	0.9143
33	1.1092	0.2077	28.0	0.67	1.75	2.97	0.9170	0.3637	0.9170
34	1.1135	0.1992	29.0	0.67	1.76	2.97	0.9195	0.3637	0.9195
35	1.1174	0.1907	30.0	0.68	1.77	2.97	0.9302	0.3637	0.9302
36	1.1335	0.1521	35.0	0.69	1.81	2.97	0.9384	0.3637	0.9384
37	1.1450	0.1201	40.0	0.71	1.84	2.97	0.9449	0.3637	0.9449
38	1.1535	0.0946	45.0	0.72	1.87	2.97	0.9501	0.3637	0.9501
39	1.1601	0.0746	50.0	0.72	1.89	2.97	0.9545	0.3637	0.9545
40	1.1655	0.0593	55.0	0.73	1.90	2.97	0.9581	0.3637	0.9581
41	1.1698	0.0477	60.0	0.73	1.92	2.97	0.9639	0.3637	0.9639
42	1.1765	0.0344	70.0	0.74	1.94	2.97	0.9682	0.3637	0.9682
43	1.1813	0.0340	80.0	0.75	1.96	2.97	0.9717	0.3637	0.9717
44	1.1850	0.0484	90.0	0.75	1.97	2.97	0.9744	0.3637	0.9744
45	1.1878	0.0798	100.0	0.76	1.98	2.97	0.9767	0.3637	0.9767
46	1.1901	0.1283	110.0	0.76	1.99	2.97	0.9816	0.3637	0.9816
47	1.1920	0.1915	120.0	0.76	2.00	2.97	0.9839	0.3637	0.9839
48	1.1948	0.3402	140.0	0.77	2.01	2.97	0.9856	0.3637	0.9856
49	1.1969	0.4770	160.0	0.77	2.02	2.97	0.9870	0.3637	0.9870
50	1.1984	0.5651	180.0	0.77	2.02	2.97	0.9882	0.3637	0.9882
51	1.1992	0.5932	200.0	0.77	2.02	2.97	0.9892	0.3637	0.9892
52	1.1973	0.5697	220.0	0.77	2.02	2.97	0.9907	0.3637	0.9907
53	1.2003	0.5120	240.0	0.78	2.03	2.97	0.9919	0.3637	0.9919
54	1.2010	0.3596	280.0	0.78	2.04	2.97	0.9928	0.3637	0.9928
55	1.1992	0.2235	320.0	0.78	2.04	2.97	0.9935	0.3637	0.9935
56	1.2020	0.1289	360.0	0.78	2.04	2.97	0.9941	0.3637	0.9941
57	1.2009	0.0710	400.0	0.78	2.04	2.97	0.9946	0.3637	0.9946
58	1.2027	0.0381	440.0	0.78	2.05	2.97	0.9950	0.3637	0.9950
59	1.2019	0.0201	480.0	0.78	2.05	2.97	0.9950	0.3637	0.9950
60	1.2012	0.0105	520.0	0.78	2.05	2.97	0.9950	0.3637	0.9950

p = 200 atm.									
JJ	R ₂ cm/sec	FZEROP	DZERO, μ	XSTPF, μ	XSTAP, μ	XSTPD, μ	XSTARD, μ	ALFAST, α^*	XMUST, β^*
1	0.0022	0.0000	0.5	0.00	0.00	10000.00	10000.00	0.1600	0.0870
2	0.0025	0.0001	1.0	0.00	0.00	10000.00	10000.00	0.2759	0.1601
3	1.3484	0.0008	1.5	0.23	0.52	5.04	6.31	0.3637	0.2223
4	1.9047	0.0032	2.0	0.34	0.80	3.05	3.57	0.4325	0.2759
5	2.0972	0.0080	2.5	0.38	0.92	2.57	2.99	0.4878	0.3227
6	2.1844	0.0156	3.0	0.41	0.99	2.37	2.77	0.5334	0.3637
7	2.2296	0.0260	3.5	0.43	1.03	2.27	2.69	0.5714	0.4001
8	2.2553	0.0389	4.0	0.45	1.06	2.21	2.66	0.6038	0.4325
9	2.2711	0.0539	4.5	0.46	1.09	2.16	2.65	0.6316	0.4616
10	2.2821	0.0704	5.0	0.47	1.11	2.12	2.66	0.6558	0.4879
11	2.2989	0.1057	6.0	0.49	1.14	2.05	2.68	0.6957	0.5334
12	2.3168	0.1413	7.0	0.50	1.17	1.94	2.70	0.7273	0.5715
13	2.3413	0.1745	8.0	0.52	1.20	1.80	2.69	0.7530	0.6039
14	2.3787	0.2039	9.0	0.54	1.24	1.60	2.65	0.7742	0.6317
15	2.4498	0.2287	10.0	0.56	1.29	1.27	2.58	0.7921	0.6558
16	2.4478	0.2487	11.0	0.57	1.30	1.42	2.47	0.8074	0.6770
17	2.3815	0.2640	12.0	0.56	1.27	2.81	2.31	0.8205	0.6957
18	2.3955	0.2751	13.0	0.57	1.29	4.51	2.09	0.8320	0.7124
19	2.4508	0.2825	14.0	0.58	1.33	7.07	1.77	0.8421	0.7274
20	2.6385	0.2865	15.0	0.63	1.44	11.50	1.02	0.8511	0.7408
21	2.2505	0.2878	16.0	0.54	1.23	21.07	2.65	0.8591	0.7530
22	2.0339	0.2867	17.0	0.49	1.11	56.90	4.09	0.8663	0.7641
23	1.8604	0.2837	18.0	0.46	1.02	10000.00	5.88	0.8727	0.7743
24	1.7207	0.2791	19.0	0.42	0.95	10000.00	8.35	0.8786	0.7836
25	1.6172	0.2732	20.0	0.40	0.89	10000.00	12.06	0.8840	0.7921
26	1.5658	0.2665	21.0	0.39	0.86	10000.00	18.29	0.8889	0.8001
27	1.5607	0.2590	22.0	0.39	0.86	10000.00	30.98	0.8934	0.8074
28	1.5787	0.2509	23.0	0.39	0.88	10000.00	70.68	0.8976	0.8142
29	1.5915	0.2425	24.0	0.40	0.89	10000.00	10000.00	0.9014	0.8206
30	1.6032	0.2339	25.0	0.40	0.90	10000.00	10000.00	0.9050	0.8265
31	1.6139	0.2252	26.0	0.41	0.90	10000.00	10000.00	0.9083	0.8321
32	1.6237	0.2164	27.0	0.41	0.91	10000.00	10000.00	0.9114	0.8373
33	1.6328	0.2077	28.0	0.41	0.92	10000.00	10000.00	0.9143	0.8422
34	1.6412	0.1992	29.0	0.42	0.93	10000.00	10000.00	0.9170	0.8468
35	1.6490	0.1907	30.0	0.42	0.93	10000.00	10000.00	0.9195	0.8511
36	1.6809	0.1521	35.0	0.43	0.96	10000.00	10000.00	0.9302	0.8696
37	1.7042	0.1201	40.0	0.44	0.98	10000.00	10000.00	0.9384	0.8840
38	1.7220	0.0946	45.0	0.44	0.99	10000.00	10000.00	0.9449	0.8956
39	1.7356	0.0746	50.0	0.46	1.01	10000.00	10000.00	0.9501	0.9050
40	1.7464	0.0593	55.0	0.46	1.02	10000.00	10000.00	0.9545	0.9129
41	1.7554	0.0477	60.0	0.46	1.02	10000.00	10000.00	0.9581	0.9196
42	1.7691	0.0344	70.0	0.47	1.04	10000.00	10000.00	0.9639	0.9303
43	1.7792	0.0340	80.0	0.48	1.05	10000.00	10000.00	0.9682	0.9384
44	1.7869	0.0484	90.0	0.48	1.05	10000.00	10000.00	0.9717	0.9449
45	1.7930	0.0798	100.0	0.48	1.06	10000.00	10000.00	0.9744	0.9501
46	1.7979	0.1283	110.0	0.48	1.07	10000.00	10000.00	0.9767	0.9545
47	1.8019	0.1915	120.0	0.49	1.07	10000.00	10000.00	0.9786	0.9581
48	1.8080	0.3402	140.0	0.49	1.08	10000.00	10000.00	0.9816	0.9639
49	1.8125	0.4770	160.0	0.49	1.08	10000.00	10000.00	0.9839	0.9682
50	1.8159	0.5651	180.0	0.49	1.08	10000.00	10000.00	0.9856	0.9717
51	1.8185	0.5932	200.0	0.50	1.09	10000.00	10000.00	0.9870	0.9744
52	1.8164	0.5697	220.0	0.50	1.09	10000.00	10000.00	0.9882	0.9767
53	1.8219	0.5120	240.0	0.50	1.09	10000.00	10000.00	0.9892	0.9786
54	1.8238	0.3596	280.0	0.50	1.10	10000.00	10000.00	0.9907	0.9816
55	1.8210	0.2235	320.0	0.50	1.10	10000.00	10000.00	0.9919	0.9839
56	1.8261	0.1289	360.0	0.50	1.10	10000.00	10000.00	0.9928	0.9856
57	1.8244	0.0710	400.0	0.50	1.10	10000.00	10000.00	0.9935	0.9871
58	1.8276	0.0381	440.0	0.50	1.10	10000.00	10000.00	0.9941	0.9882
59	1.8264	0.0201	480.0	0.50	1.10	10000.00	10000.00	0.9946	0.9892
60	1.8254	0.0105	520.0	0.50	1.10	10000.00	10000.00	0.9950	0.9900

PARABOLIC FLAME ASSUMED

PROPELLANT DATA IS

WT. PERCENT OXID. = 90.0
 PROCP. DENSITY = 0.0
 QFUEL = 25.0
 DIFF PARAM = 1000.0000
 ST PAT = 16.50
 PPI ST PAT = 8.30
 BINDER DENSITY = 0.98
 MOL WT = 20.87
 OXID. DENSITY = 1.95
 PRI MOL WT = 28.00

OXIDIZER IGNITION AND BURNING DATA IS

CIGN = 190.0
 POWIGN = 0.721
 POWD = 0.8
 LATENT HEAT = -110.0

ACTIVATION ENERGIES AND RATE FACTORS ARE

EF = 15000.
 ORDER, PF = 1.500
 ORDER, HP = 1.800
 E OX = 26000.
 RT CON, PF = 0.2500
 RT CON, HP = 0.2310
 AF = 0.2700
 ORDER, LP = 1.800
 RT CON, LP = 0.2310
 A OX = 0.3000

FLAME PROPERTIES ARE

OXID. FLM TEMP = 1400.0
 AV FLM HT FACT = 0.3000
 GAS CONDUCT = 0.00020
 CP(AVE) = 0.3000

PROPELLANT INITIAL TEMP IS 21.1 DEG CENTIGRADE

n (exponent in Eq. 19) = 2

EXPONENT FOR DIFFUSION PRESSURE DEPENDENCE IS 1.000

PPFS ATMS	PRES PSIA	JR CM/SEC	BR IN/SEC
2.00	29.4	0.1006	0.0396
3.54	52.0	0.1515	0.0597
6.34	93.2	0.2287	0.0900
11.24	165.2	0.3405	0.1341
20.00	294.0	0.5047	0.1987
35.40	520.4	0.7357	0.2896
63.40	932.0	1.0400	0.4095
112.40	1652.3	1.4896	0.5860
200.00	2940.0	2.1296	0.8384

Appendix B

HYDRAULIC ANALOGY

The analogy between one-dimensional, nonsteady flows of inviscid gases and inviscid liquids with free surfaces and between two-dimensional, steady flows of inviscid gases and inviscid liquids with free surfaces is well documented in the literature⁽²²⁾. As one might expect in this situation, the analogy also extends to two-dimensional, nonsteady flows. However, although this analogy has been exploited in several studies,⁽²²⁾ no explicit derivation of the analogy for the nonsteady, two-dimensional situation has apparently been presented.* The object of this appendix is to present a derivation for this situation.

For nonsteady, two-dimensional, irrotational flow of a perfect gas the governing equations are⁽²⁴⁾

$$\partial \rho / \partial t + \partial \rho u / \partial x + \partial \rho v / \partial y = 0 \quad (\text{B-1})$$

$$\partial u / \partial t + u \partial u / \partial x + v \partial u / \partial y + \rho^{-1} \partial p / \partial x = 0 \quad (\text{B-2})$$

$$\partial v / \partial t + u \partial v / \partial x + v \partial v / \partial y + \rho^{-1} \partial p / \partial y = 0 \quad (\text{B-3})$$

$$p / p_o = (\rho / \rho_o)^\gamma \quad (\text{B-4})$$

Employing a_o , ρ_o , p_o , l_g , t_g as reference dimensions and Eq. B-4 to eliminate p from Eqs. B-2 and B-3 yields the non-dimensional equations

$$\partial \rho^+ u^+ / \partial x^+ + \partial \rho^+ v^+ / \partial y^+ + [l_g / (a_o t_g)] \partial \rho^+ / \partial t^+ \quad (\text{B-5})$$

$$[l_g / (a_o t_g)] \partial u^+ / \partial t^+ + u^+ \partial u^+ / \partial x^+ + v^+ \partial u^+ / \partial y^+ + [\partial (\rho^+) \frac{\gamma-1}{\gamma} / \partial x^+] / (\gamma-1) = 0 \quad (\text{B-6})$$

$$[l_g / (a_o t_g)] \partial v^+ / \partial t^+ + u^+ \partial v^+ / \partial x^+ + v^+ \partial v^+ / \partial y^+ \quad (\text{B-7})$$

$$+ [\partial (\rho^+) \frac{\gamma-1}{\gamma} / \partial y^+] / (\gamma-1) = 0$$

A three dimensional, nonsteady flow of inviscid liquid over a planar surface perpendicular to the gravity vector g is governed by the equations⁽²⁴⁾

* Loh⁽²³⁾ indicates in a footnote that the analogy extends to this case.

$$\partial u / \partial x + \partial v / \partial y + \partial w / \partial z = 0 \quad (B-8)$$

$$D_u / D_t + \rho^{-1} \partial p / \partial x = 0 \quad (B-9)$$

$$D_v / D_t + \rho^{-1} \partial p / \partial y = 0 \quad (B-10)$$

$$D_w / D_t + \rho^{-1} \partial p / \partial z + g = 0 \quad (B-11)$$

Assuming that vertical water accelerations are small compared to g Eq. B-11 becomes

$$\partial p / \partial z = -\rho g \quad (B-12)$$

Integration yields

$$p(x, y, z, t) = \rho g \int_h^z dz + p(x, y, h, t) \quad (B-13)$$

where $h(x, y, t)$ is the depth of the water. However, since only pressure differences are encountered in Eq. (B-9) to (B-11) and since $p(x, y, h, t) =$ constant, that constant can be set to zero without loss of generality. Consequently,

$$p(x, y, z, t) = \rho g (h - z) \quad (B-14)$$

and

$$\rho^{-1} \partial p / \partial x = g \partial h / \partial x \quad (B-15)$$

$$\rho^{-1} \partial p / \partial y = g \partial h / \partial y \quad (B-16)$$

Analysis is directed at inviscid motion. Assume $u = u(x, y, t)$ and $v = v(x, y, t)$. Therefore, terms containing w are eliminated from Eqs. (B-9) and (B-10). However, since $w = w(z)$, $\partial w / \partial z \neq 0$. Formally integrating Eq. (B-8) from $z=0$ to $z=h$ yields (after application of Liebnitz's rule⁽²¹⁾) and the above assumption

$$\partial h u / \partial x + \partial h v / \partial y + w(x, y, h, t) = u(x, y, h, t) \partial h / \partial x + v(x, y, h, t) \partial h / \partial y \quad (B-17)$$

$$\text{Since } w(x, y, h, t) = \partial h / \partial t + u(x, y, h, t) \partial h / \partial x + v(x, y, h, t) \partial h / \partial y, \text{ Eq. (B-17)}$$

becomes

$$\partial h / \partial t + \partial h u / \partial x + \partial h v / \partial y = 0 \quad (B-18)$$

Nondimensionalizing Eqs. B-9, B-10, and B-18 with reference dimensions h_0 , $g h_0$, l_w , and t_w yields the non-dimensional hydraulic equations

$$\partial h^+ u^+ / \partial x^+ + \partial h^+ v^+ / \partial y^+ + [l_w / (\sqrt{gh_o} t_w)] \partial h^+ / \partial t^+ = 0 \quad (B-19)$$

$$[l_w / (\sqrt{gh_o} l_w)] \partial u^+ / \partial t^+ + u^+ \partial u^+ / \partial x^+ + v^+ \partial u^+ / \partial y^+ + \partial h^+ / \partial x^+ = 0 \quad (B-20)$$

$$[l_w / (\sqrt{gh_o} l_w)] \partial v^+ / \partial t^+ + u^+ \partial v^+ / \partial x^+ + v^+ \partial v^+ / \partial y^+ + \partial h^+ / \partial y^+ = 0 \quad (B-21)$$

Comparison of Eqs. (B-5) to (B-7) with Eqs. (B-19) to (B-21) shows that when $\gamma=2$ and $l_w / (\sqrt{gh_o} t_w) = l_g / (a_o t_g)$ the non-dimensional equations are equivalent if $h^+ = \rho^+$. Consequently, under these conditions an analogy exists between the gas and free surface liquid flows. In this analogy

$h^+ = \sqrt{p^+}$ [or $p^+ = (h^+)^2$], $a = \sqrt{gh}$, $h^+ = \rho^+$, $u_w^+ = u_g^+$, and $v_y^+ = v_g^+$. For conditions where $0(l_w) \sim 0(l_g)$, $0(t_w) < 0(t_g)$. In other words, time is effectively slowed in the analogy. This means that transient phenomena can often be studied visually in the hydraulic analogy. It is this fact that makes the analogy valuable for nonsteady situations.

It has been shown that an analogy exists between irrotational flow of gas with $\gamma=2$ and irrotational flow of liquid over a horizontal surface. Flows in nature are not irrotational. Therefore, of what practical value is this analogy? First, numerous experiments⁽²²⁾ have demonstrated excellent agreement with theory for simple flows. Second, there seems to be no question that the analogy provides a relatively simple way to obtain information on complex flow situations.⁽²²⁾

UNCLASSIFIED

SECURITY CLASSIFICATION OF THIS PAGE (When Data Entered)

19 REPORT DOCUMENTATION PAGE		READ INSTRUCTIONS BEFORE COMPLETING FORM	
1. REPORT NUMBER AFOSR TR-75-1553	2. GOVT ACCESSION NO.	3. RECIPIENT'S CATALOG NUMBER 9	
4. TITLE (and Subtitle) STEADY-STATE COMBUSTION OF NONMETALLIZED COMPOSITE SOLID PROPELLANT,		5. TYPE OF REPORT & PERIOD COVERED INTERIM 1 May 74 - 30 Jun 75	
7. AUTHOR(s) R. L. GLICK		6. PERFORMING ORG. REPORT NUMBER U-75-27	
9. PERFORMING ORGANIZATION NAME AND ADDRESS THIOKOL CORPORATION HUNTSVILLE DIVISION HUNTSVILLE, ALABAMA		8. CONTRACT OR GRANT NUMBER(s) F44620-74-C-0080	
11. CONTROLLING OFFICE NAME AND ADDRESS AIR FORCE OFFICE OF SCIENTIFIC RESEARCH/NA 1400 WILSON BOULEVARD ARLINGTON, VIRGINIA 22209		10. PROGRAM ELEMENT, PROJECT, TASK AREA & WORK UNIT NUMBERS 681308 AF-9711-01 61102F	
14. MONITORING AGENCY NAME & ADDRESS (if different from Controlling Office)		12. REPORT DATE Jul 75	
		13. NUMBER OF PAGES 76	
		15. SECURITY CLASS. (of this report) UNCLASSIFIED	
		15a. DECLASSIFICATION/DOWNGRADING SCHEDULE	
16. DISTRIBUTION STATEMENT (of this Report) Approved for public release; distribution unlimited.			
17. DISTRIBUTION STATEMENT (of the abstract entered in Block 20, if different from Report)			
18. SUPPLEMENTARY NOTES			
19. KEY WORDS (Continue on reverse side if necessary and identify by block number) MONODISPERSE BDP COMBUSTION MODEL NONMETALLIZED PROPELLANTS HYDRAULIC T-BURNER ANALOG VENT FLOW PHENOMENA NON-NEUTRAL PRESSURE-TIME HISTORY			
20. ABSTRACT (Continue on reverse side if necessary and identify by block number) Monodisperse BDP combustion model was extended to nonmetallized propellants with mixed, polydisperse oxidizers by embedding monodisperse model in statistical framework including mixture ratio effects. Basically, polydisperse propellant is "disassembled and rearranged" to form sequence of monodisperse pseudo-propellants whose rates are computed via monodisperse model. Reassembly provides real propellant's burning rate. Approach provides information pertaining to distribution of regression rates and surface structure among different size oxidizer particles. Preliminary results suggest that significant factor in rate increases wrought by			

UNCLASSIFIED

SECURITY CLASSIFICATION OF THIS PAGE(When Data Entered)

introduction of small oxidizer modes is mixture ratio alterations in larger modes. Hydraulic T-burner analog was constructed and employed to visualize vent flow phenomena. Studies showed that flow enters vent with axial momentum and that momentum is partially transformed to vent into Karman vortex sheet. Fact that flow enters vent with axial momentum invalidates boundary condition of Culick analysis for flow turning gain; "correct" boundary condition leads to null vent gain. Experimental facts consistent with proof that in formal one-dimensional flow vent gain violates second law of thermodynamics. Logical and consistent way to reduce solid rocket data when pressure-time history is not neutral was derived. Since current techniques are not self-consistent in this situation, these results open door to reclamation of performance data heretofore rejected.

UNCLASSIFIED

SECURITY CLASSIFICATION OF THIS PAGE(When Data Entered)